EXPLANATORY NOTES

GOVERNMENT OF WESTERN AUSTRALIA

GEOLOGY OF THE CONNAUGHTON 1:100 000 SHEET

by L. Bagas and R. H. Smithies

1:100 000 GEOLOGICAL SERIES

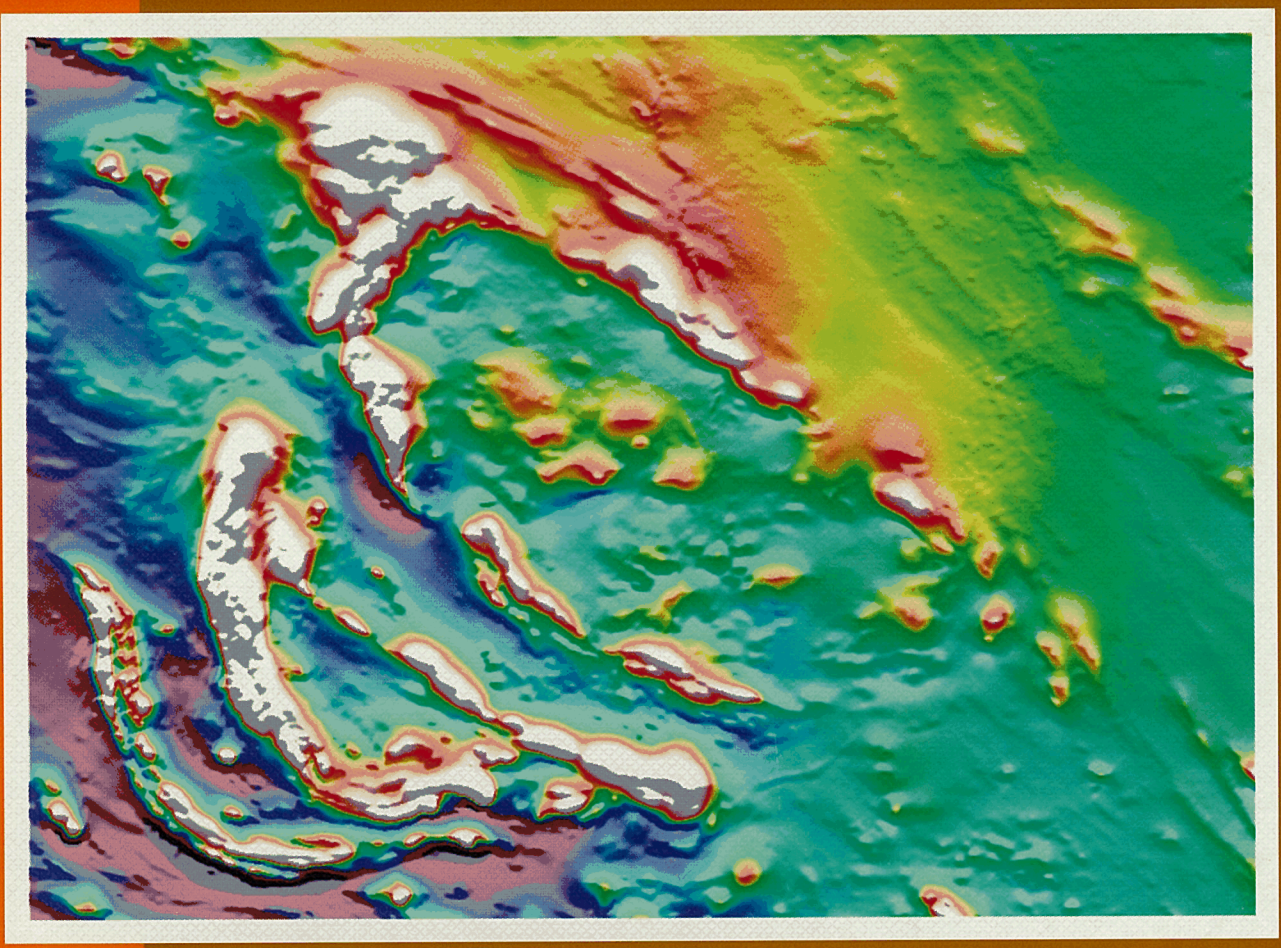

GEOLOGICAL SURVEY OF WESTERN AUSTRALIA

DEPARTMENT OF MINERALS AND ENERGY

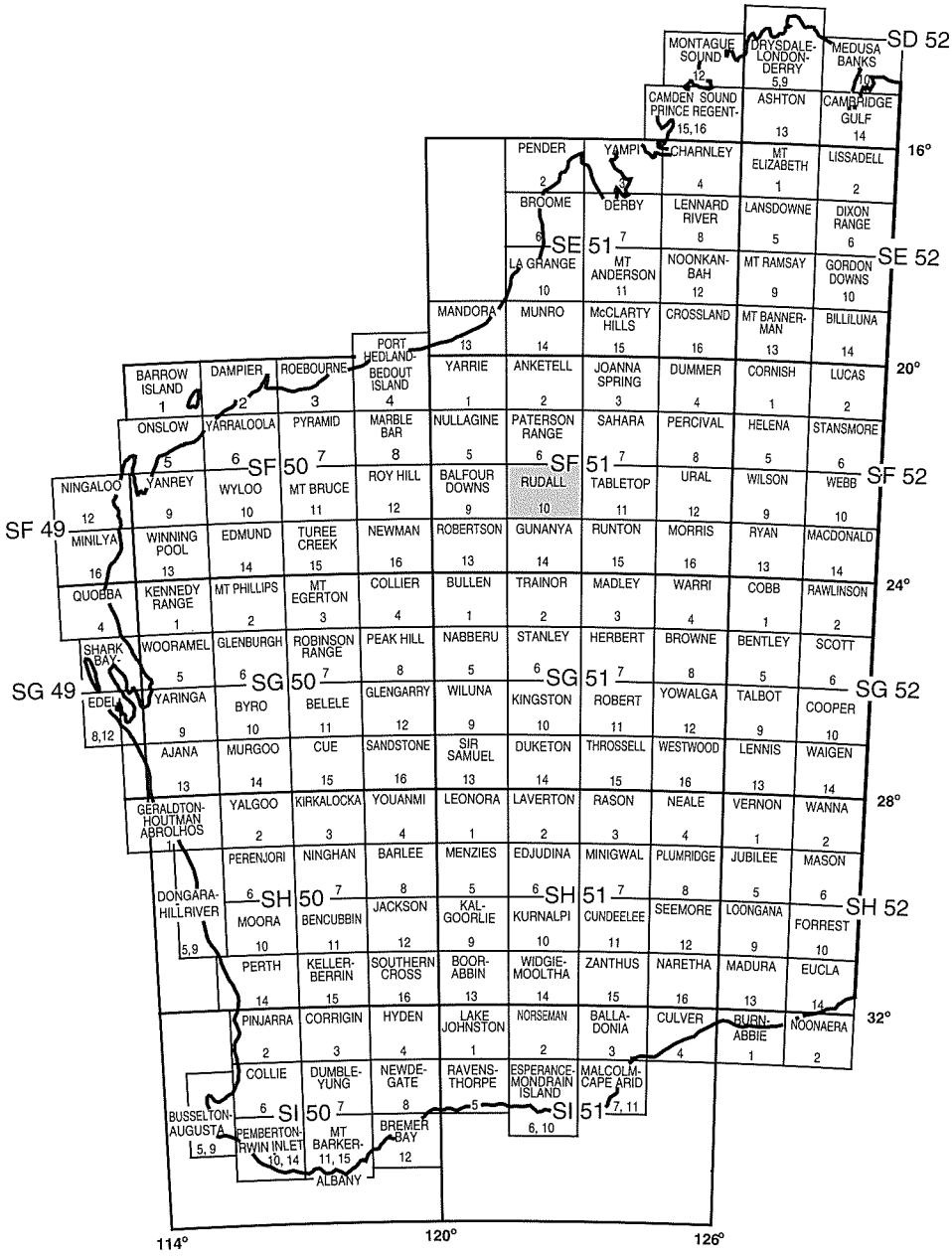

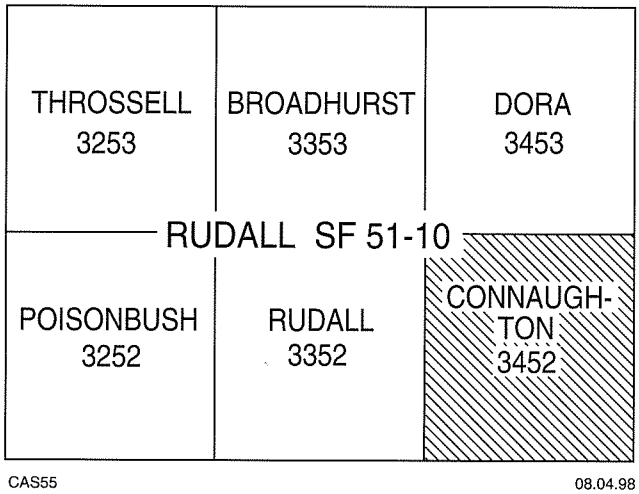

CAS55

08.04.98

GEOLOGICAL SURVEY OF WESTERN AUSTRALIA

GEOLOGY OF THE CONNAUGHTON 1:100 000 SHEET

by
L. Bagas and R. H. Smithies

Perth 1998

MINISTER FOR MINES
The Hon. Norman Moore, MLC

DIRECTOR GENERAL
L. C. Ranford

DIRECTOR, GEOLOGICAL SURVEY OF WESTERN AUSTRALIA
David Blight

Copy editor: D. P. Reddy

REFERENCE

The recommended reference for this publication is:

BAGAS, L., and SMITHIES, R. H., 1998, Geology of the Connaughton 1:100 000 sheet: Western Australia Geological Survey, 1:100 000 Geological Series Explanatory Notes, 38p.

National Library of Australia Card Number and ISBN 0 7309 6616 X

ISSN 1321–229X

The locations of points mentioned in this publication are referenced to the Australian Geodetic Datum 1984 (AGD84)

Cover photograph:
Colour-draped Total Magnetic Intensity image covering the Harbutt Range area of southeastern CONNAUGHTON. The image was provided by Australian Platinum Mines NL. Approximate scale 1:100 000.

Contents

Appendices

Figures

Tables

Geology of the Connaughton 1:100 000 sheet

by

L. Bagas and R. H. Smithies

Abstract

The CONNAUGHTON 1:100 000 sheet occupies the central part of the Paterson Orogen, and includes the Palaeoproterozoic Rudall Complex, the Mesoproterozoic to Neoproterozoic Yeneena Supergroup, the Neoproterozoic Tarcunyah Group of the greater Officer Basin, and local outliers of Permian sedimentary rocks of the Canning Basin.

The Rudall Complex consists of a broad imbricate zone of northeasterly and easterly dipping thrust sheets with cross-cutting relationships that indicate progressively younger thrusts towards the east. Some of the thrusts are major faults separating three distinct tectono-stratigraphic terranes: the Talbot, Connaughton, and Tabletop Terranes.

The Talbot Terrane, in the western part of the CONNAUGHTON sheet, comprises a metamorphosed succession of siliciclastic rocks. The Connaughton Terrane, in the central part of the sheet, comprises a succession of mafic schist and gneiss, and associated metamorphosed chemical and clastic sedimentary rocks. The poorly exposed Tabletop Terrane, in the eastern part of the sheet, comprises a sequence of amphibolite and metasedimentary rocks, and is characterized by weakly metamorphosed tonalite and leucogranite.

The Throssell Group represents the Mesoproterozoic to Neoproterozoic Yeneena Supergroup on CONNAUGHTON and is unconformably or disconformably overlain by the Neoproterozoic Tarcunyah Group. Both these groups unconformably overlie or are faulted against the Rudall Complex.

The Paterson Orogen contains evidence of at least six major deformation events. The first two deformation events (D_1 and D_2) occurred during the Yapungku Orogeny between 2000 and 1760 Ma. The D_3 and D_4 deformation events occurred during the Miles Orogeny between 1300 and 800 Ma. Structures associated with the D_5 deformation event may be contemporaneous with those in the Blake Fault and Fold Belt in the Savory Basin, south of CONNAUGHTON. The last deformation event (D_6) occurred during the redefined Paterson Orogeny.

Peak regional M_2 metamorphism was syn- to post-D_2 in both the Talbot and Connaughton Terranes. The Talbot Terrane was metamorphosed to intermediate-pressure amphibolite facies. The Connaughton Terrane, however, was metamorphosed at high pressures to amphibolite–granulite facies. The progressive deformation and high-pressure metamorphism assigned to the D_2–M_2 event was clearly related to major crustal overthickening involving overthrusting, and is consistent with a collisional orogeny. The D_2 structures were probably produced by an advancing plate from the east during continued deformation associated with the Yapungku Orogeny, between 1790 and 1760 Ma. The eastern plate may be the Tabletop Terrane or it may be concealed beneath the Canning Basin further to the east. The extent of deformation suggests Himalayan-style continent–continent collision.

KEYWORDS: Rudall Complex, Yeneena Supergroup, Tarcunyah Group, Talbot Terrane, Connaughton Terrane, Tabletop Terrane, granulite facies metamorphism, plate tectonics

Introduction

The CONNAUGHTON* 1:100 000 map sheet covers the southeastern part of the RUDALL 1:250 000 map sheet, between latitudes 22°30' and 23°30'S and longitudes 122°30' and 123°00'E (Fig. 1). The area occupies the eastern part of the Paterson Orogen (Williams and Myers, 1990) and straddles the boundary between the Great Sandy Desert and the Little Sandy Desert (Fig. 2). The Paterson Orogen consists of sedimentary and igneous rocks that were formed, intensely deformed, and variably metamorphosed during the Proterozoic.

* Capitalized names refer to standard map sheets. Where 1:100 000 and 1:250 000 sheets have the same name, the 1:100 000 sheet is implied unless otherwise indicated.

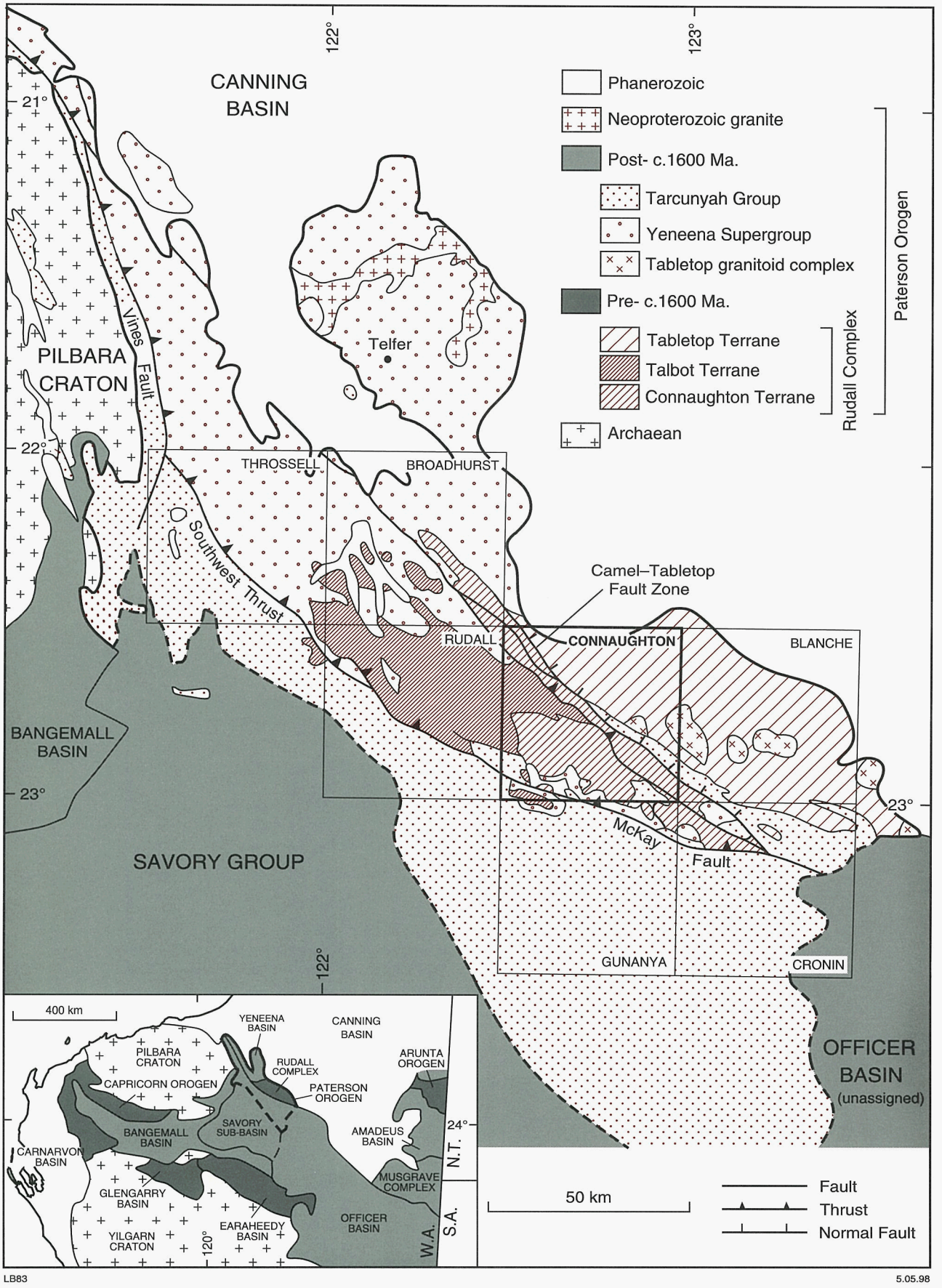

Figure 1. Regional geological setting of Connaughton

The Rudall River National Park (1 569 459 ha) covers the northern two-thirds of CONNAUGHTON and is centred on the catchment area of the Rudall River, which drains into Lake Dora, north of CONNAUGHTON.

The Parnngurr (Cotton Creek) Aboriginal community is the only permanent settlement on CONNAUGHTON. The nearest town is Telfer, about 100 km north-northwest of the sheet area. A gravel road links the Rudall River National Park to Telfer in the north and the Canning Stock Route to the southeast. A good-quality, four-wheel drive track connects the southern part of CONNAUGHTON to Newman, via Balfour Downs Homestead and the Ethel Creek – Jigalong road. Few other tracks are present in the area, and off-road access within the park requires prior approval from the Western Australian Department of Conservation and Land Management (CALM).

Previous investigations

The isolation of the Rudall River area and the lack of a permanent water supply impeded exploration until 1971, when gold was discovered at the Telfer Dome, 100 km to the north. The early exploration of the Rudall region was summarized by Chin et al. (1980).

Reconnaissance mapping of the RUDALL (1:250 000) map sheet was carried out during 1974–75 by R. J. Chin, I. R. Williams, S. J. Williams, and R. W. A. Crowe of the Geological Survey of Western Australia (Chin et al., 1980), as part of the systematic 1:250 000 geological mapping of Western Australia. The conclusions reached from that work were first reported by Williams et al. (1976), and later expanded by Williams and Myers (1990).

The Geological Survey of Western Australia (GSWA) located gossanous quartz veins with anomalous base-metal concentrations at South Rudall Dome, Mount Cotton, and the Wells Antiform during the mapping of RUDALL (1:250 000) in 1975 (Chin et al., 1980). They also located rare-earth element (La, Y, and Ce) mineralization in a massive quartz vein north of Mount Cotton (AMG 561829*).

In 1984 the Bureau of Mineral Resources (now known as the Australian Geological Survey Organisation) flew a regional airborne magnetic survey over RUDALL (1:250 000), at a line spacing of 1.6 km and a sample interval of 60 m.

In 1985 uranium was discovered at Kintyre on BROADHURST, adding new impetus to mineral exploration.

The Geological Survey of Western Australia commenced a program of detailed 1:100 000 geological mapping of the Rudall Complex in 1989, and by 1994 BROADHURST (Hickman and Clarke, 1994), RUDALL (Hickman and Bagas, in prep), THROSSELL (Williams and Bagas, in press), and CONNAUGHTON had been mapped.

These Notes and the accompanying 1:100 000 geological map are the result of detailed regional mapping during 1993–94, using 1985 1:25 000 colour airphotos and 1988 1:50 000 black-and-white airphotos. Geophysical data supplied by CRA Exploration (now known as Rio Tinto Exploration) and PNC Exploration were used to interpret structures and lithologies hidden by Cainozoic cover.

Physiography

The physiography of CONNAUGHTON (Fig. 2) is the product of several distinct events of erosion and deposition. The most important events appear to have been Permian glaciation, Tertiary peneplanation, and Cainozoic erosion and deposition.

Permian land surface

The Permian land surface (Fig. 2) includes Permian fluvial–glacial sedimentary rocks deposited in valleys during glacial retreat. Late Permian to Cainozoic erosion of high-relief areas probably contributed to deposition in continental and shallow-marine settings in the south-western part of the Canning Basin.

Tertiary land surface

Laterite, ferruginous duricrust, and silcrete deposits that cap the plateaus (Fig. 2) represent unmodified remnants of the Tertiary land surface. Smaller areas of the same deposits also cap recent dissected plateaus and ridges. The precise age of the Tertiary surface is uncertain, but it may be correlated with the Hamersley Surface in the Hamersley Ranges (Campana et al., 1964; Chin et al., 1982) or the Ashburton Surface of central Australia (Jennings and Mabbutt, 1971).

Calcrete deposits throughout CONNAUGHTON pre-date the sandplains, and are probably related to channels and lakes that were active during the Tertiary. These deposits form small mounds in low-lying areas and are composed of massive, nodular, and vuggy limestone locally replaced by chalcedony.

Recent land surface

The recent land surface has been divided into erosional and depositional surfaces.

Recent erosional land surface

Divisions within the recent erosional land surface represent various stages in the erosion of Tertiary or pre-Tertiary surfaces.

The least eroded division is the dissected plateau, which is preserved in areas underlain by quartz arenite of the Tarcunyah Group (Williams and Bagas, in prep.). The boundary of this division is usually marked by a cliff line and narrow gorges and ravines, against the more

* Localities are specified by the Australian Map Grid (AMG) standard six-figure reference system whereby the first group of three figures (eastings) and the second group (northings) together uniquely define position, on this sheet, to within 100 m.

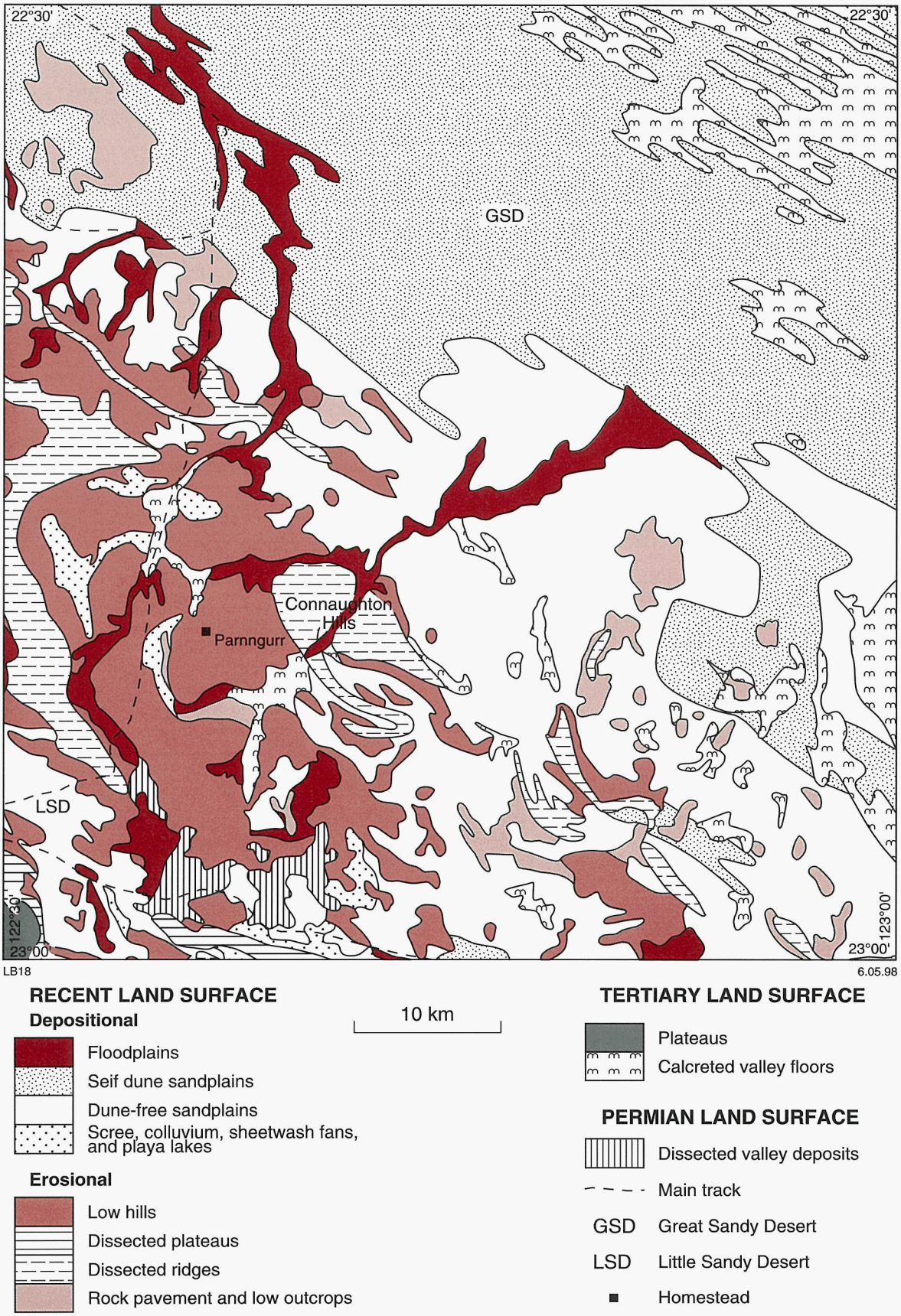

Figure 2. Physiography and main access on CONNAUGHTON

subdued landscape of adjoining divisions. Hickman and Clarke (1994) and Hickman and Bagas (in prep.) noted that the duricrust was the main barrier to erosion of the arenite.

The Connaughton Hills include dissected and, in part, sinuous quartzite ridges rising to about 450 m above sea level, separated by valleys developed over less-resistant metapelite and psammitic units. The valleys are locally filled by a thin Permian cover, establishing a pre-Permian origin for some of these narrow valleys; these areas are too small to represent on Figure 2. The ridges are bevelled to a height of about 400 m above sea level in the western part of CONNAUGHTON.

The southwestern part of CONNAUGHTON has large expanses of low hills subjected to active erosion by headwater systems, and constitutes a dissected low-lying peneplain that varies from rounded to more rugged and quartz-strewn. The rock types present influence the form of the hills — orthogneiss and paragneiss characteristically produce rounded hills and quartzite produces more-rugged country.

Rock pavements and low outcrops are mainly found in sandplain country in the central and northern parts of CONNAUGHTON, but are also found as small areas within the low hills. Erosion is restricted to wind action and water movement in small streams, and represents the last stage in the formation of a new peneplain.

Recent depositional land surface

Sandplains have been subdivided into seif dune and dune-free sandplains, which collectively are found over at least half of CONNAUGHTON. The northern part of CONNAUGHTON includes the western edge of the Great Sandy Desert. The seif (longitudinal) dune sandplains include easterly to southeasterly trending seif dunes that reach a maximum height of 30 m, are many kilometres long, and spaced up to 3 km apart. Their longitudinal profiles and steep southern slopes are consistent with prevailing winds from the east-southeast. Further descriptions of seif dunes are provided by Crowe (1975).

The dune-free sandplains are found in areas subjected to periodic flooding, and on the leeward sides of hills. The Rudall River has incised its former Tertiary drainage course, which is outlined by consolidated river gravel covered by recent alluvium.

The scree, colluvium, sheetwash fans, and playa lakes commonly flank sandplains and represent locally derived clastic detritus from streams and channels draining hilly divisions. Some of these deposits are dissected by the present drainage.

Precambrian geology

CONNAUGHTON occupies part of the Paterson Orogen (Williams and Myers, 1990), which was previously referred to as the Paterson Province (Daniels and Horwitz, 1969; Blockley and de la Hunty, 1975), and includes local outliers of Permian sedimentary rocks of the Canning Basin (Fig. 1).

The term Paterson Orogen is applied to a northwesterly trending belt of folded and metamorphosed sedimentary and igneous rocks, ranging in age from Palaeoproterozoic to Neoproterozoic, that have a common tectonic history (Williams and Myers, 1990). Archaean rocks of the Pilbara and Yilgarn Cratons flank the Paterson Orogen to the west and southwest respectively (Fig. 1).

There are three subdivisions of the Paterson Orogen on CONNAUGHTON: the Rudall Complex, Yeneena Supergroup, and Tarcunyah Group (Williams and Bagas, in prep.). The Yeneena Supergroup is a redefinition of the 'Yeneena Group' of Williams et al. (1976), and comprises the Throssell and Lamil Groups (Williams and Bagas, in prep.). The Karara Formation, previously regarded as younger than the 'Yeneena Group', is included in the Tarcunyah Group, which is now assigned to the Officer Basin (Bagas et al., 1995) rather than the 'Western Succession of the Yeneena Group' (Williams, 1990).

The term 'Rudall Complex' is restricted to Palaeoproterozoic rocks that have been deformed and metamorphosed by the 'Yapungku Orogeny' (see **Structure**). Igneous rocks that are younger than this orogeny, but probably older than the Yeneena Supergroup, have not been assigned to a group.

The Rudall Complex is situated between the West Australian and North Australian Cratons (Myers et al., 1996). The relationship between the complex and the West Australian Craton (consisting of the Yilgarn and Pilbara Cratons) is obscured by sedimentary rocks of the Throssell Group (of the Yeneena Supergroup), the Tarcunyah and Savory Groups, and the Earaheedy and Bangemall Basins (Fig. 1). Cover sequences of the Canning and Officer Basins obscure the relationship between the Paterson Orogen and the Precambrian North Australian Craton to the east (Fig. 1).

The early Rudall basin possibly trended north–south, and probably developed as a rift-basin on the eastern margin of the Pilbara Craton, after the rifting and fragmentation of Archaean continents (Myers et al., 1996).

Rudall Complex

The Rudall Complex (Williams, 1990) consists of a broad imbricate zone of northeasterly and easterly dipping thrust sheets, with cross-cutting relationships that indicate progressively younger thrusts towards the east. Some of the thrusts are major faults separating distinct tectonostratigraphic domains (Hickman and Bagas, in prep.).

The Rudall Complex outcrops in the southwestern part of CONNAUGHTON. The complex is divided into two distinct, tectonically juxtaposed packages of rocks containing foliated augen orthogneiss. The two packages are referred to as the Talbot Terrane (after

H. W. B. Talbot, an earlier explorer of the Rudall region) and the Connaughton Terrane (after the Connaughton Hills).

The rocks in the Talbot Terrane are principally siliciclastic sedimentary rocks and granitoids, metamorphosed to amphibolite facies. Similar rocks are also found in the Rudall Complex on BROADHURST and RUDALL (Hickman and Bagas, in prep.). The Connaughton Terrane comprises a succession of mafic volcanic and intrusive rocks, banded iron-formation, pelite, chert, felsic gneiss (including augen orthogneiss), minor amounts of quartzite, and ultramafic intrusive rocks, all metamorphosed to amphibolite–granulite facies. The terrane extends into the Camel Domain of northeastern RUDALL (Hickman and Bagas, in prep.).

A third, possibly exotic, terrane — the Tabletop Terrane — has been identified east of the southeasterly trending Camel–Tabletop Fault Zone. The fault separates the Tabletop Terrane from the Talbot and Connaughton Terranes. The Tabletop Terrane contains voluminous granitoids, dolerite dykes, and possibly felsic volcanic rocks dated at c. 1300 Ma by PNC Exploration (Smithies and Bagas, 1997). This magmatic event was partly contemporaneous with a major orogenic event that occurred in the Albany–Fraser Orogen between 1300 and 1100 Ma (Myers, 1990b).

Most rocks of the Rudall Complex have undergone retrogressive metamorphism to greenschist facies, characterized by the following minerals: epidote, actinolite, albite, quartz, chlorite, sericite, and calcite. To avoid lengthy petrographic descriptions, only the higher grade mineral assemblages and important retrogressive assemblages will be discussed.

Connaughton Terrane

The tectonic setting of the Connaughton Terrane is difficult to interpret because of the discontinuous nature of the rocks, the structural complexity, pervasive recrystallization, and a general lack of primary sedimentary and igneous features. Metavolcanic rocks are predominantly high-iron tholeiites in composition (Appendix 1). In the lower part of the succession the metavolcanic rocks are intimately interlayered with metamorphosed chemical sedimentary rocks (e.g. banded iron-formation and calc-silicate or carbonate rocks) and shale. In the upper part they are interlayered with mixed clastic sedimentary rocks. The contact between the metavolcanic and clastic rocks is tectonically disrupted to such a degree that it is impossible to accurately establish stratigraphic relationships. There appears to be, however, a tendency for the sedimentary rocks associated with the metavolcanic rocks to coarsen upward. The top and base of the Connaughton Terrane succession are not exposed.

Basalt and chemical and clastic sedimentary rocks were deposited in the Connaughton Terrane prior to 1780 Ma. The succession indicates extensive exhalative activity associated with mafic volcanism in either a shallow-water restricted continental basin or a deep-water outer continental-shelf environment characterized by near-saturation levels of iron, silica, and carbonate.

The term amphibolite is used here to describe recrystallized medium-to coarse-grained amphibole- and plagioclase-rich rocks in which no igneous textures are preserved. Mafic granulite, which is subordinate to the amphibolite, is characterized by the presence of brown hornblende and orthopyroxene.

Garnet amphibolite (PRag)

Medium- to coarse-grained garnet amphibolite (*PRag*) is common in and around the South Rudall Dome, and in the Connaughton Synform where it is associated with banded iron-formation, graphitic and sulfidic schist, and lesser amounts of quartzite and calc-silicate or carbonate rocks. In the Harbutt Range small outcrops of non-garnetiferous amphibolite (*PRam*) have discontinuous layers or lenses of garnet amphibolite.

The garnet amphibolite appears to be conformably overlain by a quartz–magnetite banded iron-formation (*PRi*) that is, in turn, overlain by a succession of silicified carbonate rock (*PRk*); quartz–sericite–graphite–chloritic–magnetite–carbonate schist (after calcareous black shale); quartz–feldspar–biotite gneiss (*PRnm*); quartzite, possibly after chert (*PRq*); banded iron-formation (*PRi*); and garnetiferous amphibolite. The banded iron-formation is gossanous in places, indicating that it may include sulfidic horizons.

Garnet amphibolite locally shows distinct centimetre-scale banding due to metamorphic segregation of amphibole-rich and plagioclase-rich layers (Fig. 3). In rare cases (GSWA 113016, AMG 562674; GSWA 113019, AMG 572676; and GSWA 113095, AMG 682664), garnet cores preserve sigmoidal trains of fine-grained epidote, hornblende, and titanite representing an early foliation (Fig. 4).

Garnet amphibolite contains abundant hornblende and plagioclase (andesine), a maximum of 20% quartz, and is characterized by subrounded to prismatic garnet porphyroblasts with a maximum diameter of 5 mm. Clinopyroxene (diopside) is preserved in the South Rudall Dome and Connaughton Synform areas (GSWA 112980, AMG 572694; and GSWA 113088, AMG 670655). Accessory minerals include titanite, magnetite (leucoxene), rutile, apatite, and secondary epidote, calcite, and sericite. In more foliated samples, hornblende wraps around garnet and diopside porphyroblasts, defining an early shear foliation, but no reaction relationship has been observed between garnet, clinopyroxene, and hornblende.

Clinopyroxene and quartz-bearing amphibolite (PRam)

Clinopyroxene and quartz-bearing amphibolite (*PRam*) is a common, medium-grained rock type in the Harbutt Range, where it is interlayered with thin units of garnetiferous amphibolite, felsic orthogneiss, quartz–biotite(–muscovite) schist, and quartzite. In the

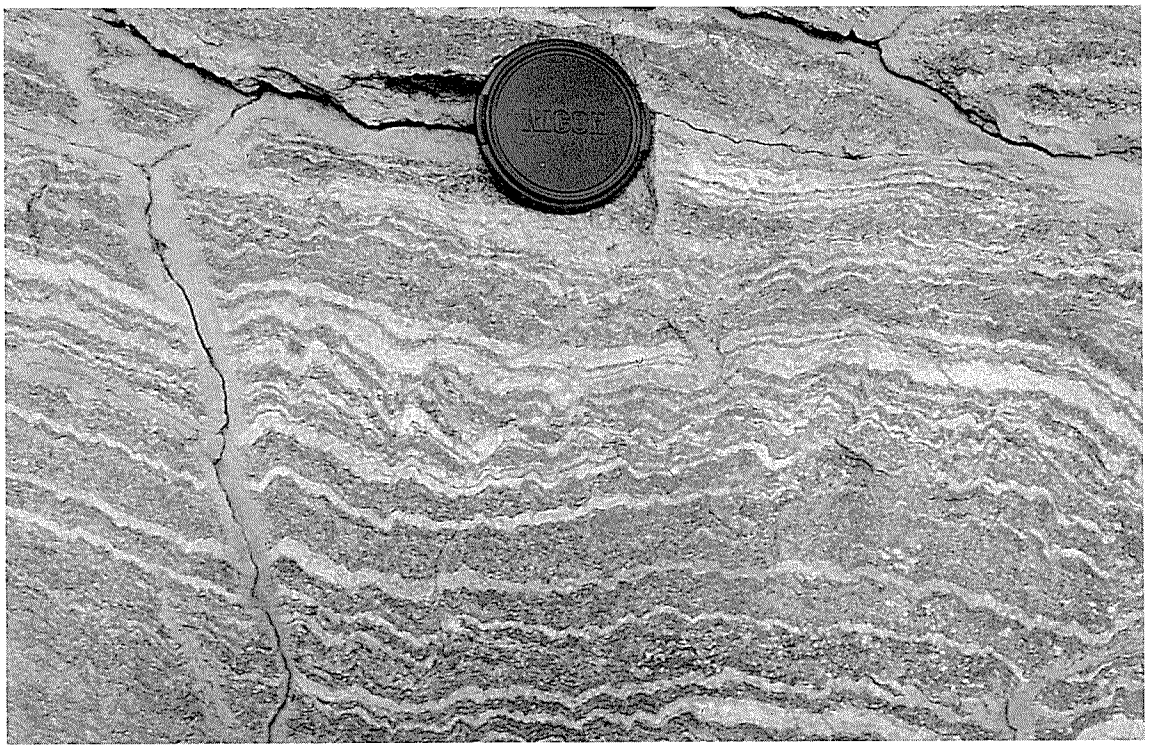

LB 85 28.04.98

Figure 3. Centimetre-scale banding in garnet amphibolite (*PRag*), showing metamorphic segregation of amphibolite-rich and plagioclase-rich layers (AMG 588743)

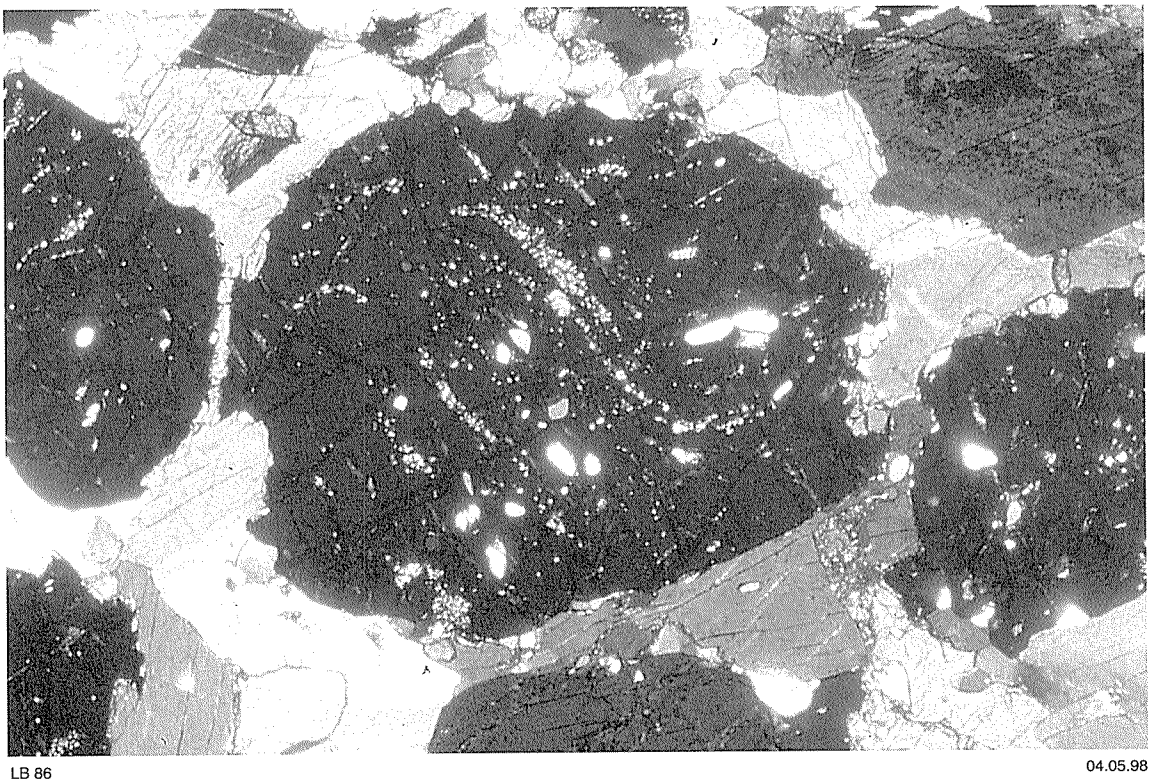

LB 86 04.05.98

Figure 4. Garnet porphyroblasts in GSWA sample 113016 (AMG 562674). Cores preserve sigmoidal trains of fine-grained epidote, hornblende, and titanite representing S_1, which is oblique to S_2 defined by hornblende and plagioclase . The garnet porphyroblast is 0.2 mm in diameter

Connaughton Synform minor outcrops of medium-grained amphibolite are associated with major shear zones and faults, and interlayered with quartzite and orthogneiss.

The amphibolite is very well foliated and locally shows distinct centimetre-scale layering due to metamorphic segregation of amphibole-rich and amphibole-poor layers. Plagioclase (andesine) and hornblende are the main constituents. The amount of quartz varies between 5 and 20%, and may be partly the product of extensive retrogressive alteration of plagioclase to epidote. Accessory minerals include titanite, apatite, magnetite (or leucoxene), rutile, biotite, and zircon.

Although clearly mafic in composition, the protolith of this rock is unclear. Some samples of the amphibolite may represent sheared and retrogressed garnet amphibolite; the least quartz-rich samples have compositions very similar to the garnet amphibolite (Appendix 1). However, the abundance of quartz in other samples (GSWA 115729, AMG 574043; and GSWA 115840, AMG 818665) indicates that the protolith may have locally included immature sediments.

Both garnet amphibolite and medium-grained amphibolite show signs of migmatization. Felsic leucosomes form irregular, discontinuous segregations and, in extreme cases, dyke-like bodies up to 1 m thick are found. The leucosomes show the same structural fabrics as their mafic hosts, and chemical analyses (GSWA 115854; Appendix 1) show them to be trondhjemite.

Fine-grained amphibolite (*PRab*)

Fine-grained amphibolite (*PRab*) outcrops 9 km north and on the eastern side of South Rudall Dome. At the former locality it is interlayered with minor amounts of chert (*PRic*), quartz–mica schist (*PRm*), and quartzite (*PRq*); at the latter locality it forms a thin layer within K-feldspar augen orthogneiss (*PRga*) and is locally epidotized (*PRae*). The rock is a recrystallized and highly foliated metabasalt consisting of fine-grained hornblende (altered to actinolite) in a very fine grained matrix of quartz and plagioclase (altered to epidote and carbonate), with accessory magnetite, epidote, carbonate, and rare relict garnet. Outcrops north of South Rudall Dome are tectonically attenuated and bound by layer-parallel faults that have been folded and faulted (see **Structure**). Xenoliths of fine-grained amphibolite are locally preserved in K-feldspar augen orthogneiss (e.g. AMG 592841), indicating that the granite precursor to the orthogneiss intruded the protolith to the amphibolite.

Orthopyroxene and clinopyroxene-bearing amphibolite (*PRac*)

Medium- to coarse-grained, orthopyroxene- and clinopyroxene-bearing amphibolite (*PRac*) outcrops northeast of Harbutt Range, east of Mount Eva, and west of Camel Rock as thin elongate pods or lenses in gneiss (usually *PRng*), or interlayered with ironstone and chert. The amphibolite is usually equigranular, well foliated to massive, and has a well-developed granoblastic texture. Amphibole (brown hornblende) and lesser amounts of plagioclase (andesine) comprise 90–95% of the rock, and are accompanied by minor amounts of clinopyroxene (diopside) and orthopyroxene (hypersthene), and accessory quartz, magnetite, titanite, and rutile. Amphibolite, containing green hornblende and lacking orthopyroxene, forms dyke-like bodies within the brown hornblende-bearing variety and is present as inclusions in leucogabbro–anorthosite (*PRan*, see below).

Coarse-grained leucocratic amphibolite (*PRan*)

Leucocratic, very coarse to coarse-grained amphibolite (*PRan*) is derived from protoliths ranging from leucogabbro to anorthosite. The amphibolite outcrops south of Harbutt Range and there are two small outcrops about 6 km south and 5 km west of Camel Rock. Coarse leucocratic amphibolite is commonly massive, but has a well-developed foliation in places. South of Harbutt Range (AMG 829604), a small outcrop of well-foliated medium-grained amphibolite appears to be cross-cut and enclosed by non-foliated coarse leucocratic amphibolite. This relationship either indicates that some outcrops of coarse leucocratic amphibolite may be younger than the medium-grained amphibolite, or that coarse leucocratic amphibolite was considerably more competent than medium-grained amphibolite during deformation. Coarse leucocratic amphibolite commonly preserves igneous textures defined by interstitial clinopyroxene (now altered to actinolite and rarely to hornblende) in a framework of plagioclase (anorthite to bytownite) euhedra. Plagioclase comprises between 60 (leucogabbro) and 90% (anorthosite) of the rock. Accessory minerals include titanite, apatite, and magnetite (leucoxene).

Garnet amphibolite interleaved with granitic gneiss (*PRao*)

Garnet amphibolite with minor interlayers of compositionally banded orthogneiss (*PRao*) is present in the southwestern part of Connaughton and southeast of South Rudall Dome. This unit is lithologically similar to the compositionally layered orthogneiss (*PRgo*) except that it has a greater proportion of amphibolite. Both units are hybrids of the orthogneiss and garnet amphibolite.

Fine-grained amphibolite and schist (*PRae*)

Fine- to medium-grained quartz–epidote(–hornblende–actinolite–biotite–sericite) amphibolite and schist (*PRae*) outcrop about 5 km southwest of Harbutt Range and east of South Rudall Dome. The unit is always in contact with orthogneiss (*PRga* and *PRgo*), and forms prominent outcrops parallel to the structural trend of the area. Mineral proportions vary widely from a maximum of 75% quartz to 70% epidote. In thin section, relic domains comprising plagioclase and hornblende indicate that the rock may be a silicified and epidotized garnet amphibolite (*PRag*) or medium-grained amphibolite (*PRam*). In places millimetre- to centimetre-scale mineralogical banding is defined by alternating layers rich in quartz, biotite, epidote, and rarely, hornblende. The fine-grained gneiss and schist is commonly well

foliated, but is massive and banded with well-developed polygonal textures in places.

Ultramafic rock (PRu)

Medium-grained serpentine–tremolite–magnetite-bearing rocks (*PRu*) are locally foliated, but commonly preserve olivine cumulate textures that identify their protoliths as either dunite or peridotite. Ultramafic rocks are most abundant about 4 km east of Mount Eva and throughout the Harbutt Range, where discontinuous layers up to 5 km long outcrop within amphibolite and metasedimentary rocks. In the Camel Rock area lenticular pods of ultramafic rocks, commonly less than 200 m wide, outcrop in orthogneiss. A small isolated outcrop of ultramafic schist is present on the eastern side of the Connaughton Synform near a major late fault.

Metamorphosed banded iron-formation (PRi)

Metamorphosed banded iron-formation (*PRi*) is the most abundant rock type in the Connaughton Synform and South Rudall Dome areas. The banded iron-formation in the South Rudall Dome area is commonly interlayered with garnet amphibolite (*PRag*), except at the dome itself, where it structurally overlies garnet amphibolite and is overlain by a very thin unit of calc-silicate or carbonate rock (*PRk*). In the Connaughton Synform the banded iron-formation is interlayered with garnet amphibolite, and overlain by a succession of interlayered calc-silicate rock, orthoquartzite (*PRq*), micaceous quartzite (*PRqm*), garnet amphibolite, and medium-grained amphibolite. Banded iron-formation in the northwestern corner of CONNAUGHTON outcrops near garnet gneiss (*PRng*), biotite gneiss (*PRnm*), and amphibolite (*PRac*). A similar outcrop of banded iron-formation immediately to the west, on RUDALL, forms an enclave in orthogneiss (Hickman and Bagas, in prep.).

Banded iron-formation is fine to medium grained, finely laminated, and consists of recrystallized quartz, aligned magnetite, accessory muscovite, about 2% apatite, and rare light-green amphibole, relict garnet, and epidote. Some iron oxides may pseudomorph amphibole, which is probably grunerite. The rock also contains sericite-rich patches, possibly after feldspar. The laminations commonly define a pervasive early foliation, and primary surfaces have not survived recrystallization, except in samples west of Camel Rock where original layering is typically on a centimetre scale. The present grain size does not reflect the protolith grain size, as indicated by the very fine sand- to silt-sized quartz and iron oxide grains preserved in garnet cores (e.g. GSWA 117773, AMG 662793). These cores are rimmed by a second growth of inclusion-free garnet associated with M_2 metamorphism, similar to that observed in the garnet amphibolite.

Metamorphosed chert and banded iron-formation (PRic)

Outcrops of quartzite (after chert) and lesser banded iron-formation (*PRic*) are found throughout the Harbutt Range, to the east of Mount Eva, and in the South Rudall Dome – Connaughton Synform area. The unit commonly forms prominent outcrops interlayered and folded with mafic schist and gneiss and micaceous quartzite, except in the far northwestern part of CONNAUGHTON where metamorphosed chert forms enclaves within gneiss (*PRnm*). The unit is mineralogically diverse, ranging from pure chert to quartz–magnetite rock, although the dominant rock type is a ferruginous chert variously comprising quartz–magnetite–garnet–diopside–grunerite(–pseudomorphed apatite).

Metamorphosed graphitic sulfidic schist (PRir)

Metamorphosed graphitic and sulfidic schist thinly interlayered with quartz–mica–garnet schist, amphibolitic schist, and minor amounts of chert and quartz–carbonate rock (*PRir*) outcrop at Mount Cotton. The rocks are extensively recrystallized and commonly chloritized, silicified, and carbonated. They are interpreted as metamorphosed and metasomatized successions of sulfidic black shale, chemical sedimentary rocks (banded iron-formation), and sedimentary rocks derived from mafic volcanic rocks.

The graphitic schist is very fine grained and consists of quartz, mica (sericite and biotite), chlorite, graphite, and disseminated sulfides (pyrrhotite, pyrite, chalcopyrite, sphalerite, and galena). The quartz–mica–garnet schist is very fine grained and comprises chloritized biotite, opaque minerals, sericite, remnant porphyroblasts of sericitized and chloritized garnet, and rare dolomite. The amphibolitic schist is fine grained and comprises hornblende (?after pyroxene)–actinolite(–epidote–quartz–biotite) sulfide schist, amphibole (anthophyllite–cummingtonite)–graphite–biotite(–quartz–sericite) sulfide schist, quartz–hornblende–epidote sulfide schist, and clinopyroxene(–orthopyroxene)–quartz–garnet–biotite(–dolomite) sulfide schist. The quartz–carbonate rock is very fine grained and consists of carbonate, quartz, sulfides (pyrrhotite, pyrite, chalcopyrite, galena, and sphalerite), and variable amounts of sericite and graphite.

These mineral assemblages reflect metamorphism at the amphibolite–granulite facies transition (see **Metamorphism**). The presence of carbonate (dolomite and ankerite), sericite, sulfides, chlorite, and epidote possibly indicate a later metasomatic alteration at greenschist facies. The sulfides also fill fractures as veins parallel to the early foliation in the rocks.

Calc-silicate or carbonate rock (PRk)

The calc-silicate or metamorphosed carbonate rock (*PRk*) unit outcrops as a thin horizon immediately above banded iron-formation in the Rudall Dome. The unit is less than 20 m thick, poorly exposed, and heavily silicified.

Mica schist (PRm)

Fine- to medium-grained quartz–biotite–muscovite(–Fe-oxide–tourmaline–garnet–K-feldspar) schist (*PRm*) outcrops south of Harbutt Range and about 10 km northeast of South Rudall Dome. South of Harbutt

Range the unit is interleaved with medium-grained amphibolite (*PRam*) and infolded with orthogneiss. North of South Rudall Dome, the schist is interlayered with quartzite (*PRq*) and fine-grained amphibolite (*PRab*). The protolith is an argillaceous sedimentary rock, possibly incorporating a minor, locally derived mafic component.

Quartzite (PRq) and micaceous quartzite (PRqm)

The quartzite (*PRq*) consists of a recrystallized fine-grained quartz mosaic with rare thin bands containing amphibole (tremolite) and carbonate. The protolith was either a chert or a fine-grained, pure quartz arenite. Micaceous quartzite (*PRqm*) consists of recrystallized quartz and muscovite with variable amounts of sericite and opaque minerals.

Quartzofeldpathic gneiss and schist of uncertain protolith

The mineralogy of some quartzofeldspathic gneiss and schist is not consistent with derivation from an igneous protolith. Other samples are sheared or recrystallized to the extent that their protolith cannot be recognized. In many outcrops, however, these rocks are associated with various orthogneisses.

Medium-grained biotite gneiss (PRnb)

Medium-grained quartz–feldspar–biotite(–muscovite) gneiss (*PRnb*) outcrops near Mount Eva, about 8 km west and 5 km southwest of Mount Eva, and about 5 km south of the Connaughton Synform. At the first two localities, the gneiss is wedged between quartzite and augen orthogneiss. The proportion of quartz roughly correlates with the degree of shearing and decreases from 60% to about 30% close to the augen orthogneiss. The more highly sheared rocks are muscovite rich, but biotite becomes the dominant mica in less sheared rocks. Medium-grained biotite gneiss west of Camel Rock is closely associated with garnetiferous gneiss (*PRng*, see below), rather than augen orthogneiss. Likewise, medium-grained biotite gneiss south of the Connaughton Synform is wedged between quartzite (*PRq*) and garnet amphibolite (*PRag*).

Microcline gneiss (PRnm)

A microcline-rich gneiss (*PRnm*) outcrops 5 km northeast of Harbutt Range and 5 km east of Mount Eva, and is associated with garnet gneiss (*PRng*). The rock is medium grained, equigranular, and commonly shows a well-developed polygonal (granoblastic) texture. Biotite is the only mafic mineral. The amount of quartz varies up to a maximum of 40%, and the feldspar is dominantly microcline with plagioclase comprising less than 10% of the feldspar.

Charnockite (PRnc)

Charnockite (*PRnc*) outcrops about 6 km northeast of Harbutt Range and is a fine- to medium-grained quartz–microcline–plagioclase–garnet–clinopyroxene (–hypersthene)–spinel–biotite gneiss. Discontinuous 10–20 mm-thick bands show variations in grain size. Discontinuous trails of garnet and hypersthene show a preference for the medium-grained bands and accentuate the gneissic fabric of the rock. Hypersthene and garnet are altered to actinolite and biotite respectively. Where only garnet remains, the rock closely resembles garnet gneiss (*PRng*). Both charnockite and garnet gneiss have peraluminous compositions (Appendix 1), and it is possible that these rocks are metamorphosed immature sedimentary rocks of a granitic provenance.

Garnet gneiss (PRng)

The garnet gneiss (*PRng*) is medium grained, equigranular, and commonly rich in biotite and feldspar. Discontinuous biotite-rich layers, or schlieren, are common and complexly folded. Small subhedral grains of garnet are distributed throughout the rock, usually as an accessory or minor phase, although some samples are garnet rich. Accessory phases include zircon, titanite, allanite, apatite, and opaque minerals. The felsic mineralogy may be consistent with derivation from igneous protoliths ranging in composition from granodioritic to granitic; however, the abundance of garnet in many samples may reflect a sedimentary origin.

Mylonite (PRns)

Mylonitic quartz–sericite(–K-feldspar–muscovite–biotite) schist outcrops west of the Camel–Tabletop Fault Zone. Early fabrics are destroyed by intense cataclasis, which has granulated the quartz and sericitized feldspar and biotite.

Talbot Terrane

The Talbot Terrane consists of a succession of siliciclastic rocks that are complexly interleaved and further complicated by thrusting during early deformation (the Yapungku Orogeny). Hickman and Bagas (1994) proposed a stratigraphy for the Talbot Terrane. On RUDALL, the rock types and changes in facies and thickness indicate that sedimentary rocks were deposited in a deep-water basin oriented in a north–south or northwest–southeast direction along a continental margin (Hickman and Bagas, 1994). The succession may have been deposited in a subsiding rift-basin along the eastern margin of the Pilbara Craton, analogous to the Bryah, Yerrida, Ashburton, and Earaheedy Basins of the Capricorn Orogen (Thorne and Seymour, 1991; Pirajno et al., 1996). The sedimentary rocks were intruded by a range of granitoids (now banded orthogneiss — *PRgx*) between 2015 and 1802 Ma (Nelson, 1995).

The basement to the Talbot Terrane is Archaean to early Palaeoproterozoic in age and may include part of the Connaughton Terrane. Xenocrystic zircons from a sedimentary component in banded orthogneiss (*PRgx*) on RUDALL have given Sensitive High-Resolution Ion Microprobe (SHRIMP) U–Pb ages of 2715–2577 Ma (Nelson, 1995).

Psammitic paragneiss (ERs)

Psammitic paragneiss (*ERs*) consists of quartz–feldspar–muscovite(–biotite) gneiss with minor amounts of quartz–mica schist and quartzite. The unit represents metamorphosed sandstone and subordinate argillaceous siltstone, and mainly outcrops in the northwestern part of CONNAUGHTON (AMG 486951). Rare, compositionally layered, rhythmic units less than 1 m thick are composed of a lower feldspathic quartzite grading upward into plagioclase–quartz–mica paragneiss, and overlain by a 0.1 m-thick layer of biotite–epidote–quartz microgneiss. These rhythmic units are possibly metamorphosed graded beds of a turbidite succession.

Banded paragneiss (ERb)

Banded paragneiss (*ERb*) outcrops in the Connaughton Hills in the western part of CONNAUGHTON, and is the eastward extension of the Butler Creek Formation defined on RUDALL (Hickman and Bagas, in prep.). The paragneiss consists of finely interlayered and metamorphosed shale, argillaceous quartzite, feldspathic greywacke, and rare banded iron-formation or sulfidic shale, which form bands up to 2 m thick. Close to a major early fault at AMG 548860, the unit contains thin, tectonically interleaved, fine-grained amphibolite (*ERab*). The pelitic units contain quartz, biotite, muscovite or sericite, secondary chlorite, and minor amounts of plagioclase. The metagreywacke is fine to medium grained and contains quartz, muscovite, minor amounts of biotite, microcline, albite, and secondary sericite. The argillaceous quartzite is fine to medium grained, and contains quartz, minor amounts of biotite and sericite, and accessory tourmaline. The metamorphosed banded iron-formation consists of iron oxides, quartz, minor amounts of sericite, and rare garnet. The relative proportions of these rock types vary. The banded paragneiss is interpreted to represent a turbidite sequence with a source area dominated by felsic igneous rocks.

The banded paragneiss is complexly folded and faulted. During deformation it formed an incompetent layer, and its contacts with other units are commonly tectonic. At and around AMG 500750, the banded paragneiss structurally overlies and is tectonically interleaved with K-feldspar augen orthogneiss (*ERga*), and is structurally overlain by quartzite (*ERq*).

Quartzite (ERq)

Quartzite (*ERq*) is either massive or compositionally layered, with a pervasive foliation defined by recrystallized quartz grains. The unit consists of fine- to medium-grained recrystallized quartz and various proportions of sericite, muscovite, opaque minerals, and rutile. Quartzite in the Connaughton Hills includes very thin intercalations of quartz–muscovite schist and structurally overlies banded paragneiss.

Quartz–aluminosilicate schist (ERqa)

Medium-grained quartz–aluminosilicate schist (*ERqa*) is a general term used for sillimanite- or kyanite-rich metasedimentary rocks, which are rare. These include quartz–garnet–sillimanite–feldspar schist east of Mount Eva and quartz–kyanite–ilmenite(–sillimanite) schist southeast and southwest of Mount Eva. The former comprises anhedral porphyroblasts of garnet and prismatic sillimanite in a medium-grained, well-foliated groundmass of quartz, microcline, and plagioclase. The porphyroblasts overprint the groundmass foliation and contain inclusions of quartz, spinel, and sillimanite. The kyanite-bearing rocks vary from well foliated to massive. Kyanite and ilmenite form anhedral porphyroblasts in a granoblastic quartz-rich matrix, but in well-foliated samples, kyanite and ilmenite are stretched out along the foliation. Sillimanite is a minor component of some samples and is present as randomly orientated fibrolite in and around kyanite.

Orthogneiss

About half of the Rudall Complex on CONNAUGHTON is composed of orthogneiss. About half of the orthogneiss comprises microcline–quartz–plagioclase–biotite(–muscovite) gneiss (*ERga*) containing numerous augen (deformed megacrysts) of K-feldspar.

K-feldspar augen orthogneiss (ERga)

The K-feldspar augen orthogneiss (*ERga*) is the only orthogneiss that outcrops in both the Connaughton and Talbot Terranes. Typically it shows a strong foliation defined by the alignment of mica; in rare cases, it is weakly foliated (e.g. AMG 565784). Microcline augen are often stretched out within the foliation plane, and are sometimes recognizable only as spindles of granular microcline. The strong mineral fabrics are the result of an early deformation event (D_2). No earlier deformation event (D_1) is evident. The protoliths to the augen orthogneiss were mainly porphyritic biotite monzogranite and biotite granite. Minor and accessory minerals include zircon, garnet, titanite, allanite, apatite, and opaque minerals. K-feldspar augen orthogneiss (*ERga*) locally contains xenoliths of amphibolite (e.g. AMG 592842).

On RUDALL and CONNAUGHTON, SHRIMP U–Pb zircon dates of 1790 ± 17, 1787 ± 5, 1769 ± 7, and 1765 ± 15 Ma have been obtained from four samples of the K-feldspar augen orthogneiss collected at four localities up to 40 km apart (Nelson, 1995, 1996). The two older dates are from highly foliated orthogneiss, and the other two dates are from moderately foliated orthogneiss. The correlation between decreasing intensity of foliation and decreasing age of the augen orthogneiss possibly indicates that the augen orthogneiss was pre- to syn-D_2, and that D_2 has a maximum age of c. 1790 Ma. The 1790 ± 17 Ma age, however, was from a sample containing six populations of zircons. The youngest population gave an age of 1790 ± 17 Ma and this is interpreted as the crystallization age of the orthogneiss protolith. The older zircon populations gave ages that reach a maximum of 2425 ± 7 Ma, and are interpreted to be xenocrystic.

The augen orthogneiss (*ERga*), more than any other group of felsic gneisses, forms a compositionally coherent group, despite an intrusive age range of 1790 to 1765 Ma. This implies episodic melting of a relatively compositionally homogeneous source region. This orthogneiss is not restricted to the Talbot Terrane of the Rudall Complex, but also outcrops in the Connaughton Terrane, and it is likely that the source had a regional extent.

Banded orthogneiss (ERgo)

Banded orthogneiss (*ERgo*) outcrops in the southwestern part of CONNAUGHTON and forms sheets within garnet amphibolite and medium-grained amphibolite, or large bodies that enclose and are interleaved with lenses of amphibolite and quartzite. The orthogneiss is commonly conspicuously banded, both in outcrop and on aerial photographs. Thin layers of quartz–feldspar–muscovite gneiss alternate with biotite-rich gneiss, quartz–feldspar gneiss, and gneissic pegmatite. The composition of the gneiss ranges from granite to granodiorite. Numerous inclusions of amphibolite and quartzite range from centimetre scale to lenses several hundred metres long.

Chin and de Laeter (1981) published a Rb–Sr date of 1333 ± 44 Ma for retrograded gneiss (their 48929 series). They suggested that the date represented the age of pervasive metamorphism of the Rudall Complex (our M_2 event, see **Metamorphism**). The rocks sampled are located between the foliated granite (*Pge*) and the Throssell Group in the southern part of CONNAUGHTON, and are apparently from an outcrop of banded orthogneiss (*ERgo*) intruded by thin granitoid dykes. About 4 km north of the sample site, the gneiss is intruded by the foliated granite to monzogranite, which contains amphibolite xenoliths and is affected by a late deformation event (D_4), but is not affected by earlier deformation events (D_2, see **Structure**). A sample of the compositionally banded orthogneiss has a SHRIMP age of 1777 ± 7 Ma (GSWA 113035, AMG 603680). This age is interpreted as the crystallization age for the orthogneiss protolith (Nelson, 1996). The geological significance of the 1333 ± 44 Ma age is therefore uncertain: it may be the approximate age for the D_4 event and associated metamorphism (M_4) in the southern part of CONNAUGHTON; the age of the foliated granite; or a meaningless composite age of the orthogneiss modified by M_4 metamorphism.

Amphibole-bearing orthogneiss (ERgh)

In Harbutt Range and northwest of Camel Rock, amphibole-bearing orthogneiss (*ERgh*) is present as sheets within amphibolite or as larger bodies enclosing blocks of amphibolite (*ERac*), ultramafic rock (*ERu*), and chert (*ERic*).

The orthogneiss (*ERgh*) differs from the banded orthogneiss (*ERgo*) in that hornblende forms a primary constituent. The gneiss is medium grained, equigranular, and commonly well foliated. Plagioclase is the dominant feldspar and biotite the dominant mafic mineral. Hornblende is commonly rimmed by biotite, and appears to decrease in abundance with increasing abundance of alkali feldspar. Accessory minerals include zircon, allanite, titanite, and apatite. Although the gneiss shows obvious signs of recrystallization (particularly of quartz), granoblastic textures typical of K-feldspar augen orthogneiss are not observed, and it is probable that the amphibole-bearing orthogneiss has not been metamorphosed higher than upper greenschist facies. The protolith to amphibole-bearing orthogneiss ranged from granodiorite to monzogranite.

Mica orthogneiss (ERgm)

Biotite–muscovite orthogneiss (*ERgm*) with a monzogranitic composition outcrops north of the Connaughton Synform (AMG 624815). The rock is a fine- to medium-grained, equigranular to slightly porphyritic, homogeneous gneiss interlayered with the K-feldspar augen orthogneiss.

Late intrusive rocks

Late intrusive rocks are restricted to the Connaughton Terrane.

Medium-grained foliated granite (Pge)

Non-porphyritic to slightly porphyritic, equigranular, medium-grained granite to monzogranite (*Pge*) is a minor constituent of the Rudall Complex on CONNAUGHTON. The unit outcrops east of South Rudall Dome (AMG 617688). The monzogranite is massive to weakly foliated, contains angular amphibolite xenoliths of various sizes, and consists of quartz, microcline, oligoclase, muscovite, biotite, and rare garnet. The unit forms a semi-circular outcrop with a diameter of less than 2 km, and appears to intrude the banded orthogneiss (*ERgo*), K-feldspar augen orthogneiss (*ERga*), and amphibolite (*ERao*). The monzogranite is affected by the D_4 event (see **Structure**), and its intrusive age may be post-D_2.

Massive to weakly foliated granitoid (Pgf, Pgl, Pgm, Pgp)

Massive to weakly foliated leucocratic granitoids comprise porphyritic (*Pgf*), equigranular (*Pgl*), or megacrystic (*Pgm*) rocks, or pegmatite (*Pgp*). Although these rocks show some signs of recrystallization, particularly of quartz, igneous textures are commonly preserved and granoblastic textures, typical of many samples of the K-feldspar augen orthogneiss, are not observed. It is probable that the rocks have not been metamorphosed higher than upper greenschist facies (M_4, see **Metamorphism**). Intrusions of the equigranular granite and pegmatite cross-cut D_2 fabrics. Porphyritic granitoid is confined to a zone west of Mount Eva, while the other granitoids are confined to the Harbutt Range area.

Equigranular granite (*Pgl*) cross-cuts early (D_2) tectonic fabrics in the eastern part of CONNAUGHTON. The

rock has been partly recrystallized (M_4), and is massive to weakly foliated (S_4, see **Structure**). A sample of the granite collected east of the Camel–Tabletop Fault Zone (AMG 851803) in the Tabletop Terrane has a SHRIMP U–Pb zircon crystallization age of 1310 ± 4 Ma (Nelson, 1996). The relationship between this granitoid and the Throssell Group cannot be determined.

Samples of pegmatite (*Pgp*), locally tectonized by a late deformation event (D_6, see **Structure**) were collected in the Connaughton Terrane (AMG 520062) near the Camel–Tabletop Fault Zone. The pegmatite cross-cuts early (D_2) tectonic fabrics and has a SHRIMP U–Pb zircon crystallization age of 1291 ± 10 Ma (Nelson, 1995).

Amygdaloidal basalt (*Pb, Pbe*)

A fine-grained amygdaloidal basalt (*Pb*) outcrops south of the Connaughton Synform (AMG 687863) in the Connaughton Terrane. The basalt unconformably overlies the Rudall Complex and is overlain by the Taliwanya Formation of the Throssell Group. Although the latter contact is not exposed, mafic clasts in conglomerate of the Taliwanya Formation (AMG 700655) indicate that the formation is younger than the basalt. The unit could be an early sill exposed by erosion prior to deposition of the Taliwanya Formation or the basal part of the Taliwanya Formation. Basalt at this stratigraphic level is unique to CONNAUGHTON.

The amygdaloidal basalt is a dark-green, non-foliated rock consisting of altered clinopyroxene, saussuritized plagioclase, accessory magnetite, and minor amounts of altered orthopyroxene, olivine, and secondary amphibole. The rock is heavily epidotized (*Pbe*) in places, and the amygdales contain quartz and calcite.

Yeneena Supergroup

Williams (1990) defined the 'Yeneena Group' as including three geographically separate packages of fluvial–marine sedimentary rocks. These packages have now been given 'group' status and, from west to east, are named the Tarcunyah, Throssell, and Lamil Groups (Williams and Bagas, in prep.). The 'Yeneena Group' has accordingly been redefined as the Yeneena Supergroup, but includes only the Throssell and Lamil Groups (Williams and Bagas, in prep.). The Tarcunyah Group unconformably or disconformably overlies the Throssell Group (see below) and for this reason, it is excluded from the supergroup. Both the Throssell and Tarcunyah Groups unconformably overlie the Rudall Complex.

Chin et al. (1980) assigned rocks in the McKay Range area to the Yeneena Group, but did not correlate it with any particular formation. Hickman and Bagas (in prep.) suggested that although the stratigraphic positions of the Gunanya Sandstone and the conformably overlying Waters Formation in the southeastern part of RUDALL were uncertain, they were comparable to the lower part of the 'Western Zone succession' (now formally named the Tarcunyah Group; Williams and Bagas, in prep.). These formations lack the penetrative foliation (S_4) and greenschist facies metamorphic (M_4) mineral assemblages observed in rocks of the Throssell Group, and may be facies equivalents of the Choorun and Nooloo Formations of the Tarcunyah Group to the northwest (Williams and Bagas, in prep.). The Karara Formation (Crowe and Chin, 1979) has also been included in the Tarcunyah Group based on its lithological, stratigraphic, and structural similarities with the Gunanya Sandstone.

Throssell Group

In the absence of continuous outcrop, the Taliwanya Formation (new name) and Pungkuli Formation (new name) are tentatively included in the Throssell Group, based on the similar tectonic fabrics, rock types, lithological successions, and interpreted environments of deposition. The Taliwanya Formation unconformably overlies the Rudall Complex and is conformably overlain by the Pungkuli Formation.

The Throssell Group can be regionally subdivided into a basal sandstone and conglomerate unit (the Coolbro Sandstone on THROSSELL, BROADHURST, and RUDALL, and the Taliwanya Formation on CONNAUGHTON) and a conformably overlying carbonaceous, pyritic, and dolomitic shale and sandstone unit (the Broadhurst Formation on THROSSELL, BROADHURST, and RUDALL, and the Pungkuli Formation on CONNAUGHTON). The basal unit of the Throssell Group is about 4 km thick on BROADHURST and tens of metres thick on THROSSELL and CONNAUGHTON. This variation in thickness was probably controlled by the topography of the region during sedimentation, or by growth faults. The conformably and transitionally overlying shale unit appears to maintain its thickness throughout the Throssell Group.

Taliwanya Formation (PTt)

The Taliwanya Formation (*Prt*) is here named after the local name for the Talawana Track, in the southern part of CONNAUGHTON. The unit is the basal formation of the Throssell Group in southern CONNAUGHTON and south-eastern RUDALL, and is present on both sides of the McKay Fault.

The Taliwanya Formation is up to 170 m thick and principally composed of polymictic conglomerate and arkosic sandstone with rare heavy-mineral bands. The formation also contains rare thin interbeds of fine-grained lithic wacke, siltstone, and shale, which become more abundant towards the conformable contact with the overlying Pungkuli Formation. The lowest beds are commonly polymictic conglomerate containing pebbles and boulders of quartzite, vein quartz, orthogneiss, rare angular ironstone, and amygdaloidal basalt (AMG 701655). The clasts are commonly rounded or subrounded, supported by an arkosic matrix, and locally display a crude upward fining into the overlying arkosic sandstone. The conglomerate is lenticular and interpreted as a channel-fill deposit. Cross-bedding and asymmetrical ripple marks are locally preserved.

Pungkuli Formation (ΣTp, ΣTpk)

The Pungkuli Formation (*ΣTp*) is here named after the local name for McKay Range in the southern part of CONNAUGHTON. The formation consists of interbedded, laminated, slightly micaceous, grey to dark-brown–black shale, locally carbonaceous shale and siltstone, thin units of sulfidic shale and sandstone, and minor amounts of carbonate rocks and chert. Lenticular bedding is common and rare wave-ripple marks are present. The Pungkuli Formation is exposed in and north of the McKay Range. The formation is about 900 m thick in the core of the McKay Antiform, but Cainozoic and Permian cover prevent an assessment of its thickness north of McKay Range.

Light-pink, grey, to cream carbonate rock (recrystallized dolarenite and dolostone) interbedded with light-grey chert, calcareous shale, siltstone, and minor amounts of black sulfidic carbonaceous shale and sandstone (*ΣTpk*) are well exposed at the base of the Pungkuli Formation in and north of the McKay Range (AMG 536644 and 636635 respectively). Individual beds are less than 0.3 m thick. Fine-scale cross-bedding and flute marks (locally preserved in the interbedded sandstone), and stromatolites (preserved in carbonate, e.g. AMG 640633) indicate sedimentation in shallow-water conditions. The interbedded sequence of carbonate and clastic sedimentary rocks (*ΣTpk*) is at least 300 m thick north of the McKay Range (AMG 636635), but thins out at AMG 680650.

Tarcunyah Group

The Tarcunyah Group unconformably overlies the Archaean Gregory Granitic Complex (Williams and Trendall, in prep.), the Manganese Subgroup (c. 1300 Ma) of the Bangemall Group (Williams and Trendall, in prep.), and the Rudall Complex (Williams and Bagas, in prep.). Palaeontological evidence from stromatolites and acritarchs found in the Tarcunyah Group indicates an age of c. 800 Ma (Bagas et al., 1995). This implies that the Tarcunyah Group is part of Supersequence 1 of the Centralian Superbasin (Walter et al., 1995), and a correlative of the basal part of the Savory Group (Williams, 1992).

The Pilbara Craton – Tarcunyah Group unconformity is at a high angle and not tectonically disturbed, and the basal conglomerate of the Tarcunyah Group contains clasts from the Pilbara Craton (Williams and Trendall, in prep.). The Throssell Group outcrops east of the unconformity and its contact with the Tarcunyah Group is a high-angle normal fault (the Vines Fault).

The contact between the Pungkuli Formation and the overlying Tarcunyah Group is obscured by Cainozoic sediments, except at AMG 593629 where highly cleaved (S_4) phyllite (*ΣTp*) is overlain by a thin granular conglomerate at the base of the Gunanya Sandstone. The rocks of the Pungkuli Formation are more deformed and metamorphosed than the overlying rocks of the Gunanya Sandstone, and the presence of a thin conglomerate at the base of the sandstone indicates that this contact is at least disconformable. The Karara Formation shows a similar relationship with the underlying Throssell Group on BLANCHE (Crowe and Chin, 1979). These observations imply that deposition of the Throssell Group was pre-tectonic and deposition of the Tarcunyah Group was syn- to post-tectonic, with respect to the Miles Orogeny (defined below). However, the differences in foliation and metamorphism may also be due to structural juxtaposition.

Gunanya Sandstone (ΣUu, ΣUup)

The Gunanya Sandstone (*ΣUu*) consists of medium- to coarse-grained, characteristically light-pink to purple, arkosic sandstone interbedded with thin pebbly horizons and beds of feldspathic grit. Abundant trough cross-beds and asymmetrical ripple marks indicate that the sandstone was deposited by southwesterly directed currents, presumably in a fluvial to deltaic environment.

Outliers of sandstone in the southeastern part of CONNAUGHTON are lithologically similar to the Gunanya Sandstone in the McKay Range and the Karara Formation on BLANCHE and CRONIN, and have been labelled ?*ΣUu*. Conglomerate (*ΣUup*) at the base of this sandstone is matrix supported and contains well-sorted and rounded pebbles of vein quartz, up to 20 mm in diameter. The conglomerate is less than 10 m thick, lensoidal, and upward fining.

Karara Formation (ΣUk)

The Karara Formation (*ΣUk*; Williams et al., 1976; Crowe and Chin, 1979) is restricted to a small area (about 2 km^2) in southeastern CONNAUGHTON, where it unconformably overlies sheared Rudall Complex in the Camel–Tabletop Fault Zone. Although dominated by cross-bedded and ripple-marked quartz arenite, the formation also includes quartz–feldspar wacke, basal lenses of conglomerate, and minor shale beds. The conglomerate contains subrounded clasts with a maximum diameter of 1 m, derived from the Rudall Complex, and fines upward to a well-bedded, fine-grained, and distinctively pink-coloured sandstone. The basal conglomerate is common within the Camel–Tabletop Fault Zone, indicating that the zone may have been an active growth fault during the deposition of the Karara Formation under shallow-water conditions. The Karara Formation closely resembles the Gunanya Sandstone, and the two units are correlated here.

Minor intrusions (*d*), gossan (*go*), quartz (*q*), and breccia (*qb, fb*)

Northerly trending dolerite dykes (*d*) intrude the Rudall Complex in the southeastern part of CONNAUGHTON, and small pods of dolerite intrude the Rudall Complex in the McKay Antiform. The dolerite clearly post-dates D_2 and D_4 structures that affect the Throssell Group. No intrusive contact has been observed in the field, although aeromagnetic data indicate that they intrude the Throssell and Tarcunyah Groups in the southeastern parts of CONNAUGHTON and BLANCHE.

The dykes occupy late, extensional, northerly trending fractures. Williams (1992) described similar dykes in the then Savory Basin and implied a post-600 Ma age, although no direct geochronology has been undertaken. At AMG 978567 a dolerite dyke intrudes amphibolite and mylonite (*PRns*). The dyke is lenticular, has a chilled margin, is about 10 m wide, and consists of microphenocrysts of plagioclase in a granular matrix of augite, plagioclase, and opaque minerals.

Gossan or gossanous rock (*go*) units are limonite–goethite concentrations formed by surface oxidation of sulfide mineralization. Such sulfide mineralization is either epigenetic (commonly accompanying quartz veining) or syngenetic (developed from sulfide-rich layers in the Throssell Group).

Silicified fault breccia (*fb*) is mainly associated with late brittle faults. Examples are found on the northern slopes of the McKay Range (AMG 487630). Angular fragments of country rock are enveloped by a silicified and ferruginized matrix of rock flour. Some microcrystalline pseudotachylyte veinlets are locally present.

Quartz veins (*q*) and quartz breccia (*qb*) are widespread, and commonly located in faults and shear zones. Some of the veins are limonitic, particularly along their margins, indicating wallrock sulfidation. Other veins contain limonite and goethite in late fractures. Some veins contain tourmaline or rutile.

Permian geology

Paterson Formation (*Pa*)

Figure 2 shows the location of Permian sedimentary rocks of the Paterson Formation, which form dissected valley deposits. Glacial striae on the Proterozoic rocks indicate that ice movement was northerly, as on BROADHURST and RUDALL (Hickman and Clarke, 1994; Hickman and Bagas, in prep.). The rocks consist of fluvioglacial sedimentary rocks and tillite, and outcrop as isolated mesas or partially dissected benches flanking larger hills. The sedimentary rocks are assigned to the Paterson Formation (*Pa*), previously described by Traves et al. (1956) and Chin et al. (1980, 1982). The tillite deposits contain well-rounded boulders, which locally exceed 5 m in diameter and include quartzite, orthogneiss, and paragneiss from a widely spread source region. Pink quartz arenite observed in the southern part of CONNAUGHTON is possibly sourced from the Tarcunyah Group.

The tillites pass upward into cross-bedded, medium- to coarse-grained sandstone, siltstone, and mudstone, with ripple marks and graded laminae.

Cainozoic geology

Areas of recent and active sedimentation are mapped as Quaternary (*Q*). Units that contain older and significantly dissected sediments are mapped as Cainozoic (*Cz*). Some of the older sediments, such as laterite and silcrete, may be Tertiary or older in age (Idnurm and Senior, 1978), but in the absence of empirical dating they have been mapped as Cainozoic.

Most Precambrian outcrops on CONNAUGHTON show some evidence of ferruginization, leaching, or silicification, typical of lateritic profiles. Gently undulating duricrust caps, including ferricrete or ironstone deposits (*Czl*), silcrete deposits (*Czz*), silicified sandstone caprock (*Czzc*), and extensively leached and silicified K-feldspar augen orthogneiss (*Czzg*) have been recently dissected to expose underlying bedrock. The duricrust represents remnants of Cainozoic weathering profiles in which the original rock structures or textures are poorly preserved. The ferricrete grades downward into leached and kaolinized deeply weathered rock. These sediments are probably Tertiary in age and may represent a Tertiary continent-wide weathering event (Idnurm and Senior, 1978).

Colluvium, sheetwash, fan deposits, and talus (*Czc*) are composed of red–brown, ferruginous gravel, sand, and silt, locally derived from a variety of sources.

Calcrete (*Czk*), consisting of massive, vuggy, or nodular sandy limestone, is only a few metres thick and found in drainage channels such as Cotton Creek. Secondary silicification locally results in incomplete replacement by a vuggy and opaline silica caprock. In the northeastern part of CONNAUGHTON, calcrete of an old, major drainage course is transgressed and overlain by seif dunes.

Quaternary deposits

Locally derived colluvial sands, soil, and gravel (*Qc*) form gently sloping scree and outwash fans. The colluvium is weakly incised by watercourses. Extensive colluvial fans locally grade downstream into alluvium.

Sand, containing laterite granules and pebbles (*Qp*), in the western part of CONNAUGHTON produces characteristically dark aerial photograph patterns. This unit is a mixture of partly residual and partly transported ferricrete granules, pebbles, and eolian sand, and commonly overlies shale, pelitic schist, or nodular laterite. The residual component indicates ferruginous bedrock.

Flat to undulating sandplain (*Qs*) covers most of the eastern and northern parts of CONNAUGHTON. The sandplain and seif dunes consist of dark-red eolian sand and clayey sand. The sand is composed of iron-stained quartz grains up to 0.5 mm in diameter. The dunes are up to 30 m in height, many kilometres long, and have a pronounced westerly to northwesterly orientation in the direction of the prevailing winds. Sand movement is confined to the dune crests, and their sides are stabilized by a cover of spinifex and small bushy eucalypts. Some dunes terminate on the eastern sides of outcrops or where cut by drainage channels. The depth of the sand between dunes is commonly less than 2–3 m, as revealed by exposed pediments.

Poorly developed red-earth sediments (*Qw*) cover the central and western parts of CONNAUGHTON. This unit is covered with dense mulga, which grows in a distinctive swayed pattern. The sediments have formed over mature deeply weathered plains or after mature alluvium, and contain varying amounts of ferricrete granules and, in places, are calcareous.

The present drainage courses and associated floodplains contain alluvium (Qa), which consists of unconsolidated clay, silt, sand, and gravel. The floodplain deposits also contain sand and clay mixed with eolian sands.

Playa lake deposits (*Ql*) consist of clay, silt, and evaporites and are present in low-lying areas marginal to drainage channels or at the termination of creeks against sand dunes. Underlying the dry lake surface is a mixture of black to brown mud, evaporites, and sand. The dry lake surfaces are not vegetated except for seasonal grasses and scattered eucalypts.

Structure

Previous work

Interpretations of the structural history of the Paterson Orogen are presented by Chin et al. (1980), Myers (1990a), Clarke (1991), Hickman and Clarke (1994), Hickman et al. (1994), Hickman and Bagas (in prep.), and Myers et al. (1996). The structural evolution of the Paterson Orogen on CONNAUGHTON is discussed within the general structural framework outlined by Hickman and Clarke (1994). However, the Yapungku Orogeny has been defined as the D_{1-2} events, the Miles Orogeny as the D_{3-4} events, and the Paterson Orogeny redefined as the D_6 event (see **Tectonic evolution**).

Table 1 summarizes structures of the various deformation events that have affected CONNAUGHTON.

Yapungku Orogeny (D_{1-2})

The Rudall Complex was intensely deformed and metamorphosed between about 2000 and 1760 Ma during two deformation events (D_1 and D_2), collectively referred to here as the Yapungku Orogeny. The orogeny is named after the local name for the South Rudall Dome on CONNAUGHTON.

D_1 structures

No large-scale D_1 structures are identified in the Rudall Complex. Evidence for D_1 is preserved in banded orthogneiss and in metasedimentary rocks, which contain a penetrative S_1 foliation deformed by isoclinal F_2 folds (Hickman and Clarke, 1994).

Pre-D_2 textures are preserved in the cores of garnets from amphibolites on CONNAUGHTON (GSWA 113016, AMG 562674; GSWA 113019, AMG 572676; and GSWA 113095, AMG 682664). These cores contain S-shaped trails of fine-grained epidote, titanite, and hornblende truncated against rims of inclusion-free garnet. They are interpreted as reflecting garnet growth (D_1) before granulite-facies metamorphism of the amphibolite host (Fig. 4). The inclusion-free overgrowths are interpreted as the product of the M_2 event (see **Metamorphism**).

D_2 structures

The second deformation event (D_2) is characterized by tight to isoclinal, northerly to northeasterly trending folds and layer-parallel foliation. A SHRIMP zircon age of 1778 ± 16 Ma (Nelson, 1995) was obtained from a post-D_2 vein of aplite cross-cutting a ?syn-D_2 ultramafic body (*ERu*) that occupies a major D_2 fault zone on RUDALL (Hickman et al., 1994). This relationship and the minimum age for *ERga,* which has D_2 fabrics, indicate a minimum age of c. 1760 Ma for the D_2 event.

The South Rudall Dome provides the least deformed exposure of the Rudall Complex. The dome is a doubly plunging antiform and the result of interference between a northerly plunging isoclinal F_2 anticline and a southeasterly trending F_4 anticline. The northern end of the dome plunges at about 35° to the north, whereas the southern end plunges at about 20° to the south-southwest. The units on the eastern and western sides dip steeply away from the core of the dome. Preliminary observations indicate that the F_2 anticline had a subhorizontal, northerly to north-northeasterly trending axis before the D_4 event.

A northerly trending fault separates amphibolite from augen orthogneiss on the eastern flank of the dome. The western flank is affected by minor cross-faulting, and shows a variation in the thickness of the amphibolites. Units near the dome show little internal deformation, and slickensides are commonly developed on unit boundaries as well as on joints and faults. Slip on lithological contacts clearly played an important role during the formation of the dome, while flattening of units was minimal.

At Mount Cotton a doubly plunging, northerly trending, asymmetric D_2 anticline is bound by northwesterly trending D_4 faults that show only minor movement. A northeasterly plunging and tectonically disrupted D_2 anticline, the Wells Antiform, is possibly the northern extension of this anticline.

Large-scale isoclinal F_2 folds are present in the Connaughton Hills in the western part of CONNAUGHTON. Here, two ridges formed by synforms of quartzite (*ERq*) are separated by an antiform occupied by banded paragneiss (*ERb*). Preliminary observations indicate that these folds also had subhorizontal axes trending in a north-northeasterly direction, before refolding and rotation during the D_4 event.

The succession of amphibolite (*ERab*), chert (*ERic*), quartz–mica schist (*ERm*), and quartzite (*ERq*), 8 km north of South Rudall Dome, is tectonically attenuated

Table 1. Summary of deformation and metamorphism on CONNAUGHTON

Event and age	*Structures*	*Metamorphism and magmatism*
Yapungku Orogeny (D_{1-2}; 2000–1760 Ma)		
D_1 (2000–1800 Ma): regional layer-parallel shear, direction unknown; identified on BROADHURST and RUDALL	S_1: penetrative layer-parallel schistosity; alignment of mica, quartz, and feldspar	M_1: amphibolite facies conditions; local melting; granitoid intrusion
D_2 (1790–1760 Ma): northerly–northeasterly trending isoclinal folds and associated thrusting	D_2:thrust zones with movement from east to west F_2: tight to isoclinal F_2 folds (axes were subhorizontal and trended north–north-northeast before D_4) S_2: schistosity due to alignment of mica and quartz L_2: stretching lineation within S_2 (Clarke, 1991)	M_2: high-pressure amphibolite to granulite facies; partial anatexis locally
Between D_2 and D_3: development of the Throssell basin	None identified	Post-D_2 and pre-D_4 granitoids
Miles Orogeny (D_{3-4}; c. 1132–800 Ma)		
D_3: local recumbent folding affecting the Throssell Group on BROADHURST; deformation in response to southwesterly directed compression	Local faulting and quartz veining of the Rudall Complex – Throssell Group unconformity	None identified
D_4: regional deformation in response to southwesterly directed compression	F_4: upright, tight folding about northerly trending axes; fold plunges low, mainly to the northwest and southeast; limbs commonly sheared out S_4: axial surface cleavage inclined steeply northeast L_4: stretching lineations plunge down-dip on S_4 (Hickman and Bagas, in press)	M_4: greenschist facies; locally intense cataclasis and dynamic recrystallization
?D_5: local deformation; west-northwest–east-southeast directed compression after D_4; possibly related to the folding in the Blake Fault and Fold Belt of the Savory Sub-basin	Northeasterly trending open folds, domal structures in the Throssell Group in southern CONNAUGHTON. Southwesterly plunging crenulations and minor folds	None identified
Paterson Orogeny (D_6; <610 Ma)		
D_6: Brittle deformation in response to north-northeast–south-southwest compression; correlated with the Petermann Orogeny 600–540 Ma) of central Australia, King Leopold Orogeny (c. 560 Ma) in the Kimberley region, and the 750–540 Ma breakup of Rodina (Myers et al., 1996)	D_6: west-northwesterly and northwesterly striking near-vertical strike-slip faults S_6: spaced cleavage, axial to conjugate kink bands, deforming S_4	None identified

along shears that juxtaposed it against K-feldspar augen orthogneiss (*PRga*). This succession is included in the Connaughton Terrane, and its contacts with the augen orthogneiss are interpreted as major D_2 thrusts dipping to the southeast. Porphyroblast tails in the augen orthogneiss define C–S fabrics, which indicate that the sense of movement along these thrusts was towards the northwest. Originally the D_2 thrusts had a roughly north–south strike, with movement towards the west. The southeasterly dipping thrust along the northern boundary of this succession marks the boundary between the Talbot and Connaughton Terranes. Northeasterly dipping D_4 faults disrupt this D_2 thrust contact to the east. The southern extension of the thrust is disrupted by faults associated with the McKay Fault. A pervasive, closely spaced, layer-parallel schistosity (S_2) is present in the amphibolite and schist, parallel to the D_2 thrusts and the axial planes of small-scale F_2 folds.

Augen orthogneiss north of the Connaughton Terrane was thrust over banded paragneiss (*PRb*) and quartzite (*PRq*) of the Talbot Terrane during the D_2 event. This thrust dips towards the southeast and has the same sense of movement as the thrusts further south, which mark the contact between the Connaughton and Talbot Terranes.

The D_2 fabrics in the area have been folded and crenulated by a major F_4 synform plunging about 65° towards 120° (Fig. 5). This F_4 synform may be the northwestern extension of the Connaughton Synform.

Ultramafic rocks on CONNAUGHTON are largely restricted to the Mount Eva and Harbutt Range areas, where peridotite outcrops along D_2 faults that were folded during the D_4 event. Therefore, the peridotite sheets were emplaced during D_2 or late D_2, and are apparently partly controlled by D_2 shear zones.

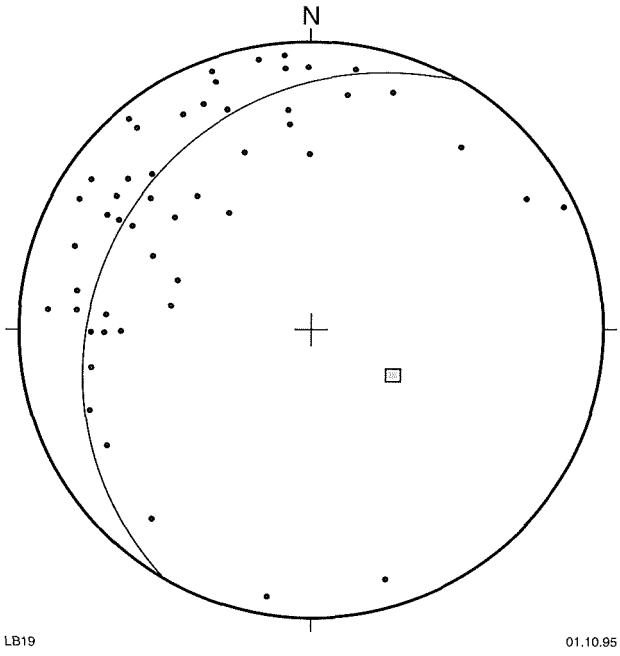

Figure 5. Stereoscopic projection of poles to the schistose S_2 foliation in fine-grained amphibolite (*ERab*) in the Connaughton Terrane north of South Rudall Dome (Schmidt equal area projection plotted on the lower hemisphere, n=50, Greater Circle = 210°/25°W, F_4 = 120°/65°)

Aeromagnetic data indicate that a poorly exposed dome, east of Harbutt Range and west of the Camel–Tabletop Fault, is about 12 km long in a northwest–southeast direction and about 6 km wide in a northeast–southwest direction. Poorly exposed gneiss and charnockite occupy the core of the dome. The surrounding rocks include banded iron-formation, amphibolite, schist, and peridotite. The lithological contacts are tectonized, and the northwesterly trending S_4 fabric and D_6 faults (related to the Camel–Tabletop Fault Zone) overprint the units. The dome may be the product of F_2/F_4 fold interference, similar to the Connaughton Synform and South Rudall Dome.

Miles Orogeny (D_{3-4})

The Miles Orogeny (named after the Miles Range on BROADHURST) is the dominant event responsible for the major northwesterly trending folds and faults on CONNAUGHTON, and does not affect the Tarcunyah Group.

D_3 structures

No D_3 structures are recognized on CONNAUGHTON. On BROADHURST, D_3 structures include reclined fold axes striking at about 120°, thrusts, local S_3 cleavage subparallel to bedding, and faulting along the Rudall Complex – Throssell Group unconformity (Hickman et al., 1994) and within the Throssell Group. In the eastern part of BROADHURST, the F_3 fold axes and associated S_3 cleavage trend about 120°. Anastomosing D_3 thrusting has resulted in stratigraphic repetition, and D_3 structures are crenulated by F_4 folds and cleaved by S_4 foliation. The general orientation of the F_3 folds indicates a north-easterly to southwesterly oriented compressional regime similar to D_4 and therefore, both are grouped into the Miles Orogeny.

D_4 structures

Chin and de Laeter (1981) reported a Rb–Sr isochron age of 1132 ± 21 Ma for pegmatite veins cutting D_2 fabrics in orthogneiss on RUDALL. They proposed that either the pegmatite was emplaced after the waning stages of D_2/M_2, and consequent recrystallization during D_4/M_4 may have been responsible for resetting the Rb–Sr isotopic system giving the younger age, or that the pegmatite could have been generated during the earlier part of of the D_4 event and not emplaced in the Throssell Group. In either case the approximate age of the D_4 event was 1132 ± 21 Ma (Chin and de Laeter, 1981).

Mineralization within the Broadhurst Formation of the Throssell Group is hosted by D_4 structures. The Broadhurst Formation is syn- to post-D_4 in age and has provided Pb-model ages of between 940 and 520 Ma (Blockley and Myers, 1990; Fletcher, I., 1993, pers. comm.; Hickman and Clarke, 1994). The t76 model ages alone, however, indicate that the age of galena mineralization is about 940–820 Ma, that the minimum age of the Broadhurst Formation is c. 900 Ma, and that the D_4 event is older than c. 800 Ma. However, recent Ar–Ar studies of the Throssell Group suggest that the minimum age for the D_4 event on BROADHURST and LAMIL is about 700 Ma (Reed, A. and Smith, S., 1995, pers. comm.).

Several massive to weakly foliated granitoids intrude the Lamil Group of the Yeneena Supergroup near Telfer, and post-date structures assigned to the D_4 event (Hickman et al., 1994). One of the weakly foliated granitoids, the Mount Crofton Granite 'Complex', has a Rb–Sr age of 598 ± 24 Ma (Trendall, 1974), a Pb–Pb age of 690 ± 48 Ma (McNaughton and Goellnicht, 1990; Goellnicht et al., 1991), and a SHRIMP U–Pb zircon age of 621 ± 13 Ma (Nelson, 1995). The nearby Minyari monzogranite has a SHRIMP U–Pb zircon age of 633 ± 13 Ma (Nelson, 1995). This demonstrates that the D_4 event and the Lamil Group are older than c. 630 Ma.

The dominant structures within the Throssell Group on CONNAUGHTON are large-scale, overturned, tight, northwesterly trending folds with a well-developed axial planar S_4 cleavage. The axial planar cleavage dips moderately to steeply to the northeast.

On RUDALL, BROADHURST, and north of the McKay Range on CONNAUGHTON, F_4 folds are commonly overturned to the southwest. The McKay Antiform, south of the McKay Fault, plunges about 40° to the east-southeast (instead of the more common southeast direction) and has a steep northern limb and a shallower

southern limb, which indicates overturning towards the east-northeast. The difference in fold style may relate to back-thrusting or local drag along the D_6 McKay Fault. Alternatively, the McKay Antiform is a D_6 structure, as F_6 folds are associated with the Vines Fault on THROSSELL (Williams and Bagas, in prep.).

In the Rudall Complex, F_4 fold geometry is complicated by late reactivation and interference with pre-existing structures. The most obvious consequence of this superimposition is that F_4 folds in the Rudall Complex commonly plunge at an angle up to 65°. This is significantly steeper than the angle of plunge of F_4 folds in the Throssell Group, although plunge directions (northwest or southeast) remain the same. An example of this is the major synform in the Rudall Complex in the eastern part of CONNAUGHTON. Common features of F_4 folds in the Rudall Complex are thrusting along the southwestern limbs of antiforms and normal faulting along northeastern limbs. Synclines are commonly broader than anticlines.

Field and aeromagnetic data indicate that major corridors of intense and anastomosing faulting or shearing are separated by zones of folding and minor faulting. The resulting structural pattern resembles augen structures in gneiss. Examples are the Connaughton Synform and structures in the Harbutt Range area. These structures are truncated by the Camel–Tabletop Fault Zone, which is a cataclastic D_6 structure.

The Connaughton Synform is a tectonically complex area of isoclinal F_2 folds and D_2 thrusts that have been refolded, faulted, and rotated during the D_4 event. The major structure in the area is a tight D_4 synform that plunges to the southeast. An interesting feature of the Connaughton Synform is the presence of a southeasterly plunging F_2 anticline on its western side. If simple F_4 folding were superimposed on a subhorizontal F_2 fold trending in a northerly direction, the resulting plunge of this refolded F_2 anticline would have been towards the north. This discrepancy can be explained by a relative anticlockwise block rotation of the anticline against the near-vertical D_4 faults bounding it to the east and west.

Most of the D_4 faults have a lineation plunging steeply to the northwest or southeast. The faults with the northwesterly plunging lineations have a dextral component of strike-slip movement and the faults with the southeasterly plunging lineation have a sinistral strike-slip component. As discussed above, faulting also includes significant block rotation. The vertical displacement of the D_4 faults on CONNAUGHTON cannot be determined; however, mapping on RUDALL indicates that vertical displacement ranges from a few hundred metres to at least 3 km (Hickman and Bagas, in prep.).

D_5 structures

In the southern part of CONNAUGHTON (AMG 640633), D_4 folds and associated S_4 cleavage in carbonate and pelitic rocks of the Pungkuli Formation are locally refolded and crenulated by open folds plunging about 20° to the southwest. A D_4 syncline in the Throssell Group (8 km east of AMG 640633), is similarly refolded by a northeasterly trending open syncline. These later folds are provisionally assigned to the D_5 event, but may relate to a later folding event (?D_7) not recognized elsewhere in the Paterson Orogen or to transpressional folding associated with the D_6 McKay Fault.

A regional reversal of the plunge of F_4 folds is observed in the central part of RUDALL (Hickman and Bagas, in prep.). This reversal is across a northeasterly trending zone and may be the result of interference with an open northeasterly trending anticline, similar in style to the late F_5 folds observed in the southern part of CONNAUGHTON. Folds with similar orientations are noted in the Blake Fault and Fold Belt of the Savory Group. This folding event is referred to as the Blake Movement (Williams, 1992), and its age is poorly constrained between about 800 and 610 Ma (Williams, 1992; Christie-Blick et al., 1995). The Blake Movement occurred before the Paterson Orogeny.

Paterson Orogeny (D_6)

Preliminary geochronological and biostratigraphic data suggest that the age of the younger part of the Savory Group (that has a D_6 fabric and unconformably overlies the Tarcunyah Group in the southwestern part of RUDALL) is about 600 Ma (Williams, 1992). This indicates that the Paterson Orogeny (D_6) is younger than 600 Ma.

Major D_6 structures on CONNAUGHTON consist of a conjugate set of northwesterly and west-northeasterly striking faults and shear zones, and an associated spaced cleavage (S_6). These faults clearly post-date D_4 folding and associated faulting, although they may follow pre-existing structures. Northwesterly trending faults, such as the Camel–Tabletop Fault Zone, display significant vertical movement as well as dextral movements, and the west-northwesterly trending faults, such as the McKay Fault and minor faults in the Harbutt Range, display a sinistral component.

The Camel–Tabletop Fault Zone is a kilometre-scale zone recognized in the Mount Eva area, and probably consists of a number of closely spaced, anastomosing faults. The Karara Formation, in the eastern part of CONNAUGHTON and western part of BLANCHE, outcrops in the Camel–Tabletop Fault Zone. Basal conglomerates are spread along this fault zone, which acted as a growth fault during the deposition of the Karara Formation and before the compressional D_6 event. It is likely that this fault is an early structure that was reactivated during the D_6 event.

The Camel–Tabletop Fault Zone separates two very different terranes. Aeromagnetic and field observations in the eastern parts of CONNAUGHTON and BLANCHE (Yeates and Chin, 1979) indicate that basement rocks to the east are Mesoproterozoic granitoids, whereas Palaeoproterozoic orthogneiss predominates to the west. The fault zone can be traced with airborne geophysical data from BROADHURST to RUNTON (1:250 000). On RUNTON

it joins the southeastern extension of the McKay Fault and then continues to the southeast, coinciding with the southern side of the Warri Gravity Ridge (Iasky, 1990). This ridge separates the West Australian Craton from continental crust to the northeast (Myers, 1993; Myers et al., 1996) and is a major structure formed during the 600–540 Ma Petermann Orogeny of central Australia (Grey, 1990; Camacho and Fanning, 1995; Walter et al., 1995). The northern extent of the Warri Gravity Ridge cannot be accurately traced due to the lack of detailed geophysical data, but it appears to continue into the Throssell Group in the eastern part of BROADHURST. This implies that it may be a long-lived structure and that the Connaughton and Tabletop Terranes were in contact before deposition of the overlying Throssell Group.

The Gunanya Sandstone in the southwestern part of CONNAUGHTON is extensively silicified, brecciated, and veined by quartz and hematite along the McKay Fault. This is a major, steeply south-southwesterly dipping fault along the northeastern edge of the McKay Range, associated with southwesterly trending sinistral splay faults. The fault has truncated both the northern limb of the McKay Antiform to the south and the contact between the Connaughton and Talbot Terranes of the Rudall Complex to the north. The antiform is east-southeasterly plunging and contains a core of quartzite, schist, and orthogneiss of the Talbot Terrane unconformably overlain by the Throssell Group. North of the hinge zone to the McKay Antiform, the Gunanya Sandstone is juxtaposed against the Pungkuli Formation and the Connaughton Terrane along the McKay Fault. This suggests that the fault has a sinistral component of movement as well as a vertical one. On geophysical evidence, the McKay Fault also appears to continue to the northwest to link with the Southwestern Thrust on RUDALL, which in turn joins with the Vines Fault on THROSSELL (Williams and Bagas, in prep.). Movement on the Southwestern Thrust is principally horizontal, with a displacement of many kilometres (Hickman and Bagas, in prep.).

The faulted contact between the Gunanya Sandstone and Talbot Terrane west of the South Rudall Dome dips to the south-southwest and is a D_6 structure parallel to the McKay Fault. Like the McKay Fault it is extensively silicified, brecciated, and veined by quartz and hematite.

Collectively, the Camel–Tabletop Fault Zone and the McKay Fault indicate maximum compression from the north-northeast with extension towards the west-northwest (Fig. 6), resulting in 'escape' of the fault block between the two faults. The late dolerite dykes (*d*) have a north-northwesterly trend and fill fracture zones that may relate to this extension.

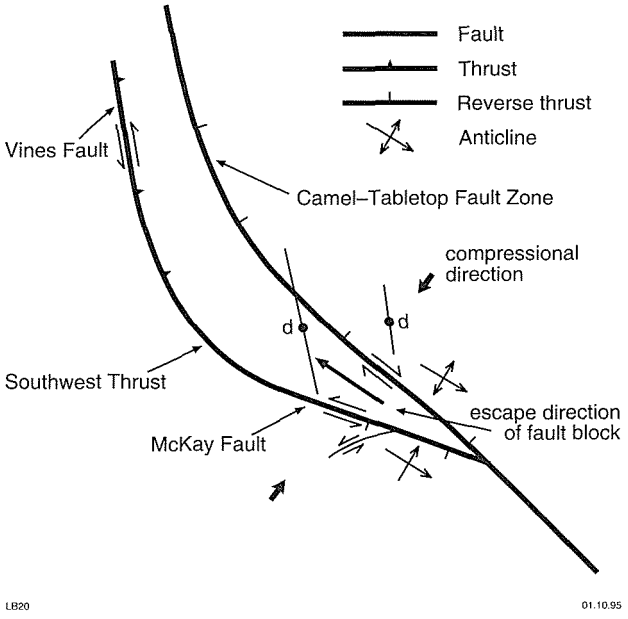

Figure 6. Cartoon showing the regional structures related to the D_6 event.

Metamorphism

The dominant structural and metamorphic features of the Paterson Orogen were produced by the D_4 event. There is abundant evidence that the Rudall Complex in the southern and eastern parts of CONNAUGHTON was metamorphosed to amphibolite–granulite facies before deposition of the Yeneena Supergroup and the Tarcunyah Group, and that this metamorphism is related to the D_2 event (Smithies and Bagas, 1997). Evidence for the M_1 event is extremely scarce on CONNAUGHTON, since subsequent tectonism and metamorphic recrystallization were intense.

The only constraint on the timing of the M_1 event is that it happened before emplacement of the post-D_1 K-feldspar augen orthogneiss (*PRga*), and is therefore older than 1790 Ma (the maximum age for *PRga*, see **Orthogneiss**). The M_2 event relates directly to the D_2 event, which deformed the augen orthogneiss. Intrusion of the protolith to the augen orthogneiss and the D_2 event occurred between 1790 and 1765 Ma (Nelson, 1995).

Greenschist metamorphism (M_4) associated with the D_4 event affected both the Rudall Complex and the Throssell Group, but some greenschist assemblages in the Rudall Complex may represent late-M_2 retrogression. Peak M_4 occurred between c. 1132 and 800 Ma (see **D_4 structures**).

Previous work

Chin et al. (1980) and Yeates and Chin (1979) recognized two metamorphic events prior to deposition of the Yeneena Supergroup. The first event, M_1, was associated with the D_1 event and produced amphibolite-facies mineral assemblages. The second event, D_2 and M_2, was thought to be a greenschist-facies event. Later metamorphism was of lower grade and dominated by dynamic effects associated with their D_3 event (D_4 of this report).

Clarke (1991) found that M_1 in the Yandagooge Inlier on BROADHURST was a low-pressure event characterized

by the assemblage andalusite–staurolite in pelitic rocks. No evidence of M_1 assemblages was found on RUDALL (Hickman and Bagas, in prep.). Clarke (1991) also recognized a middle amphibolite-facies assemblage (M_2), and established that prevailing metamorphic conditions in the Yandagooge Inlier of BROADHURST peaked at temperatures and pressures higher than 620 ± 50°C and 600 ± 100 MPa respectively (G. L. Clarke, unpublished data).

In the absence of evidence for the M_1 event on RUDALL, Hickman and Bagas (in prep.) assumed that most of the medium- to high-grade mineral assemblages related to the M_2 event. These included various combinations of kyanite, sillimanite, staurolite, and garnet in pelitic and semi-pelitic rocks; garnet, sillimanite, hornblende, kyanite, and staurolite in paragneiss and quartzite; hornblende and scapolite in amphibolite; and grunerite and garnet in banded iron-formation.

The M_4 metamorphism associated with the D_4 event did not exceed greenschist facies on BROADHURST (Hickman and Clarke, 1994), RUDALL (Hickman and Bagas, 1994), or CONNAUGHTON. The effects of M_4 metamorphism are not uniformly distributed. Recrystallization of mineral assemblages is most pronounced in zones of deformation, but is apparent to some degree in all rocks of the Rudall Complex and the Throssell Group. A characteristic of M_4 is the overprinting assemblage of epidote–actinolite–albite(–quartz–chlorite–calcite) or sericite–quartz.

Rudall Complex

Mineral assemblages in the schist and gneiss on CONNAUGHTON reflect regional metamorphism at medium to high grades.

Pelitic schist

Three pelitic units from CONNAUGHTON are distinctive in terms of their metamorphic minerals, and are mapped as micaceous quartz–aluminosilicate schist (*PRqa*). These are the quartz–sillimanite schist west-southwest of Camel Rock, quartz–garnet–sllimanite–microcline assemblages east of Mount Eva, and quartz–kyanite–muscovite–magnetite assemblages south and southeast of Mount Eva. These assemblages are indicative of medium to high grades of metamorphism. The presence of kyanite reflects moderate to high pressures. The kyanite schist southeast of Mount Eva (AMG 699863, GSWA 115669) shows prismatic kyanite rimmed by sillimanite (fibrolite, Fig. 7). Much of the sillimanite lies within the foliation, but randomly oriented fibrolite is also present, suggesting both syn- and post-tectonic growth (with respect to the D_2 event).

Gneiss

The presence of prograde garnet in charnockite (*PRnc*) and banded garnetiferous granodioritic gneiss (*PRng*)

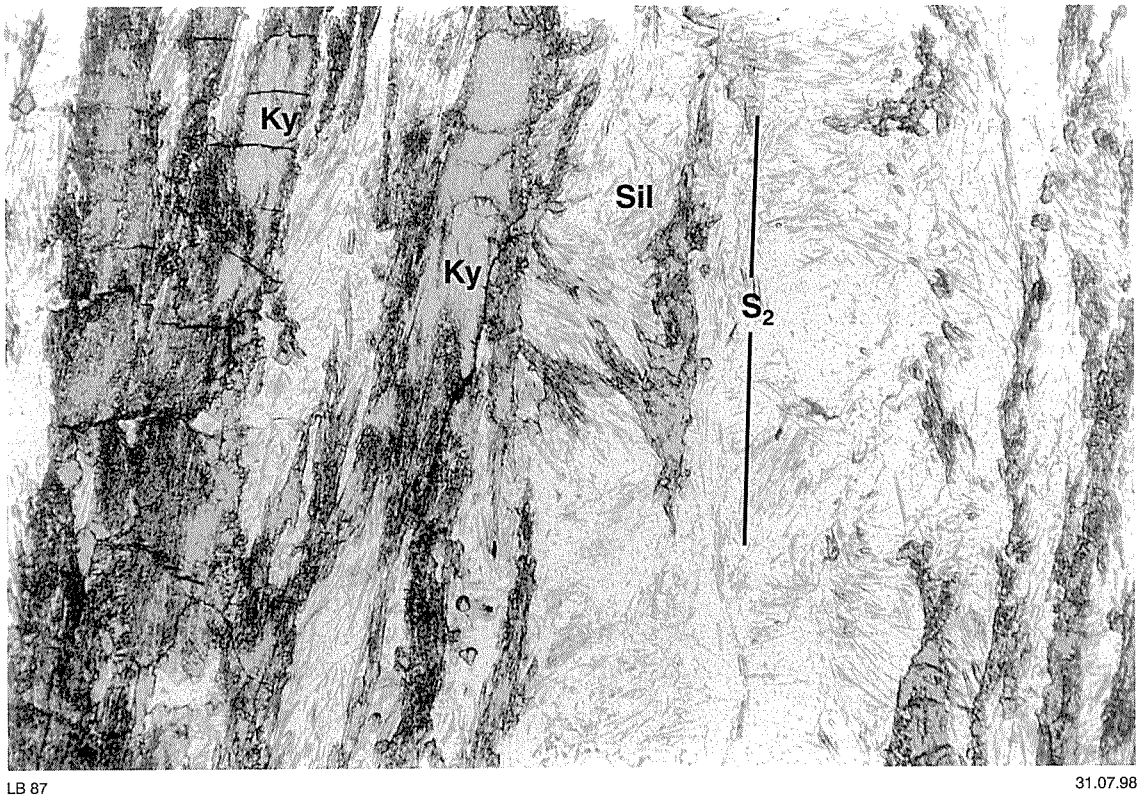

Figure 7. Foliated kyanite schist, with prismatic kyanite (Ky) rimmed by sillimanite (fibrolite, Sil). GSWA sample 115669 from southeast of Mount Eva (AMG 699863). The field of view is 0.4 mm across

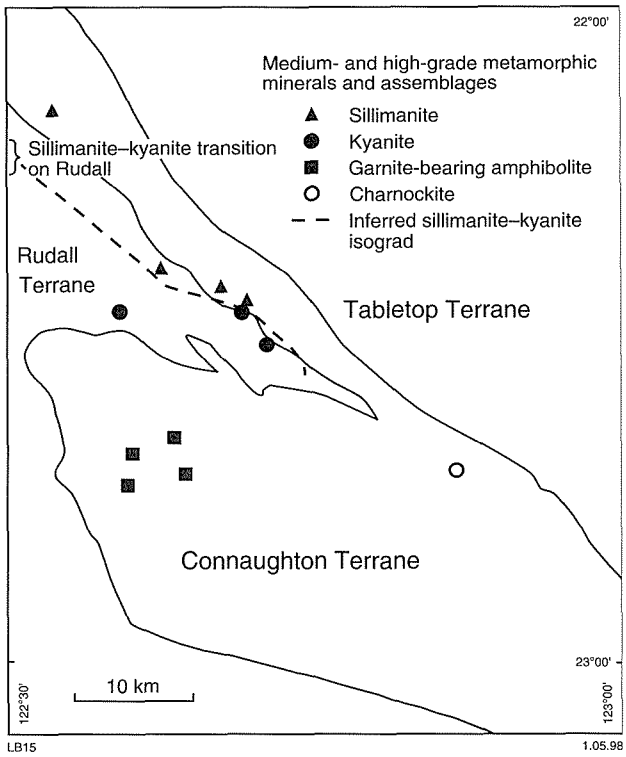

Figure 8. Plan showing the distribution of observed prograde metamorphic minerals and mineral assemblages on CONNAUGHTON.

suggests that these rocks were recrystallized at medium to high grades.

Mafic rocks

In the northeastern part of the Rudall Complex on CONNAUGHTON, amphibolite (*PRac*) contains the mineral assemblage brown hornblende–andesine–diopside–hypersthene. The presence of brown hornblende and hypersthene suggests high-grade metamorphism. Garnet amphibolite (*PRag*) is the dominant mafic rock of the South Rudall Dome – Connaughton Synform area, and is characterized by the metamorphic assemblage hornblende–andesine–almandine or hornblende–andesine–almandine–diopside. The presence of garnet suggests that the assemblage formed under moderate to high pressures and at middle to upper amphibolite facies. In rare cases (e.g. GSWA 113016, AMG 562674; GSWA 113019, AMG 572676; and GSWA 113095, AMG 682664) the cores of garnet porphyroblasts preserve sigmoidal trails of fine-grained epidote, hornblende, and titanite, representing the S_1 foliation (Fig. 4). These cores provide rare evidence for the M_1/D_1 event on CONNAUGHTON.

Distribution of M_2 indicator assemblages

Figure 8 shows the distribution of prograde metamorphic minerals on CONNAUGHTON. Sillimanite is restricted to the northwestern part of CONNAUGHTON, and kyanite is found in quartzofeldspathic rocks south of the sillimanite zone. The transition between the two zones is disrupted by the Mount Eva Thrust and the Camel–Tabletop Fault Zone. However, the distribution of metamorphic indicator minerals supports the hypothesis that the Rudall Complex on CONNAUGHTON can be divided into a northeastern sillimanite zone and a southwestern kyanite zone.

Metamorphic conditions for M_2

Quantitative assessment of the physical conditions that prevailed during pre-D_4 metamorphism (Smithies and Bagas, 1997) relies mainly on the mafic assemblages. Representative chemical analyses of mineral phases from these rocks are presented in Smithies and Bagas (1997). Table 2 shows temperatures and pressures estimated using a range of published thermobarometers.

The kyanite zone comprises the bulk of the Rudall Complex on CONNAUGHTON. Metamorphic assemblages equilibrated at temperatures of around 780°C and pressures of around 1200 MPa (Table 2). These conditions are typical of high-pressure granulites. The metamorphic minerals lie within the main regional S_2 foliation, suggesting that this metamorphic event is M_2. Evidence of a metamorphic prehistory (M_1) within the kyanite zone is provided by a relict amphibolite assemblage in the cores of some garnets in the garnet amphibolite. The sillimanite zone comprises the northeastern extremity of the Rudall Complex, extending from the northeastern part of RUDALL to the southeastern part of CONNAUGHTON. Mafic rocks in this zone equilibrated at 770–850°C (Table 2).

Pelitic schist at AMG 699863 (GSWA 115669) is situated close to or within the boundary between the two metamorphic zones, and shows kyanite being replaced by sillimanite. Fibrolite rims kyanite, but the latter remains abundant and is prismatic in habit, suggesting that either the conditions of sillimanite crystallization were close to the sillimanite–kyanite univariant curve or short-lived. Since textural relationships indicate that the sillimanite formed during the same event that foliated the quartz–kyanite schist and peak metamorphic temperatures appear slightly higher within the sillimanite zone, the preserved kyanite–sillimanite relationship is prograde rather than retrograde. This suggests that the boundary between the sillimanite zone and the kyanite zone is an isograd rather than a tectonic discontinuity, and that pressures within the sillimanite zone must have approached those at the kyanite–sillimanite univariant curve.

Peak conditions prevailing during metamorphism of the sillimanite zone, therefore, were in the order of 770–850°C at about 850–900 MPa (pressures from kyanite–sillimanite univariant curve). The change in conditions from the kyanite zone to the sillimanite zone reflects prograde decompression (Fig. 9) or a clockwise P–T–t (pressure–temperature–time) path. Overthrusting of a thick crustal slice (with at least 40 km of crust above the level of the garnet amphibolite) is the only conceivable way of achieving such trends (Carswell and O'Brian,

Table 2. Pressure and temperature estimates for the M_2 event

Lithology and GSWA sample no.	*Mineral assemblage*	*Pressure (MPa)*	*Temperature (°C)*	*Method*
Garnet amphibolite (*PRag*)				
117762	gnt, hbl, plag	1150–1200	700–730	1, 2, 3
112980	gnt, hbl, plag	1160–1230	680–710	1, 2, 3
113016	gnt, hbl, plag	1240–1250	720	1, 2, 3
112978	gnt, hbl, plag	1200	720–730	1, 2, 3
117703	gnt, hbl, plag	1130–1170	730	1, 2, 3
113088	gnt, hbl, plag, cpx	1070–1150	730–750	1, 2, 3, 4
119109	gnt, hbl, plag, cpx	1020–1100	740–770	1, 2, 3, 4
Charnockite (*PRnc*)				
115783	gnt, opx, plag	240–370	770–860	5, 6, 7, 8
Orthopyroxene- and clinopyroxene-bearing amphibolite (*PRac*)				
115642	hbl, plag	[a]700	840	3
115644	hbl, plag	[a]700	820	3
115658	hbl, plag	[a]700	810–830	3
115740	hbl, plag	[a]700	830–840	3
Garnet gneiss (*PRng*)				
115775	gnt, biot	[a]700	700	9
115744	gnt, biot	[a]700	660	9

NOTES: (a) assumed pressure gnt: garnet hbl: hornblende plag: plagioclase
cpx: clinopyroxene opx: orthopyroxene biot: biotite

SOURCES: 1: Graham and Powell (1984) 2: Kohn and Spear (1990) 3: Holland and Blundy (1994)
4: Newton and Perkins (1982) 5: Harley (1984) 6: Bhattacharya et al. (1991)
7: Lee and Ganguly (1988) 8: Harley and Green (1982) 9: Indares and Martignole (1985)

1993). Hence, metamorphic conditions during the D_2 event are most consistent with collisional tectonics involving doubly thickened crust.

Throssell Group

Greenschist facies metamorphism (M_4) associated with the Miles Orogeny has affected the Throssell Group in the southern part of CONNAUGHTON. The effects are seen in pelites and carbonates of the Pungkuli Formation, but not in the quartz arenites and shales of the Tarcunyah Group. The common metamorphic features in the Pungkuli Formation are sericite growth parallel to S_4 schistosity, silica overgrowth of rounded to subrounded quartz grains in pelite, and calcite veining parallel to and cross-cutting S_4 foliation in carbonate rocks.

Economic geology

In 1971 Otter Exploration located gossans containing subeconomic concentrations of base metals at Mount Cotton and Camel Rock. In 1974 Newmont Limited in a joint venture with Samin Limited, completed two shallow diamond drillholes at Camel Rock. The drilling totalled about 200 m in length and intersected subeconomic concentrations of base metals and barium.

In 1977 CRA Exploration (CRAE) completed an airborne radiometric and magnetic survey over the Rudall Complex on CONNAUGHTON and in the southeastern part of RUDALL. The targets were pegmatite, and metamorphic- and hydrothermal-related uranium mineralization analogous to the Alligator River region of the Northern Territory and the Athabasca region of northern Saskatchewan in Canada. Radiometric anomalies were detected, but later investigations failed to find economic mineralization, and the uranium mineralization observed was thought to be the result of secondary enrichment in calcrete.

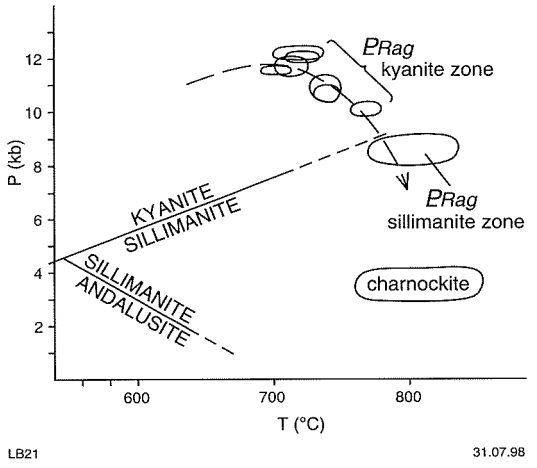

Figure 9. P–T grid showing the calculated peak metamorphic conditions for various assemblages from CONNAUGHTON

Newmont explored Mount Cotton and South Rudall Dome for base-metal mineralization in 1978. Their exploration program included geological mapping, geochemical surveys, diamond drilling, and percussion drilling.

The Paterson Orogen was explored for kimberlites by CRAE during 1978–84, based on the investigation of magnetic and geochemical anomalies.

In 1981 Aquitaine Minerals explored for uranium east of Harbutt Range. Stockdale Prospecting completed a stream-sediment geochemical survey in search of diamonds on RUDALL and CONNAUGHTON in 1984.

Agip Australia explored the South Rudall Dome, Wells Antiform, and Connaughton Synform during 1981–84 for base metals and uranium, and discovered uranium mineralization in core drilled by Newmont at Mount Cotton in 1978. CRA Exploration entered into a 'farm-in' agreement with Agip in 1984, but exploration was suspended in 1987 when an Exploration Exclusion Zone (EEZ) was imposed over the eastern part of RUDALL and west of the Harbutt Range on CONNAUGHTON as part of an Aboriginal land claim.

Since 1987 CRAE has been exploring the Rudall Complex outside the EEZ on CONNAUGHTON for uranium and other mineral commodities and in 1991 they entered into a joint venture with PNC Exploration. Exploration has targeted unconformity vein-style uranium, base-metal, gold, and platinum-group element (PGE) mineralization using geochemistry and airborne geophysics.

Mineral occurrences

As mineral exploration on CONNAUGHTON is at an early stage, no detailed information has been published on the mineralization, although unpublished information is available from company exploration reports, which can be viewed at GSWA. Mineral occurrences are shown on the CONNAUGHTON (1:100 000) geological map accompanying these Notes.

Geochemical investigation

GSWA mapping on CONNAUGHTON included routine sampling of gossans, ironstones, and sulfidic vein quartz. The AMG locations and main geochemical characteristics of anomalous samples, as well as the criteria used to identify anomalous concentrations of elements, are shown in Appendix 2.

Rare-earth elements

Anomalous concentrations of rare-earth elements (REE) are found in gossan hosted by fine-grained amphibolite (*ERab*), schist (*ERm*), and banded iron-formation (*ERi*) about 10 km north of South Rudall Dome. Sample GSWA 117747 is slightly anomalous in copper (573 ppm Cu; Appendix 2), and sample GSWA 113000 is slightly anomalous in lead (516 ppm Pb; Appendix 2).

Base and precious metals

Camel Rock

Camel Rock, in the northwestern part of CONNAUGHTON (AMG 623040), is an isolated exposure with visible copper mineralization. The rocks in the area include regularly banded magnetite–chlorite–garnet–sericite quartzite, metamorphosed banded iron-formation (*ERi*), ankerite-rich banded iron-formation (*ERi*), and minor amounts of chalcopyrite, quartz carbonate, sericite–chlorite schist, and thin bands of medium-grained amphibolite (*ERam*). The quartzite is strongly pitted after pyrite and has minor amounts of malachite, and extensive iron and manganese staining. The succession is tightly folded (F_2) and fold-hinge zones are strongly sheared. Diamond drilling by Newmont in 1974 intersected copper mineralization at depth with a maximum of 2% barium. The richest copper mineralization, with an average of 0.43% copper, was found in a 2 m-thick stockwork of magnetite, chalcopyrite, and pyrite veinlets in banded iron-formation.

Newmont delineated an airborne magnetic anomaly near Camel Rock that extends for about 8 km in a southeast–northwest direction. The anomaly was investigated but no major mineralization was detected. This region is considered highly prospective for base-metal mineralization.

Mount Cotton

Mount Cotton (AMG 594759) is a significant copper lead–zinc–uranium prospect within the core of a doubly plunging D_2 antiform that appears to continue northeastward into the Wells Antiform. The mineralization is in northeasterly trending gossanous quartz veins hosted by garnetiferous and ferruginous schist (*ERir*) and banded iron-formation (*ERi*). Work by Agip during 1981–84 indicates that the mineralization has maximum grades of 2% copper, 1.5% uranium, and 0.6% zinc, and contains traces of silver and gold (Chin et al., 1980).

Wells Antiform

The Wells Antiform appears to be the northeastern extension of the D_2 antiform at Mount Cotton. Sample GSWA 117761, from ironstone in garnetiferous amphibolite, assayed 2660 ppm lead. During 1981–84, Agip sampled a malachite-stained quartz vein just east of this locality (AMG 626792) that assayed 4.3% copper, 11 ppm silver, and 1.1 ppm gold. This area is considered highly prospective for gold and base-metal mineralization.

Connaughton Synform

Anomalous platinum, palladium, manganese, cobalt, copper, zinc, phosphorus, and lead were detected during a stream-sediment survey in the Connaughton

Synform by CRAE in 1986. Sample GSWA 117787 of a malachite-rich quartz vein exposed in alluvial rubble, collected from the southern part of the Connaughton Synform, assayed 19.4% copper, 70 ppm molybdenum, and 1 g/t gold. Sample GSWA 117789 of a malachite-rich quartz vein exposed in colluvium, from the northern part of the Connaughton Synform assayed 4% copper, 2260 ppm lead, 445 ppm zinc, and 263 ppm arsenic. The area is considered highly prospective for gold and base-metal mineralization.

South Rudall Dome

The schist, carbonate, and amphibolite succession above the prominently exposed banded iron-formation in South Rudall Dome hosts base-metal and silver mineralization.

A poorly exposed, weakly mineralized, lenticular gossan in the northern part of the dome (AMG 567731) appears to have developed in a thin band of sulfidic and graphitic schist in banded iron-formation. The gossan has a boxwork texture after pyrite, pyrrhotite, and chalcopyrite and contains traces of galena and sphalerite. Rock-chip samples collected by Agip during 1981–84 assayed up to 1500 ppm copper.

Chrysocolla, galena, and minor amounts of malachite are hosted by silicified carbonate veins in the southern part of the South Rudall Dome. The veins are enveloped by extensive silica, sericite, carbonate, and chlorite alteration, and cross-cut poorly exposed graphitic and micaceous schist (AMG 570697). Rock-chip samples from costeans, analysed by Agip, had maximum grades of 11.4% copper, 46 ppm silver, and 2.6% lead. Sample GSWA 117728, from the same locality, assayed 16.8% copper, 300 ppm silver, and 520 ppm lead. Drillhole samples analysed by Agip assayed 1.8% copper, 1.6% lead, 1.1% zinc, and 27 ppm silver.

Diamonds

A number of kimberlitic indicators and microdiamonds have been detected in the region by CRAE, although no kimberlites have yet been found. It is thought that these kimberlitic indicators and microdiamonds probably originated from Permian glacigene sedimentary rocks, having a provenance to the south.

Mineral potential

The mineral potential of the Paterson Orogen became apparent with the discovery of the Telfer Dome gold deposit in 1971 and the Kintyre uranium deposit in 1985. Comparisons between the Rudall Complex, the East Alligator River region of the Northern Territory, and the Athabasca region of Canada suggest that the potential for discovering further unconformity vein-style uranium deposits in the Paterson Orogen is high. The Rudall Complex is also considered a potential source for Palaeoproterozoic-style stratiform and stratabound base-metal and gold deposits, and for ultramafic-related platinum-group element mineralization.

During the last twenty years of exploration, numerous subeconomic (and rare economic), stratabound, fault-controlled, vein-type mineral deposits, including gold, base metals, uranium, and PGE, have been found throughout the Paterson Orogen. Many of the deposits in the Rudall Complex are hosted by carbonaceous or sulfidic schist, are hydrothermal in origin, formed late in the history of the complex, and are supergene-enriched to varying degrees.

Vein-type deposits on CONNAUGHTON are commonly hosted by sulfidic and calcareous pelites or quartz–mica schist. They are commonly associated with chlorite, sericite, or carbonate alteration and are probably late- to post-D_4 events. Banded iron-formation and ferruginous schist have potential for economic mineralization, particularly near the late granitoids around and east of the Camel–Tabletop Fault Zone.

The area north of South Rudall Dome and west of Harbutt Range has not been extensively explored. Nickel, chromium, and PGE mineralization may be present in the thick, poorly exposed, layered ultramafic complexes and serpentinite near Mount Eva. Geochemical exploration shows anomalous PGE concentrations in the Connaughton Synform. Economic concentrations of gold, silver, base metals, and uranium are present at South Rudall Dome, Mount Cotton, Wells Antiform, Connaughton Synform, and Camel Rock.

The little-explored Pungkuli Formation of the Tarcunyah Group, in the southern part of CONNAUGHTON, contains locally sulfidic or gossanous shale and carbonate, which could be prospective for Mississippi Valley-type and Mount Isa-type base-metal deposits.

Water resources

Permanent and semi-permanent pools are present along major watercourses where alluvium is sufficiently thick and extensive to hold groundwater resources. Areas of calcrete may contain large, although possibly saline, groundwater supplies. Groundwater in the Rudall Complex is likely to be restricted to shear and fault zones. Significant groundwater supplies may be found in fractured and sheared Gunanya Sandstone and Karara Formation. Permian sandstone units in the southern and northwestern parts of CONNAUGHTON may be potential aquifers, although salinity levels are untested.

Tectonic evolution

Yapungku Orogeny

The present shape and extent of the Paterson Orogen are primarily due to orogenic events after the Yapungku Orogeny. Deformation in the Connaughton Terrane may have been slightly younger as indicated by the progressively younger thrusts eastward (Hickman and Bagas, in prep.). This orogeny is similar in age to the Capricorn Orogeny and is partly synchronous with the

Strangways Orogen of central Australia (Bagas and Smithies, 1997).

Fabrics associated with D_1 are poorly preserved and restricted to bedding planes in the Talbot Terrane. On BROADHURST and RUDALL the existence of a layer-parallel penetrative schistosity, folded by F_2 folds and, in places, crenulated by a cross-cutting S_2 cleavage, indicates the presence of at least one phase of regional deformation prior to the D_2 event. The observation that S_1 is parallel to compositional layering in the paragneiss units on BROADHURST and RUDALL suggests that it may have formed axial planar to large-scale reclined isoclinal folds associated with subhorizontal thrusting (Hickman and Bagas, in prep.). The rocks in the Connaughton Terrane have been extensively recrystallized during amphibolite–granulite facies metamorphism associated with the M_2 event. In this terrane the M_1 event is preserved only in garnet cores contained within rocks with well-developed D_2 fabrics.

The banded orthogneiss in the western part of RUDALL contains both S_1 and S_2 fabrics and is intruded by protoliths of the K-feldspar augen orthogneiss (*ERga*). No structure younger than S_2 has been recognized in the augen orthogneiss. This suggests that the emplacement of the banded orthogneiss protolith was pre- to syn-D_1, and that the D_1 event occurred between 2000 and 1800 Ma. The age range for D_1 is synchronous with the initial stages of the Capricorn Orogeny (1950–1830 Ma), which formed the West Australian Craton by continental collision of the Archaean Pilbara and Yilgarn Cratons (Myers et al., 1996).

Hickman and Clarke (1994) established that the D_2 event produced tight to isoclinal folds and a regional schistosity (S_2) in all major rock units of the Rudall Complex. The S_2 cleavage has been rotated by F_4 folds and is now commonly steeply inclined, principally towards the northeast or southwest, but in the closures of F_4 folds it commonly dips to the northwest or southeast.

The D_2 event is characterized by north–south oriented isoclinal folding and faulting, overthickening of the Connaughton Terrane, and the emplacement of granitoids (e.g. the K-feldspar augen orthogneiss), peridotite–dunite rocks (*ERu*), and gabbros (some of *ERac*) on CONNAUGHTON.

K-feldspar augen orthogneiss in the Connaughton and Talbot Terranes is pre- to syn-D_2 with a crystallization age ranging from 1790 to 1765 Ma. The augen orthogneiss appears to relate to episodic melting of a compositionally homogeneous source region underlying both terranes of the Rudall Complex. The geochemistry of the augen orthogneiss (Appendix 1) suggests a dominantly igneous source region.

Peak regional M_2 metamorphism was syn- to post-D_2 in both the Talbot and Connaughton Terranes. The Talbot Terrane was metamorphosed to intermediate-pressure amphibolite facies. The Connaughton Terrane, however, was metamorphosed at high pressures (up to 1200 MPa) to amphibolite–granulite facies. The progressive deformation and high-pressure metamorphism assigned to D_2/M_2 was clearly related to major crustal overthickening involving overthrusting, and is consistent with a collisional orogeny driven by plate tectonics (Smithies and Bagas, 1997). The D_2 structures were probably produced by an advancing plate from the east during continued deformation associated with the Yapungku Orogeny, between 1790–1760 Ma. The eastern plate may be the Tabletop Terrane or concealed beneath the Canning Basin further to the east. The extent of deformation suggests continent–continent collision (Himalayan-style), similar to that in the Capricorn Orogen (Tyler, 1991).

Figure 10 is an attempt to reconstruct the Palaeoproterozoic tectonic evolution (i.e. the Yapungku Orogeny) of the Rudall Complex, and depicts the inferred positions of the various tectonic terranes. The compression deformation began with thrust repetition of the Connaughton–Talbot sequences, followed by major crustal thickening and metamorphism as the now concealed eastern crust was thrust westward.

The c. 1300 Ma magmatic event

Felsic rocks intruding the Tabletop Terrane have been dated at c. 1300 Ma by PNC Exploration (Smithies and Bagas, 1997). This magmatic event was synchronous with granitoid emplacement in the Albany–Fraser Orogen (Myers, 1990b) and the Musgrave Block (Camacho and Fanning, 1995), and it is possible that they relate to a single regional event. Clarke (1991) referred to this magmatic episode as the 'Watrara Orogeny', but correlated it with the D_2 event. Such correlations are not consistent with new geochronological data, which place the minimum age for the D_2 event on RUDALL at about 1760 Ma (see **Structure**). Therefore, it is recommended that use of the name 'Watrara Orogeny' be deferred until the significance of the c. 1300 Ma magmatic event is better understood.

The possibility that this event is related to the Miles Orogeny in the Throssell Group and that the orogeny occurred over a long period of time cannot be discounted, but an implication of this is that the Throssell Group may be older than c. 1300 Ma and partly coeval with the Bangemall Group. This would explain the higher metamorphic grade of the Throssell Group, and the non-conformable relationship between the Tarcunyah and Throssell Groups on CONNAUGHTON.

Yeneena Supergroup and Tarcunyah Group

Sedimentary environment of the Throssell Group

The basal conglomerate of the Taliwanya Formation on CONNAUGHTON is transitionally overlain by graded sandstone, and channel-fill conglomerate is common in the transitional zone. The conglomerate was deposited in a fluvial environment, possibly from a braided river

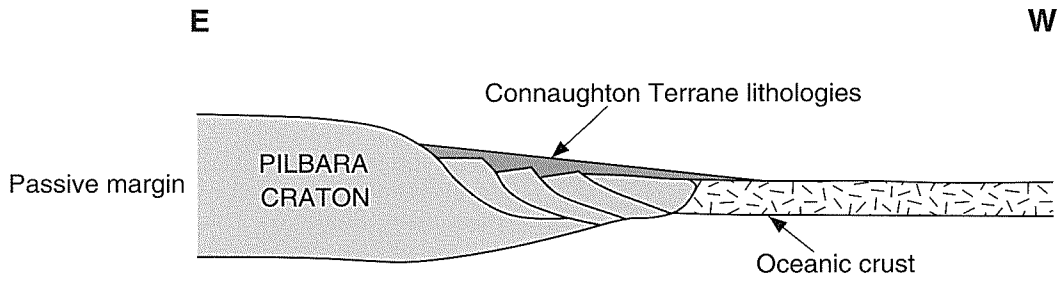

a. Rifting and deposition of rocks along the eastern 'passive margin' of the Pilbara Craton

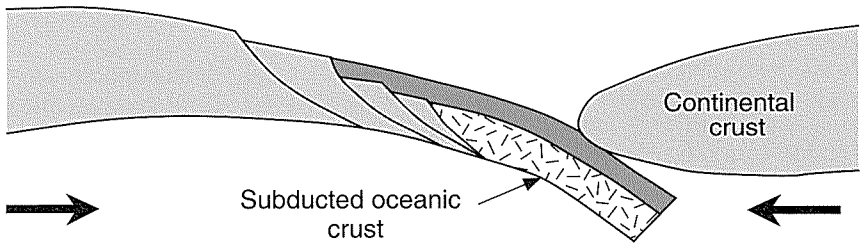

b. Active margin, pre-2000 Ma

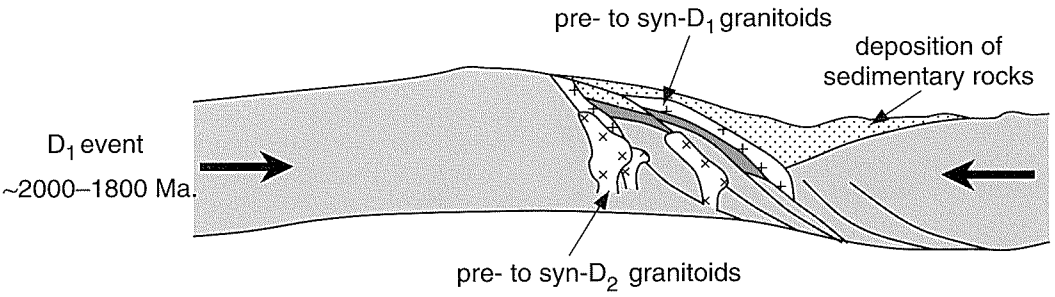

c. Collision with continental crust to the west, deposition of sedimentary rocks of the Talbot Terrane in a ?foreland basin; intrusion of pre- to post-D_1 granitoids

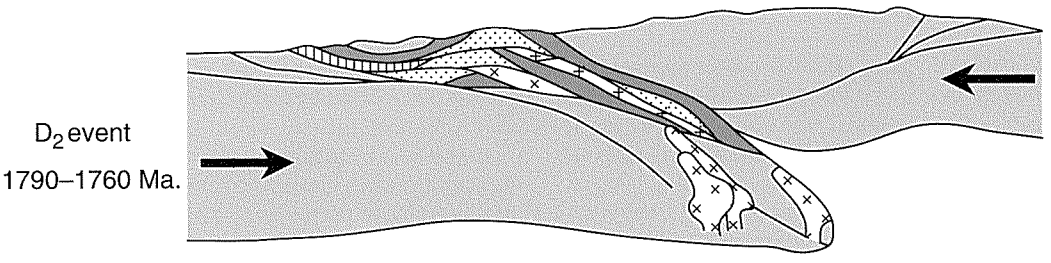

d. Major folding and thrusting accompanied by high-pressure and high-temperature metamorphism (doubly thickened crust) during D_2; reactivation of early (D_1) thrusts

LB84 6.05.98

Figure 10. Tectonic model showing the evolution of the Rudall Complex during the interval between pre-2000 and 1760 Ma

(Rust, 1981). The overlying sandstone contains unimodel palaeocurrents and common cyclic trough cross-bedding grading upward into planar bedded or massive sandstone (Hickman and Bagas, in prep.). These sedimentary features indicate that major channels were probably formed in a fluvial–deltaic environment (Rust, 1981). The palaeocurrents from the sandstone also indicate that sedimentation was from the southwest (Hickman and Bagas, in prep.) and probably, but not necessarily, from the Rudall Complex.

The sandstone is transitionally overlain by a shale unit (the Pungkuli Formation on CONNAUGHTON and the Broadhurst Formation to the northwest). The finer grained nature of the shale unit is indicative of a quieter sedimentary environment. Sedimentary features of the shale unit on CONNAUGHTON and THROSSELL (Williams and Bagas, in prep.) indicate that it was deposited in a quiet and restricted shallow-water environment. Hickman et al. (1994) suggested that the Broadhurst Formation was deposited in an anoxic pelagic environment that was affected by periodic turbidity currents towards its base. The turbidity currents were possibly produced by basin subsidence (Hickman et al., 1994).

Deposition of the Throssell Group is interpreted to have commenced in a transgressional continental environment in an extensional regime (i.e. a rift basin). Deposition progressed from a fluvial environment to a deltaic shallow-water environment, probably due to subsidence controlled by extensional growth faults. The source of the deltaic shallow-water sediments was a continental landmass to the west or southwest. Final sedimentation was in a shallow-water and restricted euxinic environment. Hickman et al. (1994) suggested that the Throssell Group developed as a strike-slip basin or, more probably, as a series of such basins.

In summary, present evidence indicates that the Throssell Group was deposited in an extensional regime (i.e. rift or sag basin) between the Pilbara Craton and the ?North Australian Craton. This was followed by deformation (Miles Orogeny) and associated greenschist-facies metamorphism.

Sedimentary environment of the Tarcunyah Group

The Tarcunyah Group is a shallow-water succession deposited in a near-shore, ?marine environment (Williams and Bagas, in prep.). In contrast, the conglomerate at the base of the Throssell Group is predominantly sourced from the Rudall Complex (see above).

Palaeocurrent data from the Gunanya Sandstone and Choorun Formation of the Tarcunyah Group support the transport of clastic material from the southwest (Hickman and Bagas, in prep.). Williams and Trendall (in prep.) indicated that the Pilbara Craton was a topographic high during the deposition of the Tarcunyah Group, and that the present northwest–southeast trend of the group broadly reflects the original orientation of the basin in which it was deposited.

Structural differences between the Yeneena Supergroup and Tarcunyah Group

The Yeneena Supergroup (Throssell and Lamil Groups) and the Tarcunyah Group (Williams and Bagas, in prep.) are commonly separated by major D_6 faults (e.g. the Vines Fault, Southwest Thrust, and McKay Fault). The contact between the Throssell and Tarcunyah Groups in the southern part of CONNAUGHTON appears to be unconformable (see above), and a discontinuity (fault or unconformity) separates the Throssell and Lamil Groups (Hickman et al., 1994). There are no direct constraints on the age of the Throssell and Lamil Groups, other than they are both younger than the Rudall Complex, and the Throssell Group is older than the Lamil and Tarcunyah Groups.

The metamorphic grade of the Throssell, Lamil, and Tarcunyah Groups is commonly low, but in the southern part of the Paterson Orogen the Throssell Group is metamorphosed to greenschist facies and the Tarcunyah Group is metamorphosed to a lower grade (Williams and Bagas, in prep.). The regional grade of metamorphism for the Lamil Group is not clear, but is low in its southern exposure (Chin et al., 1982). Geochronological data indicate that greenschist-facies metamorphism may have occurred sometime after 1132 Ma in the Talbot and Connaughton Terranes (see **D_4 structures**). This is considered to be the maximum age for the Miles Orogeny (D_{3-4}). A considerable amount of largely unpublished isotopic data (Pb–Pb, K–Ar, and U–Pb) indicates that hydrothermal events related to mineralization occurred between 940 and 820 Ma in the Throssell Group. The mineralization is hosted by D_4 structures, suggesting that these hydrothermal events occurred between 940 and 820 Ma in the Throssell Group, that the events were syn- to post-D_4, and that the D_4 event is older than about 800 Ma. Therefore, the geochronological data from the Paterson Orogen indicate that the Miles Orogeny (D_{3-4}) occurred sometime between 1132 and 800 Ma.

A further difference between the Throssell and Tarcunyah Groups is the presence of a penetrative S_4 foliation in the Throssell Group. These structural and metamorphic differences suggest that the Throssell Group has experienced an earlier deformation (D_4), although each group has experienced compression in a northeast–southwest direction. This implies that the Tarcunyah Group may be younger than the D_4 event. Up to now it has been thought that the northeasterly to southwesterly orientated compression of the Paterson Orogen had occurred during one deformation event (D_4); however, the evidence now points to a protracted period of episodic deformation. Furthermore, palaeontological evidence from stromatolites and acritarchs indicate that the Tarcunyah Group is equivalent to Supersequence 1 of the Officer Basin (Walter et al., 1995; Bagas et al., 1995). This suggests that the age of the Tarcunyah Group is about 800 Ma, that the D_6 event was younger than 800 Ma, and the D_4 event was older than 800 Ma. The Tarcunyah Group is unconformably overlain by the upper Savory Group, which is younger than 610 Ma (Williams,

1992; Walter et al., 1995), establishing the minimum age for the group as older than 610 Ma.

The nature of the contact between the Throssell Group and overlying Lamil Group remains ambiguous. However, both groups appear to have experienced deformation events associated with the Miles Orogeny. If the contact is a tectonized conformity (considered the most likely), then the Lamil Group is only slightly younger than the Throssell Group and older than at least some parts of the Tarcunyah Group.

Post-orogenic granitoids are present in the Lamil Group near Telfer, where the Minyari monzogranite (633 ± 13 Ma) and Mount Crofton Granite (621 ± 13 Ma) form discrete circular to ovoid plutons (Chin et al., 1982). Therefore, the minimum age for the Lamil Group and the Miles Orogeny in the northern part of the Paterson Orogen is 630 Ma.

Paterson Orogeny

Table 3 summarizes the geochronological and geological data into a time sequence.

The last major event recorded in the Paterson Orogen was the Paterson Orogeny (D_6), which reactivated earlier structures. The D_6 event was also a compressional event oriented in a northeast–north-northeast to southwest–south-southwest direction, and was younger than 610 Ma and possibly around 550 Ma. Myers (1990a) suggested that the Paterson Orogen marked the collision and combination of the West Australian Craton with sialic crust to the northeast, between about 750 and 550 Ma. It is inferred that this collisional event may be synchronous with the Petermann Orogeny of central Australia, which occurred between 600 and 540 Ma (Grey, 1990; Camacho and Fanning, 1995; Walter et al., 1995); the King Leopold Orogeny of the Kimberley area, which occurred c. 560 Ma (Shaw et al., 1992); the Wells Foreland Basin of the upper Savory Group (Williams, 1992; Hocking et al., 1994); and the 750–540 Ma breakup of Rodina (Myers et al., 1996).

Williams (1992) suggested that during the Paterson Orogeny, the Wells Foreland Basin succession was deposited in an incipient foreland basin along the northeastern margin of the Savory Group. This orogeny post-dates the deposition of the glacigenic Boondawari Formation that is unconformably overlain by the foreland basin succession.

Clarke (1991) used the term 'Paterson Orogeny' for the deformation event responsible for the northwesterly trending D_4 folds, faults, and associated greenschist-facies metamorphism of the Throssell Group.

Recent authors have continued to call the D_4 event the Paterson Orogeny (Hickman and Clarke, 1994; Hickman et al., 1994; Hickman and Bagas, in prep.). Myers (1993) stated that the tectonic features of the Paterson Orogeny are thrusts and folds associated with greenschist-facies metamorphism (typical of the D_4 event). He also associated the Woodroffe Thrust (of the Petermann Orogeny) in the Musgrave Block with the Paterson Orogeny. Geophysical data indicate that structures associated with the Woodroffe Thrust extend to the northwest into the Paterson Orogen. These are now recognized as D_6 structures controlling the deposition of the upper Savory Group succession and are younger than 610 Ma (Bagas et al., 1995). The D_{3-4} event is at least older than about 700 Ma (Reed, A., and Smith, S., 1995, pers. comm.) and younger than c. 1132 Ma.

Table 3. Summary of geochronological data relevant to the evolution of the Paterson Orogen

Age range (Ma)	*Geological event*
2015–1802	Crystallization of granitic protoliths included in the lithologically layered orthogneiss on RUDALL
~2000–1760	Yapungku Orogeny (includes the D_1 and D_2 events)
pre-D_1	Deposition of the Connaughton Terrane succession and the older turbiditic/shale succession in the Talbot Terrane
~2000–1802	D_1
1801–1795	Crystallization of *ERge* protolith (post-dates D_1)
1790–1765	Crystallization of *ERga, ERgd* (on RUDALL), *ERgm,* and *ERgo* protoliths
pre-D_2	Deposition of the Fingoon Quartzite in the Talbot Terrane
1790–1760	D_2 partly synchronous with M_2
1476–1286	Crystallization of post-D_2 and pre-D_4 intrusive rocks
post–D_2, pre–D_4	Deposition of the Throssell Group
1290	Maximum age for D_4/M_4 affecting the Throssell Group
1200	Maximum age for the Tarcunyah Group
1132 ± 21	Crystallization or metamorphism of pegmatite dykes, minimum age for the Throssell Group
940–820	Epigenetic galena mineralization in the Throssell Group, minimum age for the Broadhurst Formation
820	Minimum age for D_4
800	Possible age for the Tarcunyah Group
900–610	Evolution of the Savory Group (post-dating the Throssell Group, and including Supersequences 1, 3, and 4)
630–620	Emplacement of post-D_4 granitoids before the Paterson Orogeny
≤610	D_6 related to deposition of Supersequences 3 and 4 of the Savory Group, minimum possible age of the Tarcunyah Group

The term 'Paterson Orogeny' is now restricted to the D_6 event that post-dated the glacigenic Boondawari Formation of the Savory Group (Williams, 1992) and dated at c. 610 Ma (Walter et al., 1995), and is a correlative of the Petermann Orogeny (Myers, 1990a).

Acknowledgements

The authors thank CRAE and PNC Exploration for their generous assistance during the fieldwork, access to colour aerial photographs and topographic maps, and helpful discussions. Likewise, valuable logistical support from Newcrest Mining Limited (Telfer) is gratefully acknowledged.

References

BAGAS, L., GREY, K., and WILLIAMS, I. R., 1995, Reappraisal of the Paterson Orogen and Savory Basin: Western Australia Geological Survey, Annual Review 1994–95, p. 55–63.

BAGAS, L., and SMITHIES, R. H., 1997, Palaeoproterozoic tectonic evolution of the Rudall Complex, and comparison with the Arunta Inlier and Capricorn Orogen: Western Australia Geological Survey, Annual Review 1996–97, p. 110–115.

BHATTACHARYA, A., KRISHNAKUMAR, K. R., RAITH, M., and SEN, S. K., 1991, An improved set of a–X parameters for Fe–Mg–Ca garnets and refinements of the orthopyroxene–garnet thermometer and the orthopyroxene–garnet–plagioclase–quartz barometer: Journal of Petrology, v. 32, p. 629–656.

BLOCKLEY, J. G., and de la HUNTY, L. E., 1975, Paterson Province, *in* The Geology of Western Australia: Western Australia Geological Survey, Memoir 2, p. 114–118.

BLOCKLEY, J. G., and MYERS, J. S., 1990, Proterozoic rocks of the Western Australian Shield — geology and mineralization, *in* Geology of the Mineral Deposits of Australia and Papua New Guinea *edited by* F. E. HUGHES: Australasian Institute of Mining and Metallurgy, Monograph 14, p. 607–615.

CAMACHO, A., and FANNING, C. M., 1995, Some isotopic constraints on the evolution of the granulite and upper amphibolite facies terranes in the eastern Musgrave Block, central Australia: Precambrian Research, v. 71, p. 155–181.

CAMPANA, B., HUGHES, F. E., BURNS, W. G., WHITCHER, I. G., and MUCENIEKAS, E., 1964, Discovery of the Hamersley iron deposits (Duck Creek – Mt Pyrton – Mt Turner area): Australasian Institute of Mining and Metallurgy, Proceedings, no. 210, p. 1–30.

CARSWELL, D. A., and O'BRIAN, P. J., 1993, Thermobarometry and geotectonic significance of high-pressure granulites — examples from the Moldanubian Zone of the Bohemian Massif in Lower Austria: Journal of Petrology, v. 34, p. 427–459.

CHIN, R. J., WILLIAMS, I. R., WILLIAMS, S. J., and CROWE, R. W. A., 1980, Rudall, W.A.: Western Australia Geological Survey, 1:250 000 Geological Series Explanatory Notes, 22p.

CHIN, R. J., and de LAETER, J. R., 1981, The relationship of new Rb–Sr isotopic dates from the Rudall Metamorphic Complex to the geology of the Paterson Province: Western Australia Geological Survey, Annual Report 1980, p. 132–139.

CHIN, R. J., HICKMAN, A. H., and TOWNER, R. R., 1982, Paterson Range, W.A. (2nd edition): Western Australia Geological Survey, 1:250 000 Geological Series Explanatory Notes, 29p.

CHRISTIE-BLICK, N., DYSON, I. A., and von der BORCH, C. C., 1995, Sequence stratigraphy and the interpretation of Neoproterozoic earth history: Precambrian Research, v. 73, p. 3–26.

CLARKE, G. L., 1991, Proterozoic tectonic reworking in the Rudall Complex, Western Australia: Australian Journal of Earth Sciences, v. 38, p. 31–44.

CROWE, R. W. A., 1975, The classification, genesis and evaluation of sand dunes in the Great Sandy Desert: Western Australia Geological Survey, Annual Report 1974, p. 46–49.

CROWE, R. W. A., and CHIN, R. J., 1979, Runton, W.A.: Western Australia Geological Survey, 1:250 000 Geological Series Explanatory Notes, 16p.

DANIELS, J. L., and HORWITZ, R. C., 1969, Precambrian tectonic units of Western Australia: Western Australia Geological Survey, Annual Report 1968, p. 37–38.

GOELLNICHT, N. M., GROVES, D. I., and McNAUGHTON, N. J., 1991, Late Proterozoic fractionated granitoids of the mineralized Telfer area, Paterson Province, Western Australia: Precambrian Research, v. 51, p. 375–391.

GRAHAM, C. M., and POWELL, R., 1984, A garnet–hornblende geothermometer — calibration, testing, and application to the Pelona Schist, Southern California: Journal of Metamorphic Geology, v. 2, p. 13–21.

GREY, K., 1990, Birrindudu Basin, *in* Geology and mineral resources of Western Australia: Western Australia Geological Survey, Memoir 3, p. 349–362.

HARLEY, S. L., 1984, An experimental study of partitioning of Fe and Mg between garnet and orthopyroxene: Contributions to Mineralogy and Petrology, v. 86, p. 359–373.

HARLEY, S. L., and GREEN, D. H., 1982, Garnet–orthopyroxene barometry for granulites and peridotites: Nature, v. 300, p. 697–701.

HICKMAN, A. H., and BAGAS, L., 1994, Tectonic evolution and economic geology of the Paterson Orogen — a major reinterpretation based on detailed geological mapping: Western Australia Geological Survey, Annual Review 1993–94, p. 67–76.

HICKMAN, A. H., and BAGAS, L., in prep., Geology of the Rudall 1:100 000 sheet: Western Australia Geological Survey, 1:100 000 Geological Series Explanatory Notes.

HICKMAN, A. H., and CLARKE, G. L., 1994, Geology of the Broadhurst 1:100 000 sheet: Western Australia Geological Survey, 1:100 000 Geological Series Explanatory Notes, 40p.

HICKMAN, A. H., WILLIAMS, I. R., and BAGAS, L., 1994, Proterozoic geology and mineralization of the Telfer–Rudall region: Geological Society of Australia (W.A. Division), Excursion Guide 5, 60p.

HOCKING, R. M., MORY, A. J., and WILLIAMS, I. R., 1994, An atlas of Neoproterozoic and Phanerozoic basins in Western Australia, *in* The Sedimentary Basins of Western Australia *edited by* P. G. PURCELL and R. R. PURCELL: Petroleum Exploration Society of Australia, Symposium, Perth, W.A., 1994, Proceedings, p. 21–43.

HOLLAND, T., and BLUNDY, J., 1994, Non-ideal interactions in calcic amphiboles and their bearing on amphibole–plagioclase thermometry: Contributions to Mineralogy and Petrology, v. 116, p. 433–447.

IASKY, R. P., 1990, Officer Basin, *in* Geology and mineral resources of Western Australia: Western Australia Geological Survey, Memoir 3, p. 362–380.

INDARES, A., and MARTIGNOLE, J., 1985, Biotite–garnet geothermometry in the granulite facies — the influence of Ti and Al in biotite: American Mineralogist, v. 70, p. 272–278.

IDNURM, M., and SENIOR, B. R., 1978, Palaeomagnetic ages of Late Cretaceous and Tertiary weathering profiles in the Eromanga Basin, Queensland: Palaeography, Palaeoclimatology, Palaeoecology, v. 24, p. 263–277.

JENNINGS, J. N., and MABBUTT, J. A., 1971, Landform studies from Australia and New Guinea: Canberra, Australian National University Press, 434p.

KOHN, M. J., and SPEAR, F. S., 1990, Two new barometers for garnet amphibolites with applications to southeastern Vermont: American Mineralogist, v. 75, p. 89–96.

LEE, H. Y., and GANGULY, J., 1988, Equilibrium compositions of coexisting garnet and orthopyroxene — experimental determinations in the system FeO–MgO–Al_2O_3–SiO_2, and applications: Journal of Petrology, v. 29 (1), p. 93–113.

McNAUGHTON, N. J., and GOELLNICHT, N. M., 1990, The age and radiothermal properties of the Mount Crofton Granite: Australian Journal of Earth Sciences, v. 37, p. 103–106.

MYERS, J. S., 1990a, Precambrian tectonic evolution of part of Gondwana, southwestern Australia: Geology, v. 18, p. 537–540.

MYERS, J. S., 1990b, Albany–Fraser Orogen, *in* Geology and mineral resources of Western Australia: Western Australia Geological Survey, Memoir 3, p. 255–264.

MYERS, J. S., 1993, Precambrian history of the West Australian Craton and adjacent orogens: Earth and Planetary Science, Annual Review, v. 21, p. 453–485.

MYERS, J. S., SHAW, R. D., and TYLER, I. M., 1996, Tectonic evolution of Proterozoic Australia: Tectonics, v. 15 (6), p. 1431–1446.

NELSON, D. R., 1995, Compilation of SHRIMP U–Pb zircon geochronology data, 1994: Western Australia Geological Survey, Record 1995/3, 244p.

NELSON, D. R., 1996, Compilation of SHRIMP U–Pb zircon geochronology data, 1995: Western Australia Geological Survey, Record 1996/5, 168p.

NEWTON, R. C., and PERKINS, D. I., 1982, Thermodynamic calibration of geobarometers based on the assemblages garnet–plagioclase–orthopyroxene(–clinopyroxene)–quartz: American Mineralogist, v. 67, p. 202–222.

PIRAJNO, F., BAGAS, L., SWAGER, C. P., OCCHIPINTI, S., and ADAMIDES, N. G., 1996, A reappraisal of the stratigraphy of the Glengarry Basin: Western Australia Geological Survey, Annual Review 1995–96, p. 81–87.

RUST, B. R., 1981, Coarse alluvial deposits, *in* Facies Models *edited by* R. G. WALKER: Canada Geological Association, p. 9–21.

SHAW, R. D., TYLER, I. M., GRIFFIN, T. J., and WEBB, A., 1992, New K–Ar constraints on the onset of subsidence in the Canning Basin, Western Australia: Australia BMR, Journal of Australian Geology and Geophysics, v. 13, p. 31–35.

SMITHIES, R. H., and BAGAS, L., 1997, High pressure amphibolite–granulite facies metamorphism in the Palaeoproterozoic Rudall Complex, central Western Australia: Precambrian Research, v. 83 (4), p. 243–265.

TRAVES, D. M., CASEY, J. N., and WELLS, A. T., 1956, The geology of the southwestern Canning Basin, Western Australia: Australia BMR, Report 29, 76p.

TRENDALL, A. F., 1974, The age of a granite near Mount Crofton, Paterson Range Sheet: Western Australia Geological Survey, Annual Report 1974, p. 92–96.

THORNE, A. M., and SEYMOUR, D. B., 1991, Geology of the Ashburton Basin, Western Australia: Western Australia Geological Survey, Bulletin 139, 141p.

TYLER, I. M., 1991, The geology of the Sylvania Inlier and the southern Hamersley Basin: Western Australia Geological Survey, Bulletin 138, 108p.

WALTER, M. R., VEEVERS, J. J., CALVER, C. R., and GREY, K., 1995, Neoproterozoic stratigraphy of the Centralian Superbasin, Australia: Precambrian Research, v. 73, p. 173–195.

WILLIAMS, I. R., 1990, Yeneena Basin, *in* Geology and mineral resources of Western Australia: Western Australia Geological Survey, Memoir 3, p. 277–282.

WILLIAMS, I. R., 1992, Geology of the Savory Basin, Western Australia: Western Australia Geological Survey, Bulletin 141, 115p.

WILLIAMS, I. R., and BAGAS, L., in prep., Geology of the Throssell 1:100 000 sheet: Western Australia Geological Survey, 1:100 000 Geological Series Explanatory Notes.

WILLIAMS, I. R., BRAKEL, A. T., CHIN, R. J., and WILLIAMS, S. T., 1976, The stratigraphy of the Eastern Bangemall Basin and Paterson Province: Western Australia Geological Survey, Annual Report 1975, p. 79–83.

WILLIAMS, I. R., and MYERS, J. S., 1990, Paterson Orogen, *in* Geology and mineral resources of Western Australia: Western Australia Geological Survey, Memoir 3, p. 274–75.

WILLIAMS, I. R., and TRENDALL, A. F., in prep., Geology of the Pearana 1:100 000 sheet: Western Australia Geological Survey, 1:100 000 Geological Series Explanatory Notes.

YEATES, A. N., and CHIN, R. J., 1979, Tabletop, W.A.: Western Australia Geological Survey, 1:250 000 Geological Series Explanatory Notes, 19p.

Appendix 1

Analytical data for rocks collected on CONNAUGHTON

GSWA sample	*115821*	*115831*	*115892*	*115900*	*115894*	*124805*	*115847*	*115853*	*115854*	*115893*
Rock type	*Pgl*	*Pgl*	*Pgl*	*Pgl*	*Pgf*	*PRgh*	*PRgh*	*PRgh*	*Trondhj*	*PRgh*
Location (AMG)	*830660*	*817682*	*838660*	*996801*	*851615*	*910707*	*766689*	*788659*	*788659*	*950619*
						Percentage				
SiO_2	74.85	75.50	75.10	75.30	55.70	67.70	63.50	68.60	73.90	65.60
TiO_2	0.06	0.07	0.07	0.20	0.97	0.31	0.61	0.42	0.06	0.66
Al_2O_3	13.27	13.34	13.10	12.53	16.55	16.50	14.70	13.68	14.43	14.95
Fe_2O_3	0.48	0.58	0.36	0.91	2.45	1.41	2.08	1.65	0.50	1.99
FeO	0.30	0.57	0.34	0.53	4.64	1.18	3.08	2.15	0.28	2.59
MnO	0.04	0.03	0.02	0.01	0.14	0.04	0.11	0.07	0.01	0.08
MgO	0.12	0.52	0.15	0.18	4.11	0.51	2.10	1.26	0.35	1.37
CaO	0.50	0.31	0.88	1.04	5.79	3.43	3.86	2.95	2.34	3.01
Na_2O	3.99	3.92	3.82	2.82	2.73	4.83	3.35	3.40	5.45	2.76
K_2O	4.75	4.87	4.94	5.65	3.51	2.62	3.92	3.76	1.51	4.28
P_2O_5	0.02	0.03	0.02	0.02	0.41	0.12	0.18	0.10	0.01	0.21
S	<0.01	<0.01	<0.01	<0.01	0.01	<0.01	<0.01	<0.01	<0.01	<0.01
H_2O^-	0.25	0.19	0.03	0.08	0.11	0.06	0.10	0.13	0.05	0.08
H_2O^+	0.54	0.64	0.47	0.28	1.77	0.82	1.13	0.88	0.84	1.13
CO_2	0.09	0.15	0.22	0.04	0.11	0.07	0.07	0.07	0.29	0.11
LOI	nd	nd	nd	nd	nd	nd	nd	nd	nd	nd
Total	**99.26**	**100.72**	**99.52**	**99.59**	**99.00**	**99.60**	**98.79**	**99.12**	**100.02**	**98.82**
						Parts per million				
Ba	252	453	334	1 296	1 246	417	944	1 222	567	1 120
Ce	13.1	49.7	50.3	76.1	164.9	187.1	95.4	120.0	3.8	132.7
Co	2	4	3	2	29	5	18	12	2	15
Cr	5	7	7	17	71	10	71	43	10	20
Cu	38	7	5	4	28	2	15	15	10	11
Ga	19.2	20.1	17.5	17.6	26.4	21.8	23	20.3	13.5	21.8
La	7.3	22.7	36.3	38.9	68.6	100.9	38.2	56.7	2.6	61.2
Nb	17.8	18.7	2.8	2.8	17.9	9.0	16.2	16.3	1.2	15.7
Ni	11.0	3.0	2.0	3.0	43.0	2.0	31.0	17.0	6.0	14.0
Pb	23.0	23.0	36.0	30.0	21.0	54.0	36.0	41.0	64.0	28.0
Rb	227.0	169.0	187.0	185.0	175.0	52.0	187.0	131.0	34.0	146.0
Sr	15.0	57.0	43.0	93.0	298.0	100.0	264.0	244.0	124.0	170.0
Th	11.3	30.2	24.5	21.3	13.8	90.3	21.7	31.7	0.6	46.3
U	1.7	4.6	7.7	3.4	1.9	2.5	4.5	14.2	1.8	2.3
V	3.0	5.0	3.0	7.0	147.0	13.0	87.0	52.0	12.0	72.0
Y	31.1	27.2	35.1	21.9	53.2	8.0	31.2	32.7	1.0	27.3
Zn	43.0	21.0	18.0	20.0	75.0	35.0	63.0	49.0	13.0	54.0
Zr	97.9	114.1	136.5	147.3	308.4	791.4	193.1	215.0	112.4	306.2

Appendix 1 (continued)

GSWA sample	*115863*	*115865*	*115866*	*115878*	*115897*	*124806*	*115784*	*115656*	*115795*	*115797*
Rock type	*Trondhj*	*ERnc*	*ERnc*	*ERng*	*ERng*	*ERng*	*ERac*	*ERac*	*ERac*	*ERac*
Location (AMG)	*814638*	*852725*	*852726*	*817618*	*851722*	*909706*	*511064*	*663909*	*524059*	*531059*
						Percentage				
SiO_2	72.80	73.90	70.90	72.60	69.50	69.80	48.90	47.40	46.80	47.40
TiO_2	0.32	0.23	0.38	0.30	0.60	0.56	0.20	0.85	0.80	0.82
Al_2O_3	13.76	13.36	14.51	12.87	13.20	13.57	16.70	14.20	14.20	14.90
Fe_2O_3	1.10	0.58	1.18	0.92	1.63	1.18	1.63	1.39	1.08	1.75
FeO	0.93	1.34	1.85	1.07	2.95	2.49	5.14	9.02	9.45	9.16
MnO	0.02	0.08	0.08	0.04	0.09	0.09	0.18	0.23	0.18	0.19
MgO	0.52	0.51	0.80	0.36	0.87	0.81	10.15	8.93	8.09	9.36
CaO	3.72	1.48	2.28	0.98	2.39	2.00	13.90	12.90	15.00	12.70
Na_2O	4.60	2.84	3.29	2.50	2.72	2.47	1.17	1.61	1.77	1.82
K_2O	0.68	4.74	3.70	6.37	4.35	4.89	0.25	0.65	0.18	0.28
P_2O_5	0.08	0.08	0.06	0.07	0.16	0.14	0.02	0.07	0.10	0.06
S	<0.01	<0.01	<0.01	<0.01	<0.01	<0.01	0.01	<0.01	0.05	<0.01
H_2O^-	0.19	0.13	0.12	0.06	0.09	0.13	nd	nd	nd	nd
H_2O^+	0.89	0.34	<0.01	0.64	0.70	0.88	nd	nd	nd	nd
CO_2	0.04	0.04	0.04	0.26	0.04	0.04	nd	nd	nd	nd
LOI	nd	nd	nd	nd	nd	nd	1.71	1.69	2.98	1.60
Total	**99.65**	**99.65**	**99.19**	**99.04**	**99.29**	**99.05**	**99.96**	**99.94**	**100.68**	**100.04**
						Parts per million				
Ba	663	742	765	840	1 056	975	51	204	49	43
Ce	52.7	157.7	69.0	264.4	52.4	52.1	<6	<6	<6	<6
Co	4	2	9	4	12	10	45		57	53
Cr	22	19	26	12	46	29	108	295	656	198
Cu	3	5	3	5	8	4	166	129	86	83
Ga	15.3	18.9	19.5	19.3	18.5	17.3	12	15	14	16
La	22	78.9	31.6	128.4	27.8	28.4	<3	5	4	4
Nb	4.7	10.3	2.2	20.9	4.4	6.0	<7	<7	<7	<7
Ni	6.0	4.0	8.0	3.0	13.0	6.0	154	186	205	105
Pb	35.0	16.0	28.0	55.0	23.0	28.0	<4	8	8	4
Rb	155.0	10.0	102.0	247.0	145.0	123.0	<2	7	2	3
Sr	128.0	459.0	178.0	138.0	125.0	105.0	111	146	145	122
Th	7.2	48.5	9.4	91.0	<0.5	<0.5	<2	<2	<2	<2
U	0.6	5.7	<0.5	8.4	<0.5	<0.5	<2	<2	<2	<2
V	22.0	19.0	30.0	14.0	50.0	41.0	157	304	234	318
Y	30.6	10.8	17.6	37.7	26.3	30.7	5	16	22	15
Zn	21.0	10.0	36.0	17.0	47.0	40.0	66	82	100	78
Zr	97.6	423.2	127.7	240.9	166.3	193.5	12	51	52	40

Appendix 1 (continued)

GSWA sample	*115798*	*115789*	*115792*	*115840*	*115841*	*115846*	*115885*	*115888*	*115890*
Rock type	*ERac*	*ERam*	*ERam*	*ERam*	*ERam*	*ERam*	*ERam*	*ERam*	*ERam*
Location (AMG)	*544030*	*811686*	*811693*	*818665*	*818665*	*782690*	*830613*	*835620*	*838623*
					Percentage				
SiO_2	50.20	50.00	52.70	53.00	51.80	48.30	48.20	49.60	47.60
TiO_2	0.35	1.81	0.46	0.43	0.42	1.21	1.33	1.50	1.51
Al_2O_3	15.40	13.10	15.40	15.73	15.36	15.49	14.46	13.59	13.58
Fe_2O_3	1.68	6.93	3.86	2.37	2.62	3.06	3.84	5.95	3.99
FeO	6.11	7.92	5.17	4.62	5.59	7.41	7.97	8.59	9.10
MnO	0.17	0.22	0.16	0.12	0.15	0.17	0.19	0.22	0.23
MgO	9.18	5.68	6.45	6.68	6.93	6.66	6.59	5.13	6.66
CaO	13.70	8.70	9.65	11.00	10.80	10.60	10.30	9.02	10.40
Na_2O	1.19	2.94	1.69	1.51	1.71	2.68	2.42	2.54	2.37
K_2O	0.44	0.65	1.34	0.63	0.49	1.16	1.26	0.47	1.35
P_2O_5	0.04	0.18	0.06	0.08	0.07	0.10	0.14	0.12	0.16
S	0.03	<0.01	<0.01	<0.01	<0.01	<0.01	<0.01	0.06	<0.01
H_2O^-	nd	nd	nd	0.13	0.14	0.20	0.21	0.18	0.12
H_2O^+	nd	nd	nd	2.57	2.72	2.02	1.87	1.26	1.89
CO_2	nd	nd	nd	0.15	0.15	0.22	0.18	0.11	0.07
LOI	1.54	2.23	2.77	nd	nd	nd	nd	nd	nd
Total	**100.03**	**100.36**	**99.71**	**99.02**	**98.95**	**99.28**	**98.96**	**98.34**	**99.03**
					Parts per million				
Ba	95	143	405	247	194	423	250	179	405
Ce	8	21	24	34	29	27	29	16	29
Co	45	59	45	36	40	48	52	53	57
Cr	65	87	59	76	61	108	170	44	136
Cu	132	59	73	41	75	33	92	198	151
Ga	15	19	14	19	19	22	20	22	23
La	6	12	11	17	14	12	14	7	13
Nb	<7	13	<7	9	6	12	7	4	8
Ni	86	60	106	84	95	79	86	41	69
Pb	14	6	8	12	15	14	5	6	9
Rb	5	21	48	22	24	45	39	14	42
Sr	136	123	196	198	217	274	296	169	191
Th	<2	<2	5	6	4	2	2	1	2
U	2	<2	<2	2	2	1	1	<0.5	1
V	213	375	204	140	149	240	232	362	290
Y	11	29	17	15	15	17	20	25	25
Zn	60	117	68	52	65	78	98	94	98
Zr	36	127	68	70	57	84	92	98	118

Appendix 1 (continued)

GSWA sample	*124804*	*113089*	*115876*	*115877*	*115886*	*115889*	*117722*	*117730*	*113096*
Rock type	*ERam*	*ERam*	*ERag*	*ERag*	*ERag*	*ERag*	*ERag*	*ERag*	*ERag*
Location (AMG)	*916722*	*675653*	*815629*	*819618*	*830613*	*843613*	*588741*	*632729*	*682664*
					Percentage				
SiO_2	48.40	48.50	49.00	49.10	48.20	47.40	49.30	45.50	48.50
TiO_2	0.63	1.53	1.18	1.09	1.28	1.40	1.23	1.25	1.23
Al_2O_3	15.49	14.00	13.12	13.11	12.98	13.16	13.80	13.50	13.40
Fe_2O_3	4.15	4.70	4.26	2.56	3.18	4.56	3.91	3.01	3.28
FeO	7.33	7.53	8.40	9.39	10.10	8.94	9.16	9.30	9.19
MnO	0.20	0.19	0.19	0.21	0.21	0.21	0.20	0.22	0.19
MgO	6.97	6.00	6.62	7.18	6.28	6.11	6.93	5.49	5.80
CaO	10.80	11.20	10.90	10.30	10.50	10.20	11.10	14.20	11.50
Na_2O	1.79	1.98	2.14	1.76	2.03	2.51	2.04	2.78	2.06
K_2O	0.37	0.79	0.67	0.67	0.62	0.67	0.26	0.32	0.45
P_2O_5	0.07	0.15	0.09	0.09	0.12	0.11	0.10	0.20	0.10
S	<0.01	<0.01	0.05	0.03	0.11	0.06	0.03	0.11	0.05
H_2O^-	0.09	nd	0.13	0.07	0.11	0.06	nd	nd	nd
H_2O^+	2.49	nd	2.07	2.21	2.34	2.28	nd	nd	nd
CO_2	0.07	nd	0.22	0.44	0.81	1.47	nd	nd	nd
LOI	nd	2.74	nd	nd	nd	nd	1.92	4.23	3.00
Total	**98.85**	**99.31**	**99.04**	**98.21**	**98.87**	**99.14**	**99.98**	**100.11**	**98.75**
					Parts per million				
Ba	109	304	183	119	170	151	96	120	65
Ce	29	18	15	14	16	16	<6	16	7
Co	57		54	58	59	51	58	60	–
Cr	101	111	117	131	104	98	192	169	179
Cu	3	192	146	143	88	211	200	84	217
Ga	18	17	20	21	21	22	17	17	16
La	13	6	7	6	7	7	6	11	<5
Nb	4	8	4	3	5	4	<7	<7	<7
Ni	102	78	83	82	61	62	121	107	103
Pb	13	7	10	11	7	6	5	7	7
Rb	8	31	20	25	16	19	5	7	20
Sr	136	218	304	192	229	37	196	157	172
Th	1	<2	1	1	1	1	<2	<2	<2
U	<0.5	<2	<0.5	<0.5	<0.5	<0.5	<2	<2	<2
V	227	355	286	310	337	323	397	353	383
Y	16	25	20	21	22	22	21	26	23
Zn	85	107	91	92	97	95	101	140	94
Zr	59	116	79	78	84	87	80	85	78

NOTES: Major- and trace-element analyses of mafic rocks by XRF, except FeO, which was determined titrimetrically. Trace-element concentrations of felsic rocks were determined by ICP-AES (for Co, Cr, Cu, Ni, V, and Zn) or ICP-MS. All analyses preformed by Chemistry Centre (WA)
Localities are specified by the Australian Map Grid (AMG) standard six-figure reference system whereby the first group of three figures (eastings) and the second group (northings) together uniquely define position, on this sheet, to within 100 m
nd: not determined
Rock type: codes are described in the text
Trondhj: trondhjemite

Appendix 2

Analytical data for iron-rich and gossanous samples from CONNAUGHTON

GSWA sample number	*Minor*	*Major*	*112997*	*113000*	*113010*	*113012*	*113014*	*113024*	*113055*	*113059*	*113060*	*117761*	*117763*	*117787*	*117789*
Location (AMG)	*anomaly*	*anomaly*	*535752*	*564783*	*553680*	*558669*	*556654*	*575672*	*516579*	*532668*	*559665*	*624792*	*617798*	*662742*	*663775*
									Parts per million						
Ag	>50	>100	1	2	1	2	1	1	1	1	1	2	<1	11	10
As	>100	>500	6	<4	23	29	19	6	14	<4	5	<3	5	<3	[a]263
Au (ppb)	>100	>500	3	3	5	32	40	nd	16	11	8	16	7	[b]1 000	16
Ba	>1 000	>10 000	142	62	371	77	51	705	153	117	[a]1 008	21	261	343	552
Bi	>50	>100	<4	<4	<4	16	<4	<4	<4	<4	<4	5	<4	[a]51	<4
Ce	>200	>500	111	180	<6	<6	<6	132	31	<6	41	0.5	15.7	22.1	11.3
Co	>500	>1 000	33	<3	12	65	<3	nd	16	36	<3	<3	70	121	18
Cr	>500	>1 000	121	39	13	31	15	352	20	[b]1 559	69	7	[b]1 740	25	8
Cu	>500	>1 000	126	218	148	[a]584	4	46	67	152	23	29	108	[b]194 000	[b]39 900
Ga	>50	>100	4	3	<3	<3	<3	20	<3	<3	5	4	7	6	4
Ge	>10	>50	<3	<3	<3	<3	<3	<3	<3	<3	7	<3	<3	<3	4
La	>100	>500	[a]200	[a]114	<5	<5	5	64	23	<5	21	0.4	7.2	8.2	6.3
Mn	>10 000	>100 000	232	60	[a]11 050	355	<5	nd	[a]18 260	1 410	244	<5	1 810	[a]2 280	119
Mo	>50	>100	5	13	12	2	4	<2	3	<2	2	4	1	[a]70	20
Nb	>50	>150	29	<7	<7	<7	<7	[a]47	<7	<7	<7	<7	<7	<7	<7
Ni	>500	>1 000	163	31	131	10	16	283	46	[b]1 565	18	7	340	91	37
Pb	>500	>1 000	21	[a]516	6	12	5	7	161	7	14	[b]2 660	9	13	[b]2 260
Pd (ppb)	>100	>500	nd	nd	nd	nd	nd	nd	nd	nd	nd	4	3	22	15
Pt (ppb)	>100	>500	nd	nd	nd	nd	nd	nd	nd	nd	nd	<2	8	6	40
Rb	>100	>500	<2	<2	<2	3	<2	55	<2	<2	22	2	10	<2	2
Sb	>50	>100	<4	<4	<4	<4	<4	<4	<4	<4	<4	4	<4	<4	4
Sc	>50	>100	nd	nd	nd	nd	nd	nd	nd	nd	nd	<1	35	2	2
Sn	>500	>1 000	13	<4	7	4	<4	5	<4	<4	<4	<4	<4	29	<4
Sr	>500	>1 000	39	21	23	14	45	567	76	6	37	<2	40	27	10
Ta	>50	>150	nd	nd	nd	nd	nd	nd	nd	nd	nd	<5	<5	<5	<5
Te	>10	>50	<6	<6	<6	<6	<6	<6	<6	<6	<6	<6	<6	7	<6
Th	>50	>100	6	<2	<2	2	<2	10	<2	<2	4	<2	3	3	<2
U	>50	>100	3	2	7	2	<2	2	2	5	<2	<2	<2	19	10
V	>500	>1 000	89	25	88	23	50	189	53	43	164	7	173	150	63
W	>50	>100	19	4	11	5	[a]51		6	<4	8	<4	<4	<4	<4
Y	>100	>500	[a]217	19	14	37	<2	27	31	4	23	<2	12	3	<2
Zn	>500	>1 000	371	197	30	4	10	87	60	40	8	169	70	154	445
Zr	>500	>1 000	230	17	12	10	5	388	39	12	32	18	32	20	16

NOTES: Trace elements in parts per million unless otherwise specified
nd: not determined
(a) minor anomaly
(b) major anomaly
Localities are specified by the Australian Map Grid (AMG) standard six-figure reference system whereby the first group of three figures (eastings) and the second group (northings) together uniquely define position, on this sheet, to within 100 m

Appendix 2 (continued)

GSWA sample number *Location (AMG)*	*Minor anomaly*	*Major anomaly*	*113061* *563583*	*113069* *601599*	*113073* *740604*	*113094* *682661*	*117728* *570697*	*117739* *713694*	*117746* *573823*	*117747* *560829*	*117753* *519837*
						Parts per million					
Ag	>50	>100	1	1	1	1	[b]300	1	nd	<1	<1
As	>100	>500	4	<4	5	<4	49	<4	<4	3	<3
Au (ppb)	>100	>500	5	4	4	nd	nd	nd	nd	46	51
Ba	>1 000	>10 000	[a]1 000	84	[a]1 115	263	<11	247	[a]1 140	101	[a]1 810
Bi	>50	>100	<4	<4	<4	<4	5	<4	<4	<4	<4
Ce	>200	>500	42	37	12	35	54	14	18.2	[a]265	[a]250
Co	>500	>1 000	<3	<3	<3	nd	12	<3	48	42	110
Cr	>500	>1 000	44	55	24	[a]628	16	18	170	33	18
Cu	>500	>1 000	26	156	56	166	[b]167 600	43	101	[a]573	225
Dy	>5	>50	nd	nd	nd	nd	nd	nd	nd	[a]34.8	[a]22.3
Er	>5	>50	nd	nd	nd	nd	nd	nd	nd	[a]18.9	[a]12.8
Eu	>5	>50	nd	nd	nd	nd	nd	nd	nd	[a]8.8	[a]5.2
Ga	>50	>100	4	11	<3	16	<3	<3	18	<3	3
Gd	>50	>100	nd	nd	nd	nd	nd	nd	nd	[a]58.9	31.5
Ge	>10	>50	8	3	<3	<3	<3	<3	<3	<3	<3
Ho	>10	>50	nd	nd	nd	nd	nd	nd	nd	7.2	5.1
La	>100	>500	23	24	10	14	34	8	7.2	[a]270	[a]123
Lu	>5	>25	nd	nd	nd	nd	nd	nd	nd	2.7	1.7
Mn	>10 000	>100 000	236	[a]21 150	317	nd	267	[a]12 990	nd	375	5 990
Mo	>50	>100	3	<2	<2	<2	<2	<2	nd	2	4
Nb	>50	>150	<7	<7	<7	9	<7	<7	nd	<7	<7
Nd	>50	>150	nd	nd	nd	nd	nd	nd	nd	[b]245	[a]82
Ni	>500	>1 000	14	27	8	168	20	37	39	117	161
Pb	>500	>1 000	12	4	13	8	[a]520	4	<4	63	16
Pd (ppb)	>100	>500	nd	nd	nd	nd	nd	nd	nd	2	6
Pt (ppb)	>100	>500	nd	nd	nd	nd	nd	nd	nd	<2	<2
Pr	>50	>150	nd	nd	nd	nd	nd	nd	nd	[a]60	15.6
Rb	>100	>500	22	4	<2	34	<2	<2	4	3	<2
Sb	>50	>100	<4	<4	<4	<4	<4	<4	<4	<4	<4
Sc	>50	>100	nd	nd	nd	nd	nd	nd	nd	9	24
Sm	>50	>100	nd	nd	nd	nd	nd	nd	nd	48.6	18.1
Sn	>500	>1 000	<4	15	<4	4	<4	<4	<4	5	<4
Sr	>500	>1 000	38	28	19	165	3	33	247	12	59
Ta	>50	>150	nd	nd	nd	nd	nd	nd	nd	<5	<5
Tb	>50	>150	nd	nd	nd	nd	nd	nd	nd	6.8	4.2
Te	>10	>50	<6	<6	<6	<6	<6	<6	<6	<6	<6
Th	>50	>100	5	<2	3	6	2	2	1.7	<2	<2
Tm	>5	>25	nd	nd	nd	nd	nd	nd	nd	3	2.1
U	>50	>100	<2	<2	<2	<2	4	<2	0.2	7	5
V	>500	>1 000	169	120	41	336	104	27	339	73	335
W	>50	>100	4	<4	5	nd	<4	5	<4	20	23
Y	>100	>500	25	25	5	24	18	12	21.6	[a]154	[a]203
Yb	>50	>150	nd	nd	nd	nd	nd	nd	nd	16.7	10.9
Zn	>500	>1 000	7	71	4	104	290	3	110	185	[a]750
Zr	>500	>1 000	24	41	20	173	25	7	146	8	29

AUSTRALIA 1:100 000 GEOLOGICAL SERIES

CONNAUGHTON

GEOLOGICAL SURVEY OF WESTERN AUSTRALIA

SHEET 3452

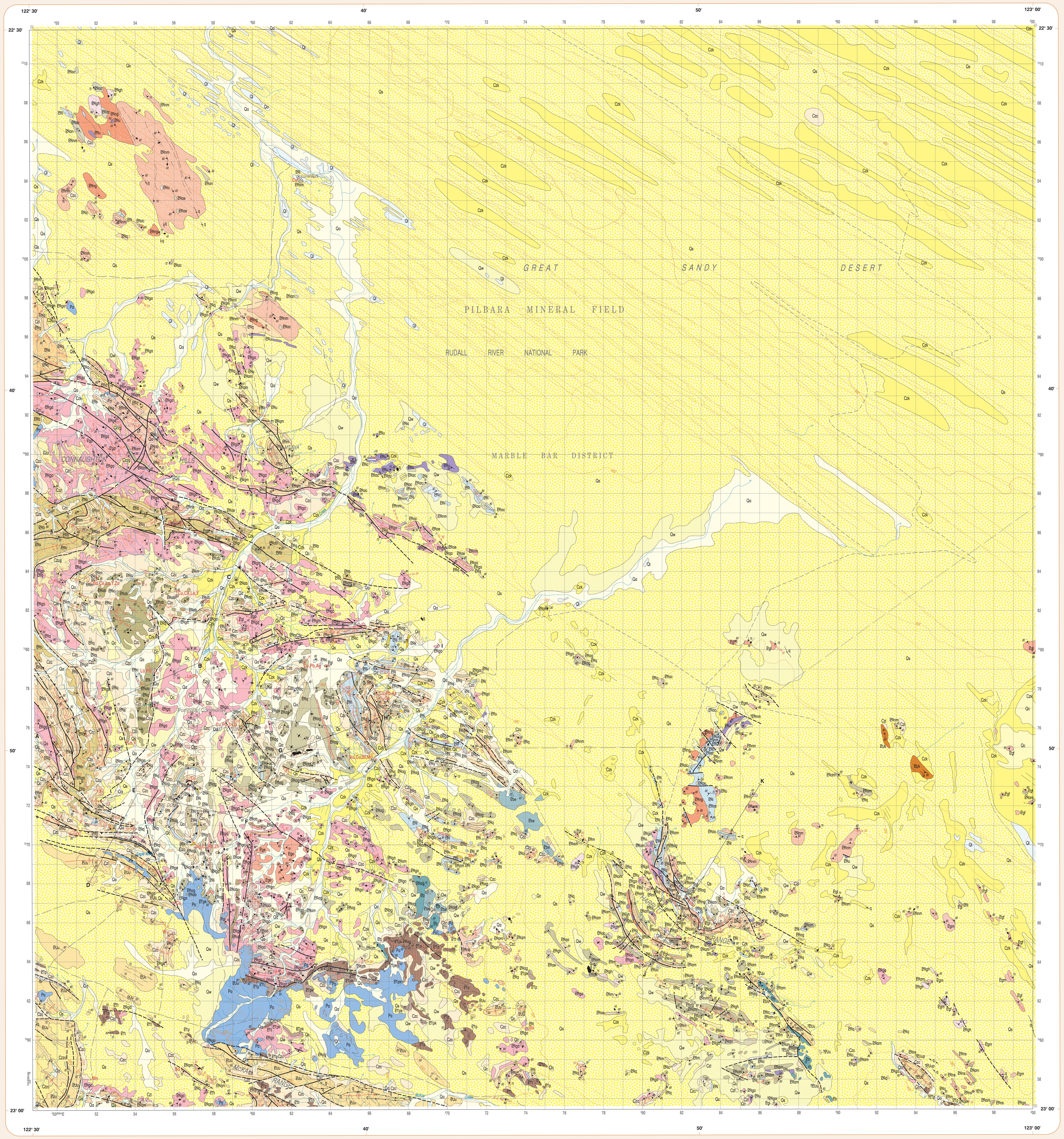

DIAGRAMMATIC SECTIONS

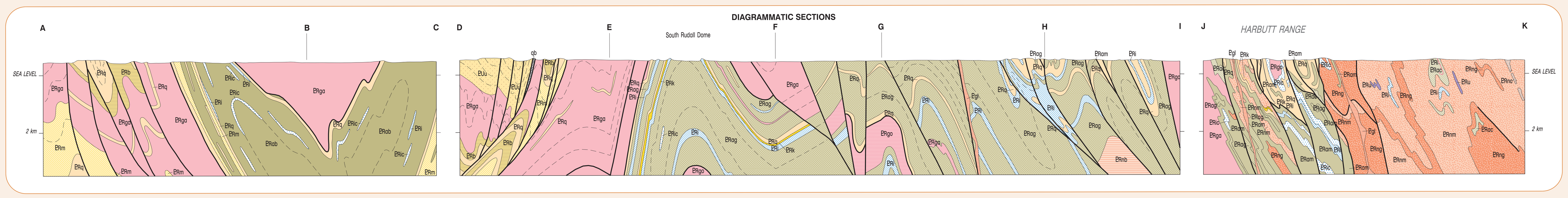

PHANEROZOIC — CAINOZOIC — QUATERNARY

Qa	Qc	Ql	Qp	Qs	Qw

Qa Alluvium—sand and gravel in drainage channels, and sand, partly reworked by wind action, on floodplains
Qc Colluvium—locally derived sand and gravel; in scree and outwash-fan deposits
Ql Playa and claypan deposits—clay and silt; saline and gypsiferous in part
Qp Lag and eolian deposits—sand with ferricrete pebbles and sand-sized particles
Qs Eolian sand; includes seif dunes and intervening sandy valleys
Qw Colluvial and alluvium—silt, sand, and gravel on distal outwash deposits in poorly drained areas; numerous small claypans

Czc	Czk	Czl	Czz	Czzc	Czzg

Czc Colluvium—variably cemented outwash talus; dissected by present drainage
Czk Calcrete—massive, nodular, and cavernous sandy limestone; locally silicified
Czl Laterite—ferruginous duricrust on tops of hills; remnants of Tertiary peneplain
Czz Silcrete—siliceous caprock with angular quartz grains
Czzc Silicified sandstone cap rock with thin veneer of colluvium; restricted to tops of hills
Czzg Leached and variably silicified granitic orthogneiss; alteration product of ᏢRga

PERMIAN

Pa **PATERSON FORMATION** : sandstone, claystone, conglomerate, and boulder beds; tillite and fluvioglacial deposits — CANNING BASIN

d	q	qb	fb	go

d Dolerite
q Quartz vein
qb Quartz breccia
fb Fault breccia and silicified rock adjacent to faults
go Gossan, or zone of gossanous rock

PROTEROZOIC — PATERSON OROGEN

c. 800 Ma — Tarcunyah Group

ᏢUk **KARARA FORMATION** : quartz arenite and quartz-feldspar wacke; minor beds of shale and conglomerate
ᏢUu **GUNANYA SANDSTONE** : arkose and medium- to coarse-grained sandstone; local beds of conglomerate and siltstone
ᏢUup Conglomerate, sandstone, and siltstone

> 900 Ma — Yeneena Supergroup — Throssell Group

ᏢTp **PUNGKULI FORMATION** : shale, reddish brown to grey; minor sandstone, carbonate, and pyritic shale; metamorphosed
ᏢTpk Carbonate rock, grey, cream to pink and finely laminated; minor sandstone, shale, and pyritic shale; metamorphosed
ᏢTt **TALIWANYA FORMATION** : arkose to arkosic sandstone, medium- to coarse-grained; local basal conglomerate and coarse sandstone; metamorphosed

Ᏽb Amygdaloidal basalt; metamorphosed
Ᏽbe Amygdaloidal basalt; heavily epidotized; metamorphosed

1310 ± 4 Ma

Ᏽgp	Ᏽge	Ᏽgm	Ᏽgl	Ᏽgf

Ᏽgp Pegmatite; quartz-K-feldspar-biotite-muscovite bearing; massive to weakly foliated
Ᏽge Syenogranite and monzogranite; even-grained; massive to weakly foliated
Ᏽgm Leucogranite; coarse-grained with K-feldspar megacrysts; massive to weakly foliated
Ᏽgl Leucogranite; medium- to coarse-grained; massive to weakly foliated
Ᏽgf Granitoid rock with feldspar phenocrysts; massive to strongly foliated

Rudall Complex (stratigraphic succession incompletely determined)

ᏢRu Metamorphosed ultramafic rock; serpentinite

ᏢRnb	ᏢRnc	ᏢRnm	ᏢRng	ᏢRns

ᏢRnb Quartz-feldspar-biotite(-muscovite) gneiss
ᏢRnc Charnockite; quartz-K-feldspar-plagioclase-garnet-orthopyroxene gneiss
ᏢRnm Quartz-microcline-plagioclase-biotite(-muscovite) gneiss
ᏢRng Quartz-K-feldspar-plagioclase-garnet(-muscovite) gneiss
ᏢRns Mylonite; quartz-sericite(-K-feldspar-plagioclase-muscovite-biotite) rock

1765 - 1790 Ma

ᏢRgh	ᏢRgm	ᏢRga	ᏢRgo

ᏢRgh Orthogneiss to strongly foliated granodiorite to monzogranite; hornblende-bearing; medium- to coarse-grained; generally interleaved with and containing inclusions of amphibolite
ᏢRgm Leucocratic, muscovite-rich orthogneiss derived from medium-grained granite
ᏢRga Orthogneiss derived from porphyritic biotite granitoid rock; generally contains K-feldspar augens
ᏢRgo Compositionally layered orthogneiss derived from fine- to medium-grained granite or monzogranite; alternating biotite- and feldspar-rich layers; lenticular inclusions of mafic rocks

ᏢRs	ᏢRq	ᏢRqm	ᏢRqa

ᏢRs Psammitic paragneiss; includes fine-grained quartz-feldspar-muscovite gneiss, quartz-mica schist, and layers of quartzite
ᏢRq Quartzite; commonly micaceous; thin intercalations of quartz-muscovite schist
ᏢRqm Muscovite quartzite; subordinate intercalations of quartz-muscovite schist
ᏢRqa Quartz-aluminosilicate schist; quartz-kyanite-ilmenite schist, quartz-sillimanite-K-feldspar schist, and quartz-sillimanite-K-feldspar-garnet schist

ᏢRb	ᏢRm	ᏢRi	ᏢRic	ᏢRir	ᏢRk

ᏢRb Banded paragneiss containing layers of quartz-feldspar(-biotite) gneiss, quartz-biotite schist, micaceous quartzite, quartz-muscovite schist, and amphibole-chlorite schist
ᏢRm Quartz-mica schist; metamorphosed argillaceous sedimentary rock
ᏢRi Metamorphosed banded iron-formation, metachert, and pyrite-graphite schist
ᏢRic Metachert and locally metamorphosed banded iron-formation
ᏢRir Graphite-quartz-garnet-biotite-sulfide schist and metamorphosed banded iron-formation; minor metachert
ᏢRk Calc-silicate gneiss and schist; metamorphosed carbonate rock and calcareous sandstone

ᏢRan	ᏢRab	ᏢRae	ᏢRam	ᏢRao	ᏢRac	ᏢRag

ᏢRan Amphibolite; leucocratic, coarse- to very coarse-grained, plagioclase-amphibole rock; massive to foliated; meta-leucogabbro and meta-anorthosite
ᏢRab Epidote and quartz-bearing amphibolite; fine-grained
ᏢRae Amphibolite; mesocratic to leucocratic, silicified and epidotized; foliated
ᏢRam Clinopyroxene and quartz-bearing amphibolite; foliated and locally gneissic
ᏢRao Garnet, clinopyroxene and quartz-bearing amphibolite interleaved with granitic gneiss (ᏢRgo); foliated
ᏢRac Orthopyroxene and clinopyroxene-bearing amphibolite; massive to foliated and locally gneissic
ᏢRag Garnet, clinopyroxene, and quartz-bearing amphibolite; foliated and locally gneissic

Geological boundary
- exposed
Fault
- exposed
- concealed
- concealed, position uncertain
- thrust or reverse, showing dip
- lag
- strike-slip, showing relative horizontal displacement
Fold, showing trend and plunge direction
- anticline; exposed, concealed
- syncline; exposed, concealed
- overturned anticline; exposed, concealed
- overturned syncline; exposed, concealed
Minor fold, showing trend and plunge direction
- minor anticline
- minor syncline
- minor fold, showing nature of vergence (Z, M or S profile)
Bedding, showing strike and dip
- inclined
- overturned
- trend, from aerial photography
Glacial striae, showing direction of ice movement
Way-up indicator
- cross-bedding
Direction and sense of movement of sediment-bearing currents
- asymmetrical ripple marks
- cross-stratification
Metamorphic foliation, showing strike and dip
- inclined
- vertical
- trend (section only)
Cleavage, showing strike and dip
- inclined
- vertical
Lineation, showing direction of plunge
- mineral lineation
- axis of crenulation
Airphoto lineament
- structural trend

Major track, maintained
Track
National park boundary
Breakaway
Sand dune
Contour line, 20 metre interval
Watercourse, ephemeral
Rockhole ... RH
Abandoned ... (abd)

Prospect ... Mt Cotton
Mineral occurrence
Geochemical anomaly from gossan assay (anomaly criteria: > 1000 ppm, except for Ba > 1%; Mn > 10%; Au > 0.5 ppm)

Arsenic	As
Barite	Ba
Bismuth	Bi
Cerium	Ce
Chromium	Cr
Copper	Cu
Gold	Au
Lanthanum	La
Lead	Pb
Manganese	Mn
Molybdenum	Mo
Niobium	Nb
Silver	Ag
Tungsten	W
Uranium	U
Yttrium	Y
Zinc	Zn

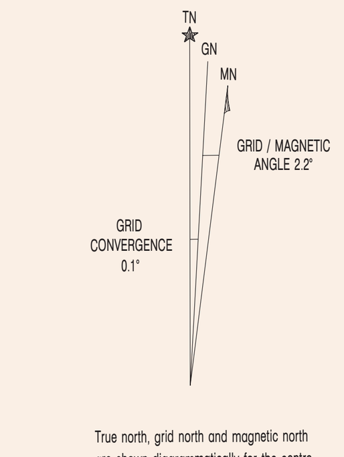

True north, grid north and magnetic north are shown diagrammatically for the centre of the map. Magnetic north is correct for 1996 and moves easterly by about 0.1° in 4 years.

SIMPLIFIED GEOLOGY

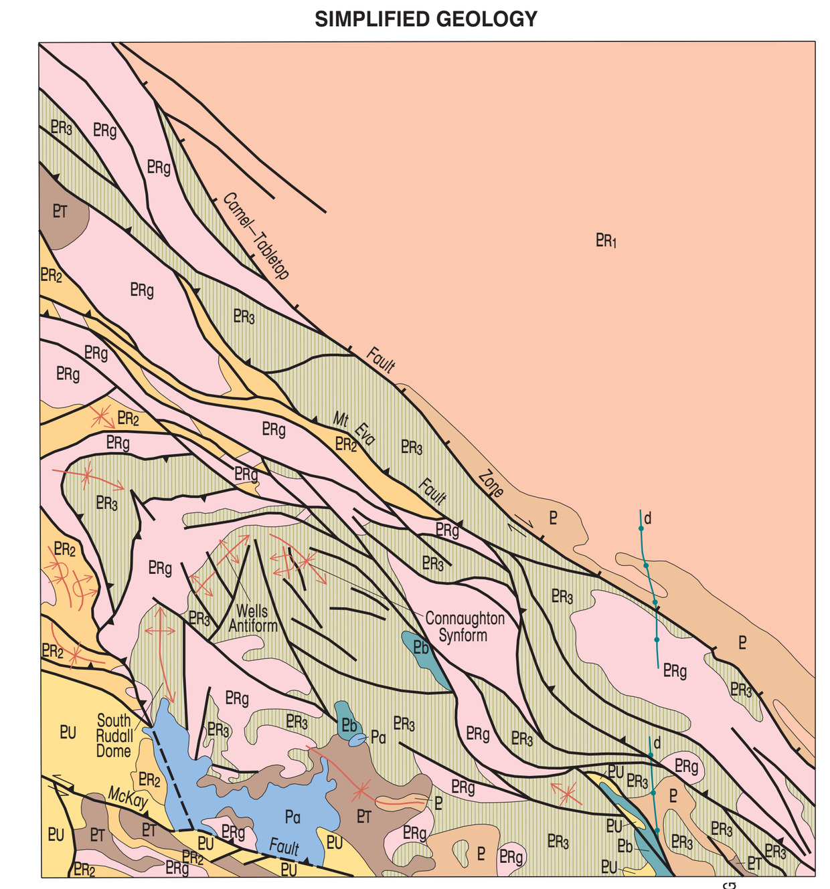

Pa Paterson Formation — CANNING BASIN
d Dolerite dyke
ᏢU Tarcunyah Group — PATERSON OROGEN
Ᏽ Tarcunyah and Throssell Groups; undifferentiated
ᏢT Throssell Group
Ᏽb Amygdaloidal basalt
ᏢRg Orthogneiss, granitoid rock; undifferentiated — Rudall Complex
ᏢR1 Tabletop Terrane; granitoid rock, amphibolite, metamorphosed banded iron-formation, and orthogneiss
ᏢR2 Talbot Terrane; quartzite, psammitic paragneiss, banded paragneiss, and pelitic schist
ᏢR3 Connaughton Terrane; amphibolite, metamorphosed banded iron-formation, chert, calc-silicate gneiss, quartzite, pelitic schist, and metamorphosed ultramafic rock

SCALE 1:500 000
0 5 10 15 20 Kilometres

SHEET INDEX

THROSSELL 3253	BROADHURST 3353 RUDALL	DORA 3453	TRIWHITE 3553	AULD 3653 TABLETOP	NANGABBITTA-JARRA 3753
POISONBUSH 3252	SF 51-10 RUDALL 3352	CONNAUGHTON 3452	BLANCHE 3552	SF 51-11 TABLETOP 3652	MUJINGERRA 3752
STACEY 3251	Mc FADDEN 3351 GUNANYA	GUNANYA 3451	CRONIN 3551	SURPRISE 3651 RUNTON	MIDWAY 3751
KNIGHT 3250	SF 51-14 DURBA 3350	DISAPPOINTMENT 3450	RUNTON 3550	SF 51-15 LEEMING 3650	BEJAH 3750

1:100 000 maps shown in black
1:250 000 maps shown in brown

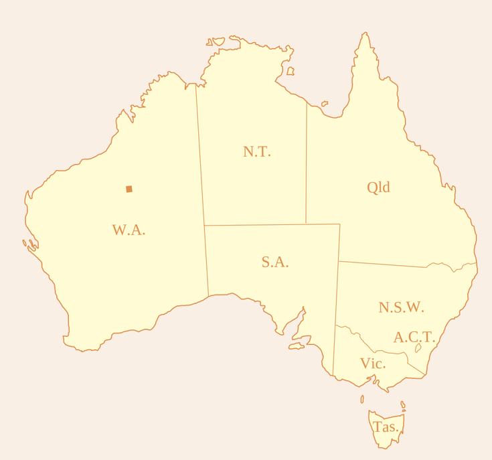

DEPARTMENT OF MINERALS AND ENERGY
L. C. RANFORD, DIRECTOR GENERAL

GOVERNMENT OF WESTERN AUSTRALIA
HON. NORMAN MOORE, M.L.C.
MINISTER FOR MINES

GEOLOGICAL SURVEY OF WESTERN AUSTRALIA
PIETRO GUJ, DIRECTOR

SCALE 1:100 000

1000 Metres 0 1 2 3 4 5 6 7 8 9 10 Kilometres

UNIVERSAL TRANSVERSE MERCATOR PROJECTION
HORIZONTAL DATUM: GEOCENTRIC DATUM OF AUSTRALIA 1994
VERTICAL DATUM: AUSTRALIAN HEIGHT DATUM

Grid lines indicate 1000 metre interval of the Map Grid Australia Zone 51

The Map Grid Australia (MGA) is based on the Geocentric Datum of Australia 1994 (GDA94)
GDA94 positions are compatible within one metre of the datum WGS84 positions

Reference points to align maps based on the previous datum, AGD84, have been placed near the map corners

Geology by L. Bagas and R.H. Smithies 1993-4
Edited by D. Ferdinando and G. Loan
Cartography by P. Taylor
Topography from the Department of Land Administration Sheet SF 51-10, 3452, with modifications from geological field survey
Published by the Geological Survey of Western Australia. Copies available from the Mining Information Centre, Department of Minerals and Energy, 100 Plain Street, East Perth, WA, 6004. Phone (09) 222 3459, Fax (09) 222 3444
This map is also available in digital form
Printed by Allwest Print, Western Australia
The recommended reference for this map is: BAGAS, L., and SMITHIES, R.H., 1996, Connaughton, W.A. Sheet 3452: Western Australia Geological Survey, 1:100 000 Geological Series

CONNAUGHTON

SHEET 3452 FIRST EDITION 1996
Version 1.1 — December 2004